



UNIVERSITÀ DEGLI STUDI DI PARMA

Dipartimento di Chimica

Ph.D. in Science and Technology of
Innovative Materials

XXV Cycle

**Supramolecular sensing
at the solid-liquid interface
with phosphonate cavitands**

Daniela Menozzi

Coordinator: **Prof. Enrico Dalcanale**

Supervisor: **Prof. Enrico Dalcanale**

Author: **Daniela Menozzi**

© Daniela Menozzi, Parma, 2013

*Alla mia Famiglia
E a Marco*

Contents

CHAPTER 1.....	1
Introduction: supramolecular chemistry with tetraphosphonate cavitands	
1.1 Supramolecular chemistry.....	2
1.2 Non-covalent interactions.....	4
φ Hydrogen bonding.....	4
φ Ion-dipole interactions.....	7
φ CH- π interaction.....	8
1.3 Cavitands as molecular receptors.....	9
φ Thermodynamics of host-guest interactions.....	13
φ Specific sensing: biosensors.....	15
φ Specific sensing with cavitands: microcantilevers.....	16
φ Thermodynamics at the solid-liquid interface.....	18
1.4 References.....	21
CHAPTER 2.....	25
Thermodynamics of host-guest interactions between methylpyridinium salts and phosphonate cavitands	
2.1 Introduction.....	26
φ General scenario.....	26
2.2 Results and discussion.....	27

⊗ Cavitands and guests.....	27
⊗ X-Ray structure.....	28
⊗ ITC measurements.....	30
2.3 Conclusions.....	33
<i>Acknowledgements</i>	33
2.4 Experimental section.....	34
2.5 References.....	40

CHAPTER 3.....	43
----------------	----

Self-assembly of a cavitand-stopped rotaxane

3.1 Introduction.....	44
⊗ Top-down versus bottom-up approach.....	44
⊗ Bottom-up approach: atoms or molecules?.....	44
⊗ Catenanes, rotaxanes, pseudorotaxanes.....	45
⊗ Non-covalent interactions in rotaxanes.....	49
⊗ Aim of the work.....	50
3.2 Results and discussion.....	53
⊗ Axle, cavitand and crown.....	53
⊗ Working principle.....	56
⊗ Titration experiments.....	57
❖ Crown-axle interaction.....	57
✓ Acetonitrile titration.....	58
✓ Acetone titration.....	60
❖ Cavitand-axle titrations.....	62
✓ Acetonitrile/chloroform experiment.....	63
✓ Acetone experiment.....	65

❖ Pseudorotaxane assembly.....	68
✓ Acetonitrile/chloroform experiment.....	69
✓ Acetone experiment.....	71
3.3 Conclusions.....	74
<i>Acknowledgements</i>	74
3.4 Experimental section.....	75
3.5 References.....	81
CHAPTER 4.....	87
Nanomechanical recognition of <i>N</i>-methylammonium salts	
4.1 Introduction.....	88
⌀ General scenario.....	88
4.2 Results and discussion.....	91
⌀ Cavitands and guests.....	91
⌀ MC experiments: protocol.....	92
⌀ ITC experiments: protocol.....	93
⌀ MC experiments: results.....	93
⌀ ITC experiments: results.....	97
⌀ MC experiments <i>versus</i> ITC experiments.....	101
⌀ Glycine <i>versus</i> Sarcosine detection in water.....	102
4.3 Conclusions.....	104
<i>Acknowledgements</i>	104
4.4 Experimental section.....	105
4.5 References.....	111

CHAPTER 5..... 115

Towards a cavitand-based MC sensor for drugs

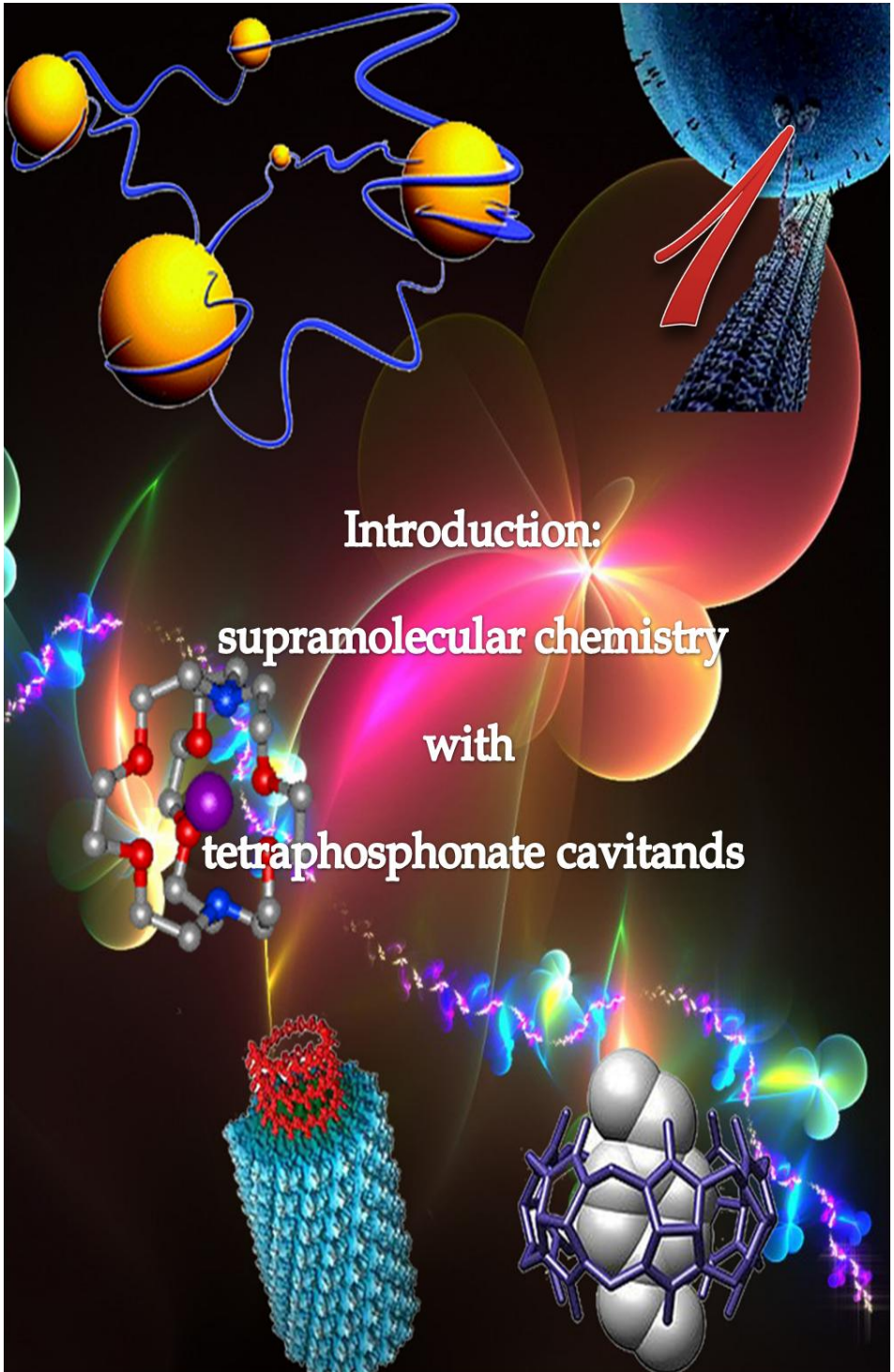
5.1 Introduction.....	116
⊘ General scenario.....	116
⊘ Cocaine.....	118
❖ Synthesis.....	119
⊘ ATS substances.....	120
❖ Synthesis.....	122
⊘ Drug sensors devices: state of the art.....	123
⊘ The excipients concern.....	125
5.2 Results and discussion.....	128
⊘ Cavitands and guests.....	128
⊘ NMR qualitative tests.....	129
⊘ Assessment of non specific interactions.....	131
⊘ Biphasic system.....	131
⊘ MC experiments.....	133
5.3 Conclusions.....	137
<i>Acknowledgements</i>	137
5.4 Experimental section.....	138
5.5 References.....	139

CHAPTER 6..... 143

Michael Walker: traffic lights on a branched track

6.1 Introduction.....	144
-----------------------	-----

ϕ General scenario.....	144
ϕ Small molecules that walk along a track.....	148
5.2 Results and discussion.....	151
ϕ Choice of the traffic lights.....	151
ϕ Tracks and walker.....	153
ϕ Selective Boc deprotection studies.....	154
ϕ Model track synthesis.....	158
ϕ Stability in walking conditions.....	159
ϕ Teoc deprotection studies.....	160
❖ KF cleavage agent.....	160
❖ TBAF cleavage agent.....	161
❖ TFA cleavage agent.....	162
6.3 Conclusions.....	164
<i>Acknowledgements</i>	164
6.4 Experimental section.....	165
6.5 References.....	168
<i>Acknowledgements</i>	171
<i>The author</i>	173



Introduction:

supramolecular chemistry

with

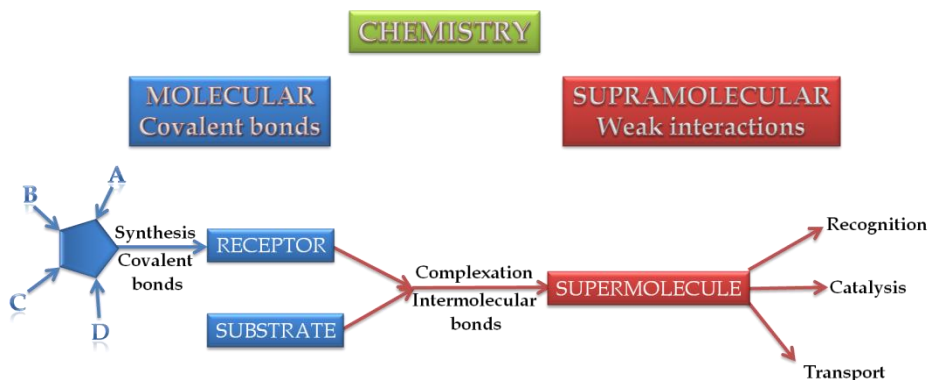
tetraphosphonate cavitands

1.1 SUPRAMOLECULAR CHEMISTRY

"Just as there is a field of molecular chemistry based on the covalent bond, there is a field of supramolecular chemistry, the chemistry of molecular assemblies and of the intermolecular bond" (Lehn, 1978).¹

"Supramolecular chemistry can be considered as the chemistry beyond the molecule" (Lehn, 1988).²

Supramolecular chemistry aims to build and develop chemical systems with an high degree of complexity based on two or more molecular components glued together by non-covalent interactions. The transition from molecular to supramolecular chemistry is explained in scheme 1: molecular chemistry starts with the synthesis of molecules via the formation of new covalent bonds. In this way the receptors and the substrates are formed. Then the molecular chemistry leaves the stage to the supramolecular chemistry: the interaction mode of the receptor•substrate complex exploits intermolecular bonds, leading to the *supermolecules* that can be addressed to many goals, like molecular recognition, catalysis and molecular transport.



Scheme 1. From molecular to supramolecular chemistry.¹

In table 1 the different features of covalent and non-covalent synthesis are summarized.

Feature	Covalent synthesis	Non-covalent synthesis
Constituent bond types	Covalent	Ionic, hydrophobic, hydrogen bonds, CH- π forces
Bond strengths (kcal/mol)	25-200	0.1-20
Stability of bonds in the product	Kinetically stable	Kinetically reversible
Contributions to ΔG	Usually dominated by ΔH	ΔH and $T\Delta S$ are often comparable
Strategy of design	Selective reaction	Directed equilibrium
Importance of solvent effects	Secondary	Primary
Other characteristics		Cooperative behavior important

Table 1. Comparison between covalent and non-covalent synthesis.

The molecular recognition phenomena in biological systems started to be a real interest in the early seventies, after the accidental discovery of crown ethers by C. Pedersen.³ In fact, in 1974 Lehn² and Cram⁴ began to work on molecular receptors for small charged and neutral molecules. For their studies they were awarded with the Nobel Prize in 1987. 30 years of researches in this field have highlighted how the weak interactions are the glue and the key issue for the construction of chemical structure with higher and higher degree of complexity.⁵

In the present thesis, the field of molecular recognition is analyzed in many aspects. The receptor-substrate motif is the guideline of the work done, starting from the monitoring of the host-guest interaction in solution, passing by the solid state via crystal structures analysis and ending with molecular recognition at interfaces.

1.2 NON-COVALENT INTERACTIONS

In the area of molecular chemistry, molecules are collections of atoms connected by a continuous network of strong and high energy covalent bonds (50-200 Kcal mol⁻¹), while in the field of supramolecular chemistry, molecules can interact without formation of kinetically stable bonds but through much weaker and kinetically labile non-covalent interactions (0.1-20 Kcal mol⁻¹)⁵ such as van der Waals forces, H-bonding, dispersive forces that are all known with the name of non-covalent interactions. The importance of these interactions starts from the biological processes, in which they have a key role, like in the protein folding processes, or in the expression and transfer of genetic information. Herein a brief discussion of the weak interactions exploited in this thesis is given.

Hydrogen bonding. H-bonds connect atoms X and Y that have electronegativities larger than that of hydrogen, namely, C, N, O, F, P, S, Cl, Se, Br, and I.⁶ The XH group is generally referred to as the "proton donor" (D) and the Y atom is called the "proton acceptor" (A) group. The strength of a H-bond increases with an increase in the dipole moment of the X-H bond and the electron lone pair on atom Y. Hence, the strongest H-bonds are formed between atoms N, O, and F acting as X and Y, although C-H can also act as a donor.⁷

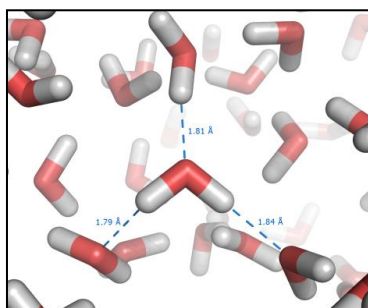


Figure 1. *Hydrogen bonds in liquid water (molecular dynamics simulation).*

Initially, the hydrogen bonding was described as a pure electrostatic interaction between the partially positive hydrogen and the lone electron pair on the acceptor, but this interaction is in reality a lot more complicated, and it is the result of five different contributes:

- 1) electrostatic or coulomb energy;
- 2) exchange repulsion;
- 3) polarization energy;
- 4) charge-transfer energy or covalent bonding;
- 5) dispersion forces.

A modified Lennard-Jones potential is often used to evaluate the hydrogen bonding strength:⁸

$$E_{H-Bond}(R) = \varepsilon \left[A \left(\frac{R_0}{R} \right)^{12} - B \left(\frac{R_0}{R} \right)^{10} \right] (\cos \theta_{D-H \cdots A})^4$$

where

- R = the distance between D and A;
- R₀ = the equilibrium distance;
- ε = the depth of the potential;
- A and B = adjustable parameters.

In the equation is present also an angle dependent term, from which we can assume that the hydrogen bonding energy has a maximum value when the donor and the acceptor are collinear.

Herein we report some selected hydrogen bonding values:

- F-H ⋯ F (155 kJ/mol)
- O-H ⋯ N (29 kJ/mol)
- O-H ⋯ O (21 kJ/mol)
- N-H ⋯ N (13 kJ/mol)
- N-H ⋯ O (8 kJ/mol)

Hydrogen bonding has the key feature to be tunable, i.e. contrary to what happens in covalent bonds, hydrogen bonding is reversible and highly solvent dependent. For example in aprotic, apolar solvents the hydrogen bonding is a

stable interaction, while protic and polar solvents can be used to decrease or to modify the strength of this force.

Secondary interactions also play a very important role in the H-bonding strength. In figure 2 the influence of those secondary interactions is shown, both for attractive and repulsive forces.⁹ Favorable and unfavorable secondary electrostatic interactions between adjacent hydrogen-bonding sites were considered to be the origin of the difference in association energy for, ad example, triple hydrogen-bonded complexes (see figure 3 for an example). The total hydrogen bond is more stable when all the proton donor-acceptor pairs are arranged in the same direction: AAA-DDD.

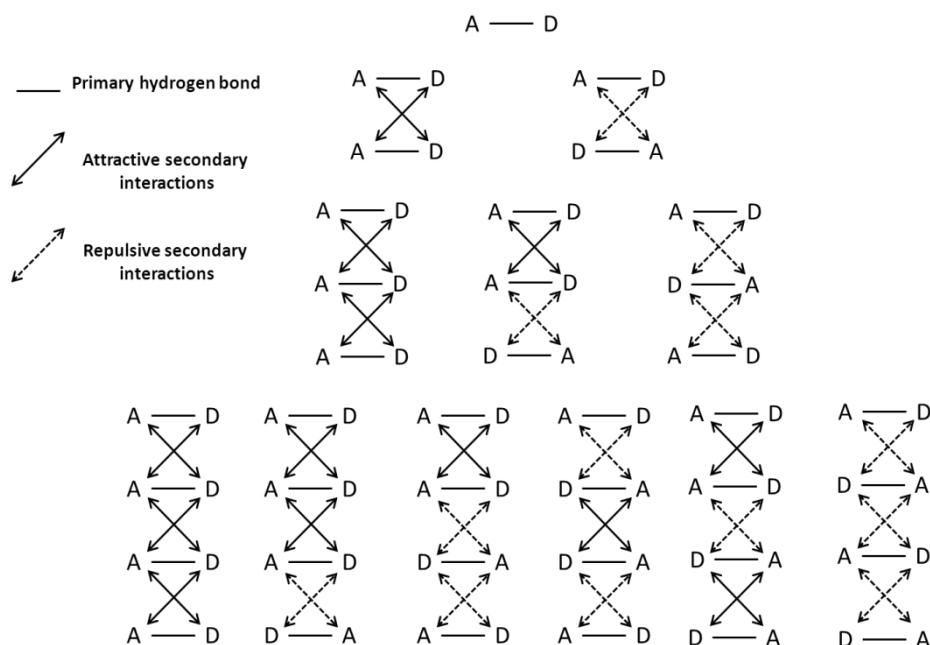


Figure 2. Schematic representation of complexes containing one to four H-bond together with the secondary attractive or repulsive electrostatic interactions.

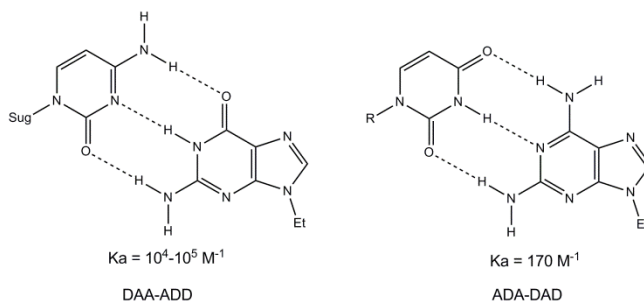


Figure 3. Differences in the association constants of two triple hydrogen bonded complexes. The complex on the right presents secondary destabilizing interactions that are responsible for the lower association constant compared with the complex on the left.

Ion-dipole interactions. Ion-dipole interactions occur between ions and polar groups of molecules (or induced dipoles). The energy is generally comprised between 50 and 200 KJ/mol.

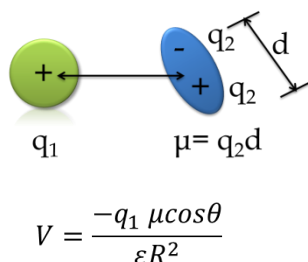


Figure 4. Schematic representation of a charge-dipole interaction (top) and the equation that describes the interaction (bottom).¹⁰

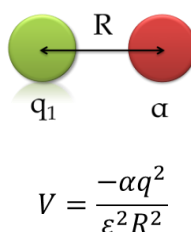


Figure 5. Schematic representation of a charge-induced dipole interaction (top) and the equation that describes the interaction (bottom).

Many examples presented in the literature are based on these weak interactions: the binding of protonated amines in cucurbituril macrocycle¹¹ rather than the inclusion of alkali-metal and alkaline-earth cations by crown ethers and related compounds.¹²

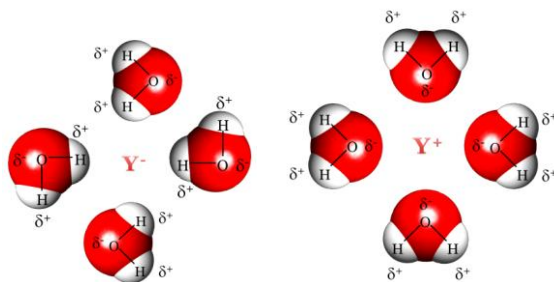


Figure 6. Example of ion-dipole interactions.

CH- π interactions. In the CH- π interactions the donor species is an aromatic, an acetylenic or an alkylic CH with a double/triple bond or an aromatic that acts like an acceptor species. In other terms, this type of interactions occurs between soft acids (CHs in an alkyl group) and soft bases (π -systems). Despite their low energy (2-8 KJ/mol), CH- π interactions can count on multiple interactions and on a variety of different geometries.

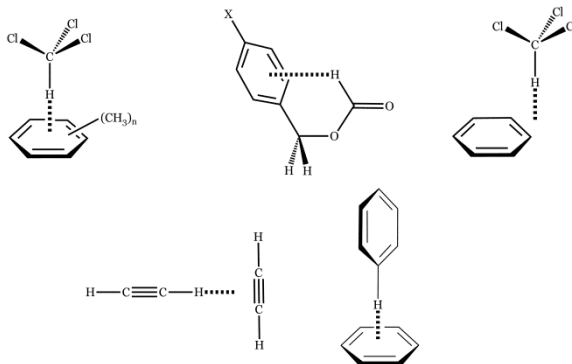


Figure 7. CH- π interactions between different species and with different geometries.

The stabilization of these interactions comes from the dispersive forces and the charge-transfer phenomenon. For what concerns the electrostatic forces contribution, this is very small in “typical” CH- π interactions of alkanes while

in the case of the acetylene, for example, the large positive charge on the hydrogen atom enhances the electrostatic interactions.¹³

CH- π interactions play a crucial role in determining the selectivity of organic reactions and the properties of solid materials (graphite and fullerene for example).

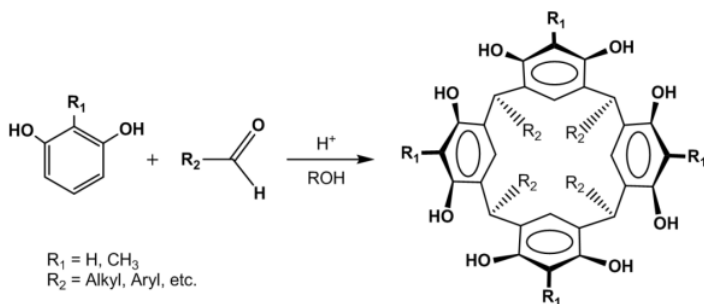
1.3 CAVITANDS AS MOLECULAR RECEPTORS

"Molecular receptors use intermolecular interactions for the selective bind of substrate" (Lehn, 1978).¹

The base of supramolecular chemistry rests on molecular recognition, that is the selective recognition of substrate molecules (guests) by synthetic receptors (hosts). Host-guest complexation involves receptor molecules containing hollow and enforced spaces and smaller species that can be located inside them. In the last decades many efforts have been oriented to the design and the development of a variety of new receptors for the binding of both neutral and charged species. The initial inspiration for this research came from the realm of biology, in which specific molecular interactions provide the basis of the working features of biotic molecules (catalysis, transport, regulation).¹⁴ Many different receptors based on cryptands,¹⁵ crown ethers,³ calixarenes,¹⁶ cyclodextrins¹⁷ and cyclic polyamines¹⁸ are described in the literature. In the present thesis we will deal with a specific class of molecular receptors, namely tetraphosphonate cavitands.

"Cavitands are synthetic organic compounds with enforced cavities large enough to complex complementary organic molecules or ions" (Cram, 1983).¹⁹

Cavitands are based on a resorcin[4]arene-type scaffold, obtained by an acid condensation between resorcinol and aldehyde (scheme 2).²⁰ The choice of a different R group in the resorcinol or in the aldehyde (R₁ or R₂, see scheme 2) provides different entry points for derivatization both at the upper and at the lower rim, that can be exploited in the molecular recognition process and in the design of the cavitand receptor.



Scheme 2. *Synthesis of a resorcin[4]arene.*

The resorcin[4]arene presents a flexible pseudo cavity, not suitable for a proper host-guest recognition. The bridging reaction of the phenolic OH on the upper rim gives to the receptor the desired rigidity and concavity. In particular, in the design of the cavitand, the choice of the bridging group is pivotal since it determines shape, dimensions and complexation properties of the final cavitand.

In our case the introduction of phosphonate groups imparts to these systems special complexing properties toward positively charged species, such as alkali-metal and alkaline-earth cations,²¹ or ammonium²² and *N*-methylpyridinium salts.²³

The presence of four stereogenic centers in the tetraphosphonate cavitands gives rise to six possible diastereomeric isomers, differing from each other for the orientation of the P=O moieties, inward (i) or outward (o) the cavity (figure 8).¹⁴

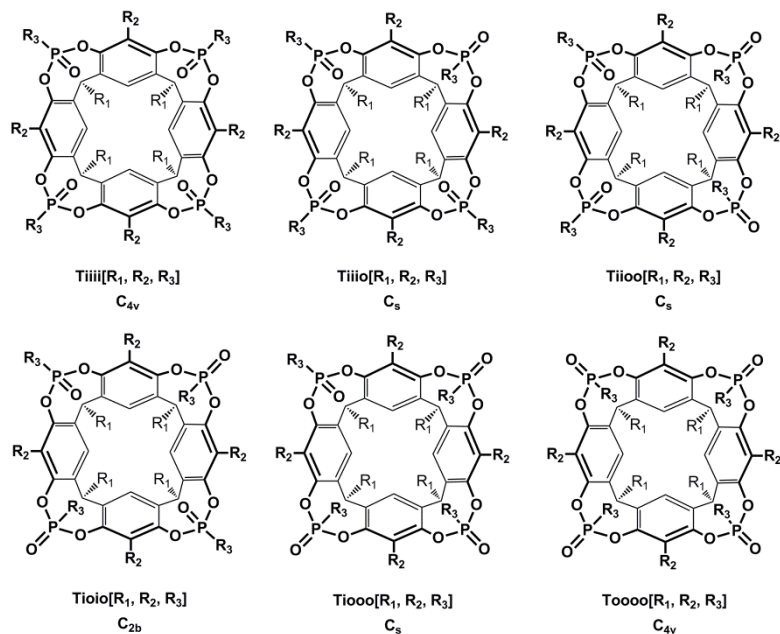


Figure 8. Isomers of tetraphosphonate bridged cavitands.

As shown in previous works,^[21, 24] increasing the number of P=O groups pointing inward the cavity leads to an enhancement of the molecular recognition properties. The receptor that showed the best recognition properties is the cavita nd with all the four P=O groups oriented inward the cavity. In particular, tetraphosphonate cavita nd presents remarkable recognition properties toward *N*-alkylammonium and *N*-methylpyridinium salts which can be attributed to three synergistic interaction modes which can be activated either individually or in combination by the host according to the guest requirements :

1. $\text{N}^+ \cdots \text{O}=\text{P}$ cation-dipole interactions;
2. $\text{CH}_3-\pi$ interactions of the acidic $^+\text{N}-\text{CH}_3$ group with the π basic cavity;
3. single or multiple hydrogen bonds involving P=O bridges and the nitrogen protons of the guest.

In figure 9 the complexation mode of tetraphosphonate cavita nds towards *N*-methylpyridinium salts (left) and *N*-alkylammonium salts (right) is shown.

In the first case the recognition process is driven by cation-dipole and $\text{CH}-\pi$ interactions, while in the second one all the three synergistic interactions are

presents, causing the higher affinity of the *N*-methylammonium toward the cavity.

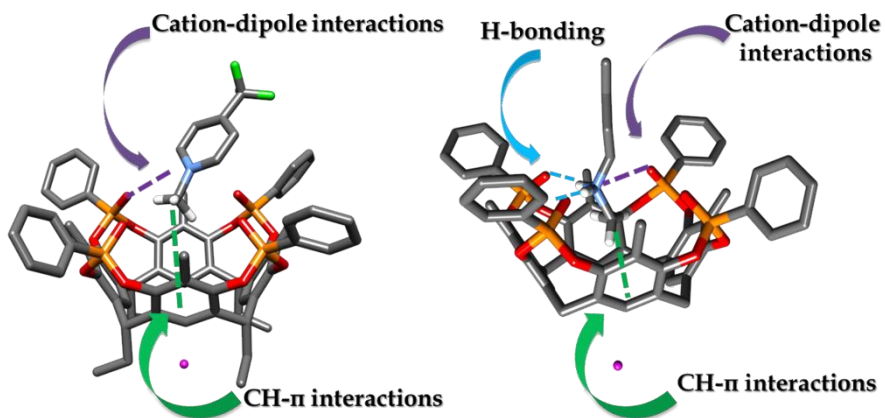


Figure 9. Complexation mode of tetraphosphonate cavitands towards *N*-methylpyridinium salts (left) and *N*-alkylammonium salts (right).

When the P=O moieties are replaced by the P=S ones, the structurally related tetrathiophosphonate cavitands²⁵ are obtained (figure 10). Those receptors are excellent hosts towards soft metals (Ag^+ , Hg^{2+} , ...) ²⁶ but there is no recognition process with the ammonium and pyridinium guests (see chapter 2 for details) because of the much weaker H-bonding and cation-dipole interactions.

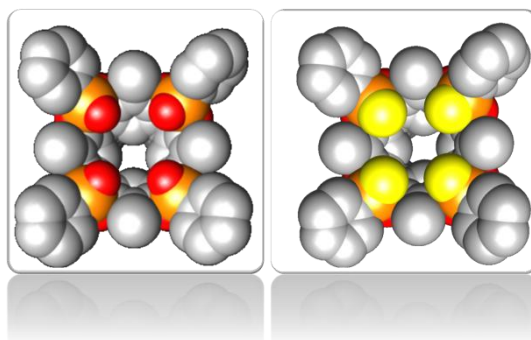


Figure 10. Top view of tetraphosphonate (left) and tetrathiophosphonate cavitands (right).

Thermodynamics of host-guest interactions. The complexation properties of tetrakisphosphonate cavitands have been previously studied in the solid state,²⁷ in solution²⁸ and in the gas phase.²⁹ In the present thesis, in chapters 2 and 4, an extensive study in solution of the host-guest recognition processes will be presented. In particular, the attention will be focused for the first time on the cavitand complexation properties towards methylpyridinium and alkylammonium salts from a thermodynamic point of view.

Isothermal Titration Calorimetry (from now on referred to as ITC)³⁰ is one of the most straightforward way to evaluate thermodynamics and association constants of interactions like host-guest ones. The principle on which this technique is based on is that every compound in solution can interact with all other species present in the environment, leading to an energetic response that can be dissected and quantified into its enthalpic and entropic components. In succession (figure 11) we report the scheme of the instrument used.

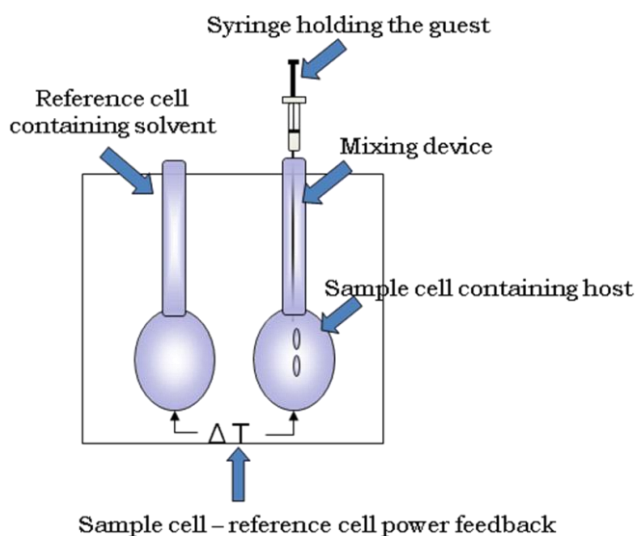


Figure 11. Schematic representation of the instrumental setup of a power compensation calorimeter.

The instrument is composed by two identical cells: one contains the pure solvent (reference cell) and the other the solution of host/guest (sample cell). An electrical power heater is attached to both cells to minimize the temperature difference between the two. On the top of the sample cell there is a syringe

filled with the solution of the guest/host. When the guest/host is dropped inside the host/guest solution, if there is an association between the two, there will be an evolution or a consumption of heat that leads to a change in the sample cell temperature. This deflection in the temperature causes the feedback regulator to adjust the electrical power needed to maintain the two cells at the same temperature. The change in the feedback current is the first signal observed and is called heat pulse (see upper panel in figure 12). The plotting of the integral of every single heat pulse versus the molar ratio of the guest gives the final data output (see lower panel in figure 12) from which is possible to extrapolate the stoichiometry (from the relative position of the inflection point with respect to the x-axis), the enthalpy (from the step height of the curve) and the K_{ass} (from the slope of the inflection point). The Gibbs free energy can be derived from the association constant and then the entropy can be calculated.

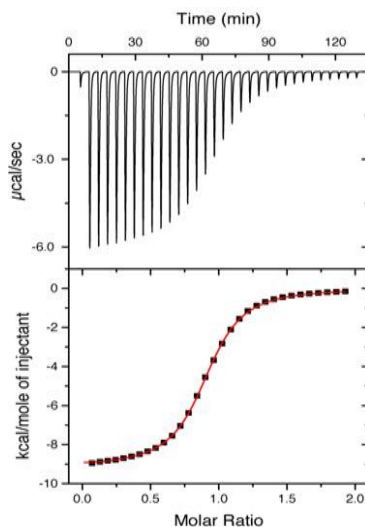


Figure 12. Example of a typical data output for an exothermic reaction monitored by ITC.

The experiments performed highlighted how the recognition processes of the host cavitands towards methylpyridinium salts and alkylicammonium salts are both enthalpy and entropy driven. The unusual entropic gain can be coarsely interpreted in terms of an increase in solvent entropy associated with the desolvation of both host and guest upon complexation (see chapters 2 and 4 for details).

The information obtained by the ITC in the recognition process of the receptor towards methylpyridinium salts were then exploited for the design of a cavitand-stopped rotaxane, shown in chapter 3.

In chapter 4, instead, ITC was used as an independent tool for confirmation and rationalization of the results obtained with microcantilevers-based sensor for the ammonium salts series.

Specific sensing: biosensors. Specific sensing pushes molecular recognition at its limits, mimicking biological receptors.

The synthetic equivalent is very seldom achieved due to the difficulty in preparing truly specific synthetic receptors.

A biosensor is a device which detects the presence or activity of molecules with the help of biomolecules.³¹ A biosensor consists of two basic elements (figure 13): one is a layer of biomolecules which can bind or interact with sample molecules and serves as the recognition element, defining the specificity of the sensor; the second element is a solid state device able to transduce the recognition event into a suitable signal for further processing. Examples of convenient physical signals that can be processed to correlate them to the presence of the target analytes are: fluorescence signals, mass changes, refractive index changes or changes in electric potential.

Depending on the detection principle one can differentiate between label-free and non-label-free sensors: the first ones detect the original and unmodified molecules and they can be used for the on-line monitoring. Although this approach remains the most desirable, problems related to the detection limits and the low-weight of some target classes of analytes are common. In fact molecules are often easier to detect when first labeled with a chemical modification. The presence of the label acts as an indicator of the presence of the molecule (see figure 13b). An example of a type of chemical tag is the use of fluorescent moieties. Despite the easier detection, this approach has some disadvantages that come from the time and costs consuming since the molecules need to be chemically modified before the investigation.

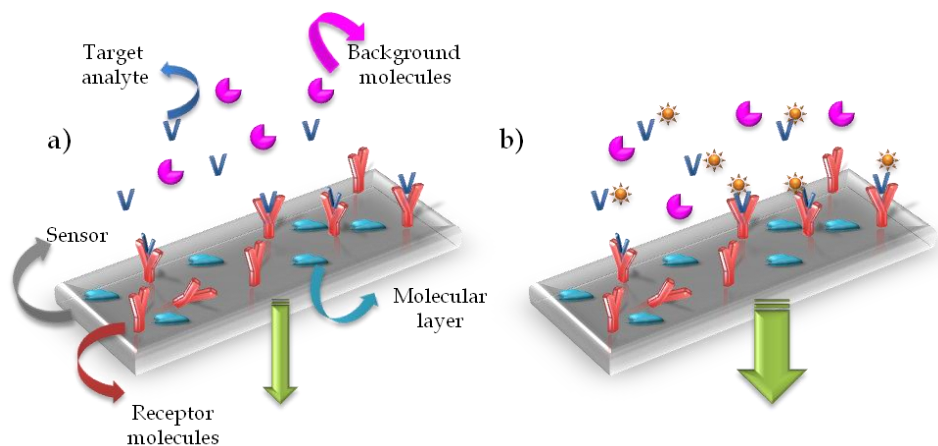


Figure 13. *Biosensing principle: a) the layer of receptor molecules attached to the sensor recognizes selectively the target analytes and doesn't bind the background molecules (interferents). The molecular layer prevents the interaction with the sensor via unspecific binding; b) same recognition process but with labeled molecules.*

Specific sensing with cavitands: microcantilevers. In the present thesis the host-guest recognition was investigated exploiting cavitand coated microcantilevers (MC). The biosensing principle beyond the cantilever-based sensors relies in the mechanical stresses produced upon molecular binding. Molecular adsorption on a solid surface is driven by surface Gibbs free energy reduction that leads to a change in the surface stress. If the solid is of proper material and shape, it responds to this stress by a mechanical response (i.e. by a deflection of the cantilever itself) that can be detected and transduced into a reliable readout signal.

Cantilevers can operate in different modes, but in this work we will deal exclusively with the so called "surface stress" or "static" mode: changes in the environment around or directly on the surface of the cantilevers create a mechanical stress in the surface which leads to an expansion or a contraction of the cantilever surface. If this stress acts only on one side of the cantilever then the structure will bend and the cantilever will deflect (figure 14).

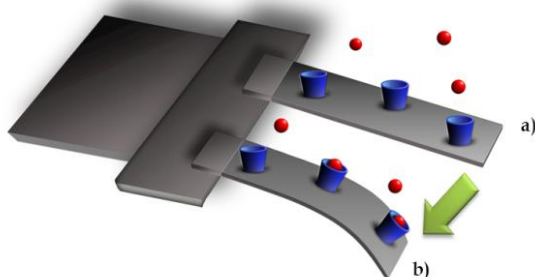


Figure 14. Simplified representation of a microcantilever working in a static mode: a) represents the state 0 of the cantilever, in which no molecular recognition occurs; b) represents the bending of the cantilever caused by the mechanical stress originated by the molecular interaction.

The most commonly used readout system for cantilever bending is the beam deflection or optical lever method introduced in 1988³² and shown in figure 15. A laser beam is focused on the flexible end of a cantilever and is reflected off onto a position-sensitive detector. The change in position of the reflection spot on the light-sensitive detector can be calculated back into a cantilever deflection. To improve this readout scheme, cantilevers can be covered with a thin reflecting metal layer (typically gold) on one side.

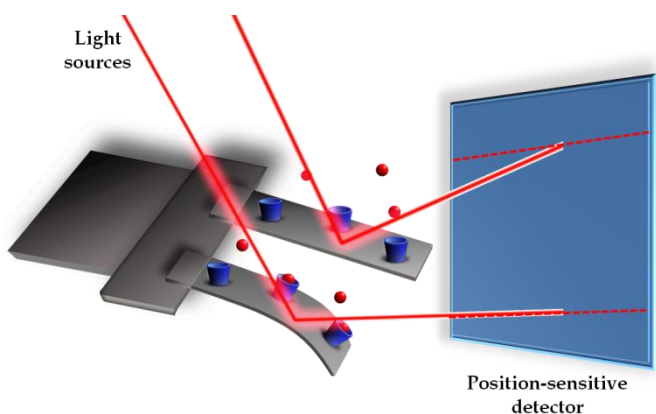


Figure 15. Simplified representation of a microcantilever array readout by optical beam deflection. Nanometer deflections of cantilevers are translated into a change of position of the reflected laser spot on a position-sensitive detector.

Thermodynamics at the solid-liquid interface. In figure 16, the two main and consecutive moments that describe the Ligand-Receptor (L-R) interaction are shown.

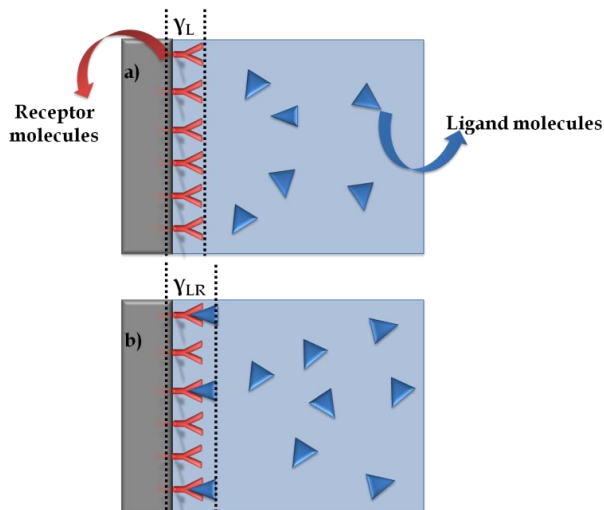


Figure 16. Sketch of the binding of ligand (L) molecules coming from solution to receptor (R) molecules which are grafted onto a solid surface. a) initial stage; b) equilibrium.

Just before the recognition process begins, the R coated surface is in equilibrium with the solvent forming an interfacial phase of interfacial tension γ_R and a given thickness τ_R (figure 16a).

After the interaction has taken place, the L molecules start to bind to the R molecules till equilibrium is reached (figure 16b). Therefore the reaction changes the molecular composition of the interfacial phase, thus changing its physicochemical properties. This transformation can be modeled by assuming that equilibrium is attained provided the substitution of the γ_R interfacial phase with a novel one, characterized by different interfacial tension, γ_{LR} , and thickness τ_{LR} .

Hence, the chemical equilibrium confined at a solid-solution interface could be described by equation (1).

$$\Delta_r G^0 = -\frac{\Delta\gamma}{\Gamma_{LR}} - RT \ln K \quad (1)$$

Where K is the equilibrium constant and Γ_{LR} is the interfacial excess density of moles of LR molecules but since in this system all the LR molecules are confined at the interface, Γ_{LR} is directly correlated to the number of LR moles per interface unit.

Equation (1) indicates that the whole standard work of the reaction $\Delta_r G^0$ splits into chemical and surface work. $\Delta\gamma = (\gamma_{LR} - \gamma_R)$ represents the work involved in the creation of the novel interfacial phase driven by the receptor/ligand binding reaction.

Instauration of this novel interfacial phase physically appears as a surface pressure π , that can be therefore defined as follows

$$\pi = \gamma_R - \gamma_{LR} = -\Delta\gamma \quad (2)$$

By substituting $-\Delta\gamma$ with π , equation (1) becomes

$$\Delta_r G^0 = \frac{\pi}{\Gamma_{LR}} - RT \ln K \quad (3)$$

It is worth noticing that, according to equation 3, a spontaneous interaction can exert either a positive or negative π .³³

In the last fifteen years these sensors have attracted more and more interest from a growing number of researchers and have impressed by their wide range of applications: to date, cantilever sensors have been used as artificial noses to detect gaseous analytes, they have detected pH, temperature changes, and ions; in the life sciences they have been used to detect nucleic acids, proteins, and bacteria; not to mention applications for infrared detection or the identification of explosives.³⁴

In chapter 4 is described how the microcantilever technique has been pushed forward, reaching an unprecedented real-time label-free selective screening towards alkylammonium salts, analytes that possess a mass equal or lower than 150 Da and that differ from each other for one, two or three methyl groups attached to the ammonium moiety. This unprecedented selectivity was achieved by the use of tetraphosphonate cavitands coating on the gold surface of the microcantilevers.

This approach has been then benchmarked by differentiating biological important molecules like sarcosine and glycine in water, reaching unique performances.

The results described in chapter 4 opened the route to use microcantilevers for the online monitoring and the label-free sensing of biologically active ammonium-based molecules like drugs.

In chapter 5 the first experiments made to assess the recognition properties of tetraphosphonate cavitands towards drugs at the solid-liquid interface are described.

1.4 REFERENCES

- ¹Lehn, J.-M. *Pure & Appl. Chem.* **1978**, *50*, 871-892.
- ²Lehn, J.-M. *Angew. Chem. Int. Ed.* **1988**, *27*, 89-112.
- ³a) Pedersen, C. J. *J. Am. Chem. Soc.* **1967**, *89*, 7017-7036; b) Pedersen, C. J. *Angew. Chem. Int. Ed.* **1988**, 1021-1027.
- ⁴Cram, D. J. *Angew. Chem. Int. Ed.* **1988**, *27*, 1009-1020.
- ⁵Reinhoudt, D. N.; Crego-Calama, M. *Science* **2002**, *295*, 2403-2407.
- ⁶Prins, L. J.; Reinhoudt, D. N.; Timmerman P. *Angew. Chem. Int. Ed.* **2001**, *40*, 2382-2426.
- ⁷Gu, Y.; Kar, T.; Scheiner, S. *J. Am. Chem. Soc.* **1999**, *121*, 9411-9422.
- ⁸Jensen F. in *Introduction to Computational Chemistry*, Wiley, Chichester, **1999**.
- ⁹(a) Jorgensen, W. L.; Pranata, J. *J. Am. Chem. Soc.* **1990**, *112*, 2008-2010; (b) Pranata, J.; Wierschke, S. G.; Jorgensen, W. L. *J. Am. Chem. Soc.* **1991**, *113*, 2810-2819.
- ¹⁰For an extensive study see: Yoder, C. H. *J. Chem. Educ.* **1977**, *54*, 402-408.
- ¹¹(a) Lagona, J.; Mukhopadhyay, P.; Chakrabarti, S.; Isaacs, L. *Angew. Chem. Int. Ed.* **2005**, *44*, 4844-4870; (b) Lee, J. W.; Samal, S.; Selvapalam, N.; Kim, H. J.; Kim, K. *Acc. Chem. Res.* **2003**, *36*, 621-630.
- ¹²Nielsen, K. A.; Cho, W. S.; Jeppesen, J. O.; Lynch, V. M.; Becher, J.; Sessler, J. L. *J. Am. Chem. Soc.* **2004**, *126*, 16296-16297.
- ¹³For selected references of CH- π interactions see: a) Nishio, M.; Hirota, M.; Umezawa, Y. *The CH- π Interactions*, Wiley-VCH, New York, **1998**; b) Dougherty, D. A.; Stauffer, D. A. *Science* **1990**, *250*, 1558-1560; c) Kim, E.-I.;

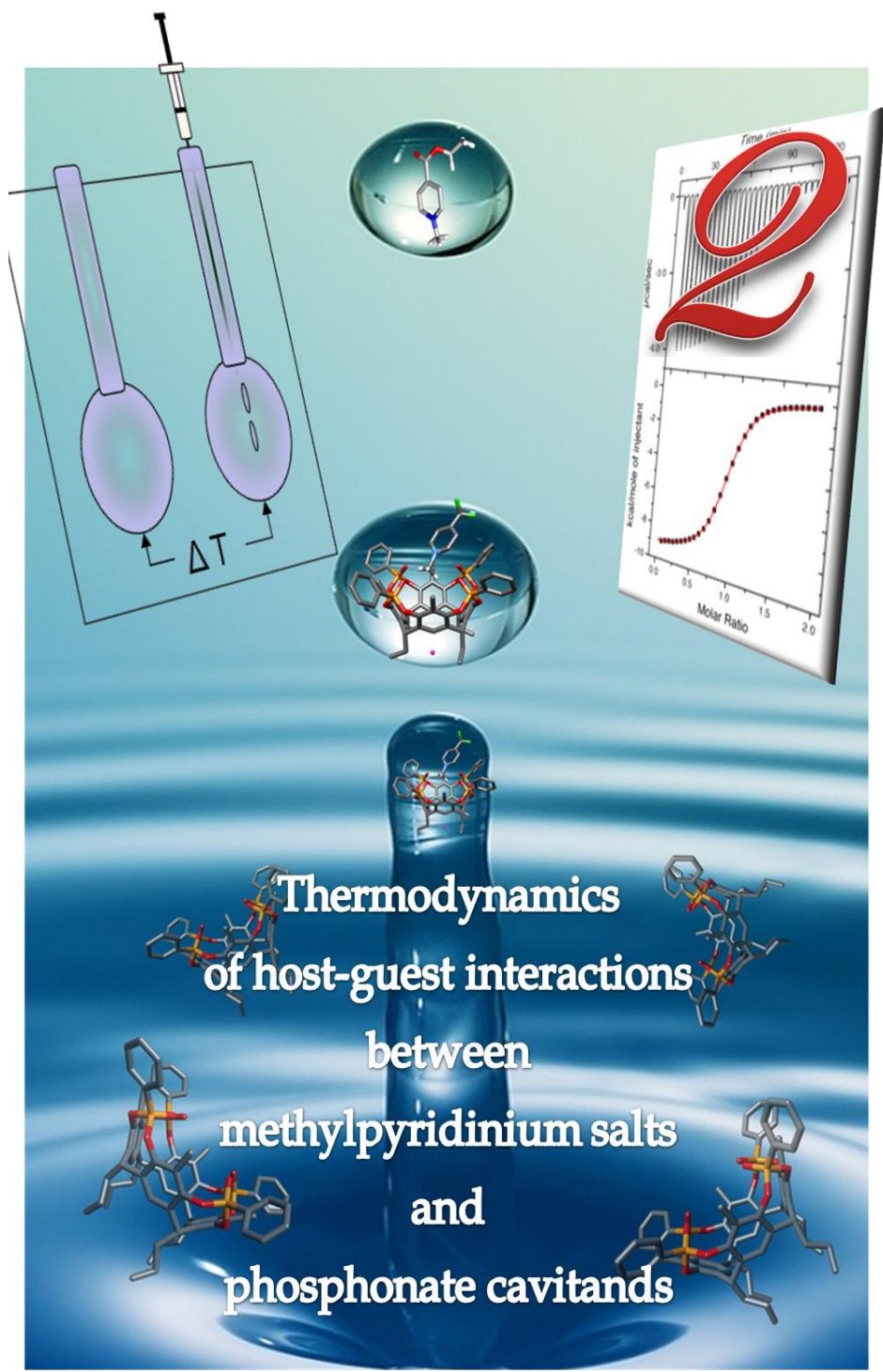
- Paliwal, S.; Wilcox, C. S. *J. Am. Chem. Soc.* **1995**, *120*, 11192-11193; d) Piatnitski, E. L.; Flowers II, R. A.; Deshayes, K. *Chem. Eur. J.* **2000**, *6*, 999-1006; e) Tsuzuki, S. *Annu. Rep. Prog. Chem., Sect. C: Phys. Chem.* **2012**, *108*, 69-95.
- ¹⁴Pinalli, R.; Suman, M.; Dalcanale, E. *Eur. J. Org. Chem.* **2004**, 451-462.
- ¹⁵a) Dietrich, B.; Lehn, J.-M.; Sauvage, J. P. *Tetrahedron Lett.* **1969**, 2885-2888; b) Dietrich, B.; Lehn, J.-M.; Sauvage, J. P.; Blanzat, J. *Tetrahedron* **1973**, *29*, 1629-1645; c) Dietrich, B.; Lehn, J.-M.; Sauvage, J. P.; Blanzat, J. *Tetrahedron* **1973**, *29*, 1647-1658; d) Lehn, J.-M. *Struct. Bonding* **1973**, *16*, 1-69.
- ¹⁶a) Valliyaveettil, S.; Engbersen, J. F.; Verboom, W.; Reinhoudt, D. N. *Angew. Chem. Int. Ed. Engl.* **1993**, *32*, 900-901; b) Beer, P. D.; Gale, P. A.; Heseck, D. *Tetrahedron Lett.* **1995**, *36*, 767-770, c) Eliseev, V.; Schneider, H.-J. *Angew. Chem. Int. Ed.* **1993**, *32*, 1331-1333; d) Manabe, K.; Okamura, K.; Date, T.; Koga, K. *J. Am. Chem. Soc.* **1992**, *114*, 6940-6941.
- ¹⁷a) Breslow, R. *Chem. Soc. Rev.* **1972**, *1*, 553-580.
- ¹⁸a) Mertes, M. P.; Mertes, K. B. *Acc. Chem. Res.* **1990**, *23*, 413-418; b) Hosseini, M. W.; Lehn, J.-M.; Jones, K. C.; Plute, K. E.; Mertes, K. B.; Mertes, M. P. *J. Am. Chem. Soc.* **1989**, *111*, 6330-6335.
- ¹⁹Cram, D. J.; Cram, J. M. in *Container Molecules and Their Guests* (Ed.: Stoddart, J. F.) **1994**, The Royal Society of Chemistry, Cambridge, Chap. 5.
- ²⁰Tunstad, L. M.; Tucker, J. A.; Dalcanale, E.; Weiser, J.; Bryant, J. A.; Sherman, J. C.; Helgeson, R. C.; Knobler, C. B.; Cram, D. J. *J. Org. Chem.* **1989**, *54*, 1305-1312.
- ²¹Delangle, P.; Mulatier, J.-C.; Tinant, B.; Declercq, J.-P.; Dutasta, J.-P. *Eur. J. Org. Chem.* **2001**, 3695-3704; (b) Dutasta, J.-P. *Top. Curr. Chem.* **2004**, *232*, 55-91.
- ²²Dionisio, M.; Oliviero, G.; Menozzi, D.; Federici, S.; Yebeutchou, R. M.; Schmidtchen, F.-P.; Dalcanale, E.; Bergese, P. *J. Am. Chem. Soc.* **2012**, *134*, 2392-2398.

-
- ²³Biavardi, E.; Favazza, M.; Motta, A.; Fragalà, I. L.; Massera, C.; Prodi, L.; Montalti, M.; Melegari, M.; Condorelli, G. C.; Dalcanale, E. *J. Am. Chem. Soc.* **2009**, *131*, 7447-7455.
- ²⁴a) Pinalli, R.; Nachtigall, F. F.; Ugozzoli, F.; Dalcanale, E. *Angew. Chem., Int. Ed.* **1999**, *38*, 2377-2380; b) Melegari, M.; Suman, M.; Pirondini, L.; Moiani, D.; Massera, C.; Ugozzoli, F.; Kalenius, E.; Vainiotalo, P.; Mulatier, J.-C.; Dutasta, J.-P.; Dalcanale, E. *Chem. Eur. J.* **2008**, *14*, 5772-5779.
- ²⁵Yebeutchou, R. M.; Tancini, F.; Demitri, N.; Geremia, S.; Mendichi, R.; Dalcanale, E. *Angew. Chem. Int. Ed.* **2008**, *47*, 4504-4508.
- ²⁶Bibal, B.; Declercq, J.-P.; Dutasta, J.-P.; Tinant, B.; Valade, A. *Tetrahedron* **2003**, *59*, 5849-5854.
- ²⁷Cram, D. J.; Karbach, S.; Kim, H.-E.; Knobler, C. B.; Maverick, E. F.; Ericson, J. L.; Helgeson, R. C. *J. Am. Chem. Soc.* **1988**, *110*, 2229-2237.
- ²⁸a) Tucker, J. A.; Knobler, C. B.; Trueblood, K. N.; Cram, D. J. *J. Am. Chem. Soc.* **1989**, *111*, 3688-3699; b) Soncini, P.; Bonsignore, S.; Dalcanale, E.; Ugozzoli, F. *J. Org. Chem.* **1992**, *57*, 4608-4612; c) Haino, T.; Rudkevich, D. M.; Shivanyuk, A.; Rissanen, K.; Rebek, Jr. *J. Chem. Eur. J.* **2000**, *6*, 3797-3805; d) Paek, K.; Cho, J. *Tetrahedron Lett.* **2001**, *42*, 1927-1929.
- ²⁹(a) Vincenti, M.; Dalcanale, E.; Soncini, P.; Guglielmetti, G. *J. Am. Chem. Soc.* **1990**, *112*, 445-447; (b) Vincenti, M.; Pelizzetti, E.; Dalcanale, E.; Soncini, P. *Pure Appl. Chem.* **1993**, *65*, 1507-1512.
- ³⁰Schmidtchen, F.-P., *Isothermal Titration Calorimetry in Supramolecular Chemistry*, in: *Analytical Methods in Supramolecular Chemistry* (Schalley, C.A. ed.), Wiley-VCH, Weinheim, **2007**, 55-78.
- ³¹For a tutorial review on cantilevers biosensors see: Fritz, J. *Analyst* **2008**, *133*, 855-863.

³²a) Lavrik, N. V.; Sepaniak, M. J.; Datskos, P. G. *Rev. Sci. Instrum.* **2004**, 75, 2229-2253; b) Meyer, G.; Amer, N. M. *Appl. Phys. Lett.* **1988**, 53, 1045-1047.

³³For the complete data treating see: Bergese, P.; Oliviero, G.; Alessandri, I.; Depero, L. E. *Journal of Colloid and Interface Science* **2007**, 316, 1017-1022.

³⁴For selected reviews see: a) Ziegler, C. *Anal. Bioanal. Chem.* **2004**, 379, 946-959; b) Carrascosa, L. G.; Moreno, M.; Alvarez, M.; Lechuga, L. M. *Trends Anal. Chem.* **2006**, 25, 196-206 and the references herein.



**Thermodynamics
of host-guest interactions
between
methylpyridinium salts
and
phosphonate cavitands**

2.1 INTRODUCTION§

General Scenario. Phosphonate cavitands have established themselves as one of the most promising classes of molecular receptors¹ thanks to their diversified complexation properties, spanning from cationic species such as ammonium, methylpyridinium and inorganic salts to neutral guests like alcohols. In particular their complexation prowess toward methylpyridinium salts has been exploited in the generation of functional surfaces^[2,3] and supramolecular polymers.⁴ The key player of the whole class is the tetrakisphosphonate cavitand Tiiii,^[5,6] presenting all four P=O bridging groups oriented inward with respect to the cavity⁷ (see scheme 1). Its peculiar complexation ability is the result of three interaction modes, which can be activated either individually or in combination by the host according to the guest requirements: (i) multiple ion-dipole interactions between the inward facing P=O groups and the positively charged guests;⁸ (ii) single or multiple H-bonding involving the P=O groups;⁹ and (iii) CH₃- π interactions between an acidic methyl group present on the guest and the π -basic cavity of the host.¹⁰ Depending on the type and number of interactions activated, the measured K_{ass} in nonpolar solvents can vary between 10^2 M^{-1} for short chain alcohols to 10^7 M^{-1} for methylpyridinium salts¹¹ and even higher for *N,N*-methylalkylammonium salts.⁴

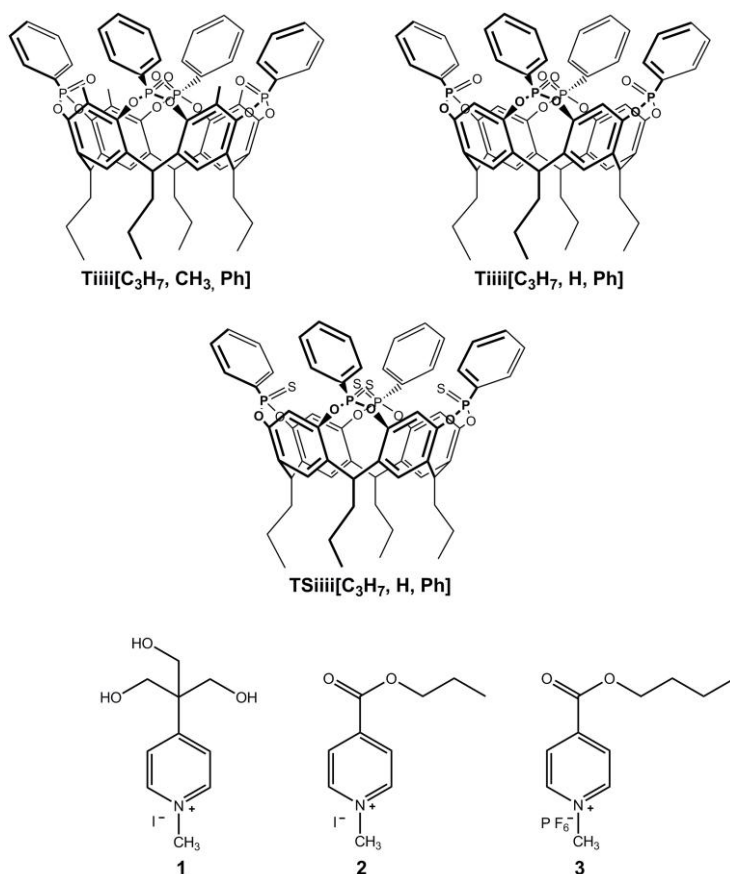
An understanding of the intimate features of the host-guest interactions and their thermodynamic signatures is essential in order to optimize selectivity and strength in guest uptake. In this case ³¹P NMR is a diagnostic tool to assess complexation in solution, due to the presence on the host of four interacting P=O units. However, in the case of methylpyridinium guests, the association constants exceed the upper limit revelation of the NMR ($10 < K_{\text{ass}} < 10^4 \text{ M}^{-1}$). In this situation, Isothermal Titration Calorimetry (ITC) represents the best alternative since it can determine association constants within the range $10^2 < K_{\text{ass}} < 10^7 \text{ M}^{-1}$ ^[12, 13] and it provides directly the thermodynamic parameters in the form of K_{ass} , ΔH , ΔS , ΔG and ΔC_p .

§ This chapter is based on: Menozzi, D.; Biavardi, E.; Massera, C.; Schmidtchen, F.-P.; Cornia, A.; Dalcanale, E. *Supramol. Chem.* **2010**, *22*, 768-775.

This article reports an ITC study of the influence of the following parameters on the complexation properties of the four tetraphosphonate/thiophosphonate cavitands reported in scheme 1 towards methylpyridinium guests: (i) solvation; (ii) nature of the guest counterion; (iii) presence of substituents in the apical positions of the receptor; (iv) P=O versus P=S bridging units.

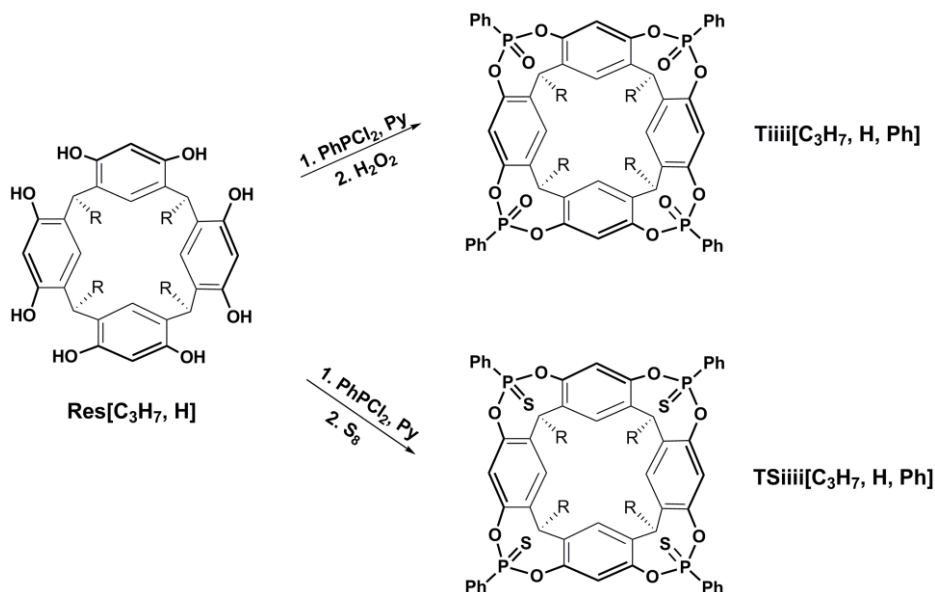
2.2 RESULTS AND DISCUSSION

Cavitands and guests. Compounds used in the present work are showed in scheme 1.



Scheme 1. Cavitand hosts and methylpyridinium guests utilized in the present work.

The preparation of cavitand **Tiiii**[C₃H₇, CH₃, Ph] has been already reported.¹¹ Cavitands **Tiiii**[C₃H₇, H, Ph] and **TSiiii**[C₃H₇, H, Ph] were prepared via a two step procedure. The acid-catalyzed condensation between resorcinol and butyraldehyde led to the propyl-footed resorcinarene **Res**[C₃H₇, H], which was then bridged with dichlorophenylphosphine and oxidized *in situ* either with hydrogen peroxide or S₈ to give **Tiiii**[C₃H₇, H, Ph] and **TSiiii**[C₃H₇, H, Ph] respectively (scheme 2). The methylpyridinium guests **1-3** reported in scheme 1 were all prepared via alkylation of the corresponding pyridine precursors with methyl iodide, followed by anion exchange with NH₄PF₆ in the case of guest **3**.



Scheme 2. Synthesis of **Tiiii**[C₃H₇, H, Ph] and **TSiiii**[C₃H₇, H, Ph] cavitands.

X-Ray structure. The determination of the thermodynamic data from the ITC curves requires the knowledge of the binding stoichiometry of the formed complex. In our case, clear evidence of 1:1 binding was given in the solid state,² and in solution¹¹ for ester derivatives **2-3** with the **Tiiii** hosts. For triol substituted guest **1**, the 1:1 stoichiometry in the solid state is proven by the crystal structure of **Tiiii**[C₃H₇, CH₃, Ph] · (C₁₀H₁₆INO₃) · 5CH₃CN complex (figure 1). The presence of the four apical methyl substituents does not change stoichiometry and complexation mode with respect to the parent **Tiiii**[C₂H₅, H, Ph] cavitand.²

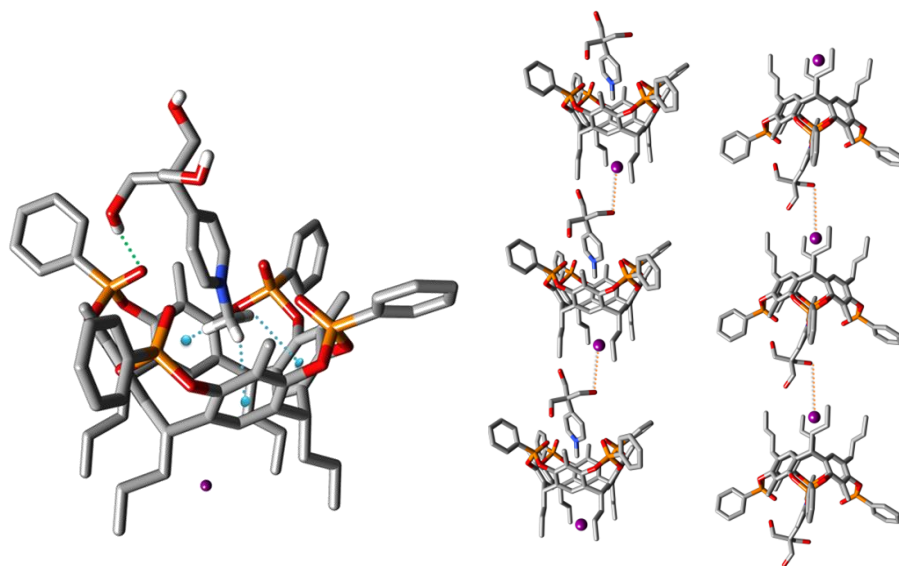


Figure 1. Crystal structure (left) and crystal packing (right) of $\text{Ti}^{\text{III}}[\text{C}_3\text{H}_7, \text{CH}_3, \text{Ph}] (\text{C}_{10}\text{H}_{16}\text{INO}_3) \cdot 5\text{CH}_3\text{CN}$ complex. Color code: I, purple; P, orange; O, red; C, grey; H, white. H-bonding, green line; $\text{CH}_3\text{-}\pi$ interactions, blue line. Hydrogen atoms, except for the triol, and acetonitrile solvent molecules are omitted for clarity.

The reported crystal structure evidences the different synergistic interactions between the tetraphosphonate cavitand $\text{Ti}^{\text{III}}[\text{C}_3\text{H}_7, \text{CH}_3, \text{Ph}]$ and guest **1** (see figure 1 left). The inclusion of **1** in the cavity is driven by dipolar interactions between the positively charged nitrogen atom and two P=O groups at the upper rim of the cavitand ($\text{P}=\text{O} \cdots \text{N}^+$: 3.056(3) and 3.116(3) Å). One of these P=O moieties is also involved in a hydrogen bond with a OH group of the guest ($\text{O} \cdots \text{O}=\text{P}$ 2.992(4) Å, $\text{O}-\text{H} \cdots \text{O}=\text{P}$ 170.4(2)°). Further stabilization is provided by three $\text{C}-\text{H} \cdots \pi$ interactions between the methyl hydrogens of the cation and three aromatic rings of the cavity (the $\text{C}-\text{H} \cdots$ centroid distances are of 2.667(4), 2.828(3) and 3.129(2) Å, with angles of 126.44 (3), 136.15(2) and 166.64(1)°, respectively). The iodide counterion is located below the cavity at 1.808(2) Å from the least-square plane defined by the four CH_2 carbons, roughly in the middle of the four alkyl chains at the lower rim. This position is stabilized by four $\text{C}-\text{H} \cdots \text{I}$ interactions with the first CH_2 groups of the chains, which range in length from 2.9985(5) to 3.1674(5) Å. The iodide ion also forms two hydrogen bonds (one stronger and one weaker) with two OH groups of the guest of a neighboring complex ($\text{O} \cdots \text{I}$ 3.392(2) and 3.563(4) Å; $\text{O}-\text{H} \cdots \text{I}$ 166.8(1)

and 165.9(2) °, respectively). This influences the crystal packing which shows a typical columnar disposition along the *a* axis of the unit cell (see figure 1 right). The distance between I⁻ and the positive nitrogen of the guest is of 7.679(3) Å. All the above values are in good agreement with similar complexes reported in the literature.^[2, 14]

ITC measurements. The first set of ITC measurements was made to assess the solvent effect on the complexation. For this purpose dichloroethane (DCE) and methanol were chosen. The first one does not compete for the cavity due to its size and its low propensity to form hydrogen bonds with the P=O units of the cavitand. Vice versa, in the case of methanol, crystal structures showed its inclusion in the cavity of Tiiii receptor,¹⁰ driven by the synergistic action of H-bonding with the phosphonates and CH₃-π interactions with the cavity. The different affinity of the two solvents for the cavity is clearly reflected in the complexation of guests **2** and **3** by Tiiii[C₃H₇, CH₃, Ph]. A decrease of the association constant of two orders of magnitude was determined for both guests by moving from DCE to MeOH (table 1, entries I and II). In both cases the reduced affinity in MeOH is mainly enthalpic in origin, with the ΔH reduction attributable to the solvent competition for the cavity and the electrostatic stabilization of the cationic guest by the more polar solvent. Interestingly, the counterion does not influence complexation, leading to comparable values of ΔG and K_{ass}. Such unexpected silence in impact may be attributed to the preferential positioning of both iodide and PF₆⁻ within the alkyl chains, as was proven in NMR studies in chloroform.¹⁴ Yet, the absence of evidence of a role for the counterions in the binding process can also arise from an adventitious cancellation of enthalpic and entropic effects of complexation at the less structured, well solvated and solvent-like site of the host compound.

Entry	Host	Guest	Solvent	$K_{AS} \pm \delta K_{AS}$ (M^{-1})	$\Delta H \pm \delta H$ ($KJ \cdot mol^{-1}$)	$\Delta G \pm \delta G$ ($KJ \cdot mol^{-1}$)	$T\Delta S \pm T\delta S$ ($KJ \cdot mol^{-1}$)
I	 Tiiii[C ₃ H ₅ , CH ₃ , Ph]	 2	MeOH	$3.4 \pm 0.3 \cdot 10^4$	-17.2 ± 0.3	-26.3 ± 0.3	9.1 ± 0.1
			DCE	$5.8 \pm 0.6 \cdot 10^6$	-25.7 ± 0.2	-39.2 ± 1.4	13.5 ± 2.4
II	 Tiiii[C ₃ H ₇ , CH ₃ , Ph]	 3	MeOH	$3.9 \pm 0.1 \cdot 10^4$	-11.3 ± 0.1	-26.7 ± 0.1	15.4 ± 0.1
			DCE	$3.1 \pm 0.3 \cdot 10^6$	-20.9 ± 0.1	-37.7 ± 0.1	16.8 ± 0.2
III	 Tiiii[C ₃ H ₇ , H, Ph]	 2	DCE	$2.8 \pm 0.4 \cdot 10^5$	-8.2 ± 0.2	-31.6 ± 0.1	23.4 ± 0.2
IV	 Tiiii[C ₃ H ₇ , H, Ph]	 3	DCE	$1.3 \pm 0.4 \cdot 10^5$	-6.8 ± 0.2	-29.7 ± 2.1	22.9 ± 3.9
V	 TSiiii[C ₃ H ₇ , H, Ph]	 2	DCE	NO INTERACTION DETECTABLE			
VI	 TSiiii[C ₃ H ₇ , H, Ph]	 3	DCE	NO INTERACTION DETECTABLE			

Table 1. Results of ITC titrations of Tiiii[C₃H₇, CH₃, Ph], Tiiii[C₃H₇, H, Ph] and TSiiii[C₃H₇, H, Ph] with 2 and 3 in DCE and in CH₃OH at 303 K.

Next, the role of the cavity structure on complexation was investigated. The presence of four methyl groups in the apical positions of **Tiiii**[C₃H₇, CH₃, Ph] deepens the cavity and enhances its π -basic character. Their removal should reduce the complexation efficiency of the receptor. Experimentally, a decrease of the K_{ass} of one order of magnitude was observed for the titration of methyl depleted cavitand **Tiiii**[C₃H₇, H, Ph] with guests **2** and **3** in DCE, as compared to the original ones (table 1, compare entry **I** with entry **III** and entry **II** with entry **IV**).

A large enthalpic drop was determined, only partially compensated by an entropic gain. This is ascribed to the reduced contribution of CH₃- π interactions¹⁵ to the overall binding and to the enhanced solvation of the more open cavity of the de-methylated host **Tiiii**[C₃H₇, H, Ph]. The latter origin is also suggested by the entropic outcome which testifies to more dramatic cavity desolvation and guest mobility in the case of **Tiiii**[C₃H₇, H, Ph] upon binding, while the guest desolvation is comparable in the two cases. It is worth noting that the methylpyridinium binding remains both enthalpy and entropy driven. As shown in table 1 (entries **III** and **IV**), the thermodynamic parameters of **Tiiii**[C₃H₇, H, Ph] complexation in DCE are not influenced by the counterions, confirming the results reported for the parent **Tiiii**[C₃H₇, CH₃, Ph].

In order to probe the contribution of cation-dipole interactions on the overall binding, tetrathiophosphonate cavitand **TSiiii**[C₃H₇, H, Ph] was prepared (scheme 2). It is structurally identical to the corresponding tetraphosphonate **Tiiii**[C₃H₇, H, Ph], except for the presence of four inward facing P=S instead of four P=O. The P=S group is more polarizable than the P=O counterpart, but it has a much smaller dipole moment.¹⁶ Its larger size does not preclude the insertion of methyl groups into the cavity,¹⁷ therefore the introduction of four P=S bridges has little influence on CH- π interactions. As a corollary, this substitution should decrease substantially the cation-dipole interactions with the charged methylpyridinium guests. The ITC results were beyond our expectations: the affinity of the cavitand for guests **2** and **3** was completely shut off (table 1, entries **V** and **VI**). Therefore, the cation-dipole interactions are indispensable for binding methylpyridinium guests. Without P=O, the complexation is negligible, well below the detection limit of ITC.

2.3 CONCLUSIONS

The selective complexation of methylpyridinium salts by tetraphosphonate cavitands relies on two interactions, namely cation-dipole and CH₃- π interactions, which operate synergically.

The crystal structure of the reported complex clearly evidences this synergy in the solid state.

Using ITC, the thermodynamic profile in the formation of several host-guest complexes was determined. They all are driven both by enthalpy and entropy,^[18, 19] reflecting for the importance and substantial participation of solvent interactions for the binding process. The relative weights of the two direct mutual interaction modes have been dissected by changing two structural parameters on the cavitands. The dominant role of cation-dipole interactions was revealed by substituting the P=O bridges with the P=S ones, which completely suppressed complexation. The relevance of CH- π interactions was highlighted by the removal of the four methyl groups in the cavity apical positions, which led to the decrease of one order of magnitude in the K_{ass} of both **2** and **3**.

On the guest side, the counterion does not play a significant role in complexation, which can be due to an adventitious cancellation of effects, but may also emerge from the basic lack of binding.

The solvent instead affects the binding significantly, particularly when the solvent competes with the guest for the cavity space, like in the case of methanol.

Acknowledgements

We thank the German-Italian exchange Program (Vigoni Program) for financial support.

2.4 EXPERIMENTAL SECTION

General Methods. All commercial reagents were ACS reagent grade and used as received, except for 4-picoline which was purified by fractional distillation before use. Solvents were dried and distilled using standard procedures. ^1H NMR and spectra were recorded on Bruker Avance 300 (300 MHz) and on a Bruker FT-DPX b 200 NMR spectrometers. All chemical shifts (δ) were reported in parts per million (ppm) relative to proton resonances resulting from incomplete deuteration of NMR solvents. ^{31}P NMR spectra were recorded on AMX-400 (162 MHz) and all chemical shifts were reported to external 85% H_3PO_3 at 0 ppm. Electrospray ionization mass spectrometry (ESI-MS) experiments were performed on a Waters ACQUILITY UPLC SQ Detector. ITC measurements were performed with a fully computer-operated MicroCal ITC-MCS instrument at 303 K by adding 2-10 μL aliquots of the guest solution into the thermostated solution of the host compound present in about 10fold lower concentration in the calorimetric cell (1.35 mL).

To obtain a good quality data output it is essential to choose the best experimental conditions. One adjustable parameter that needs optimal setting is the c parameter:

$$c = n \times [A]K_{\text{ass}}$$

Where n is the stoichiometric factor, $[A]$ is the concentration of the titrate compound in the cell (M) and K_{ass} is the affinity constant (M^{-1}). In order to obtain a sigmoidal output curve from which the K_{ass} , the stoichiometric factor n and the ΔH are derived, the c parameter should be set within the range 5-500. Adjusting the titrate concentration is the key factor to reach a good shaped curve.

Cavitand **Tiiii** [C_3H_7 , CH_3 , Ph],¹¹ resorcinarene **Res** [C_3H_7 , H]²⁰ and guests **2**³ and **3**¹¹ were prepared following a published procedure.

Synthesis.

Cavitand **Tiiii** [C_3H_7 , H , Ph].

To a solution of resorcinarene **Res** [C_3H_7 , H] (517 mg, 0.80 mmol) in freshly distilled pyridine (20 mL), dichlorophenylphosphine (0.447 mL, 3.39 mmol) was added slowly, at room temperature. After 3 hours of stirring at 80°C, the solution was allowed to cool to room temperature and 8 mL of a mixture of 35%

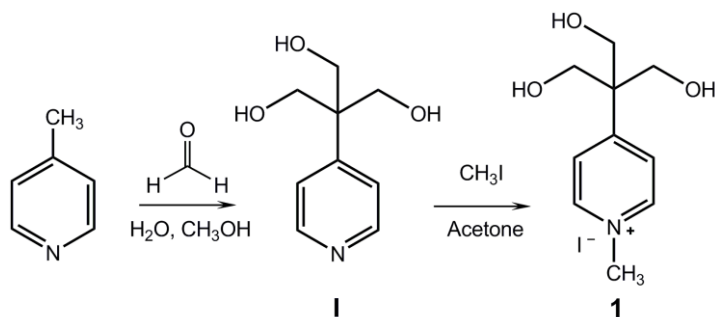
H₂O₂ and CHCl₃ (1:1) was added. The resulting mixture was stirred for 30 minutes at room temperature, then the solvent was removed under reduced pressure and water was added. The precipitate obtained in this way was collected by vacuum filtration, and purified by re-crystallization (H₂O:CH₃CN 8:2). The product is a fine white powder (870 mg, 95%).

¹H NMR (300 MHz, CDCl₃): δ (ppm) 8.09 (m, 8H, POArH_o), 7.61 (m, 4H, POArH_p), 7.52 (m, 8H, POArH_m), 7.13 (s, 4H, ArH_{down}), 6.51 (s, 4H, ArH_{up}), 4.81 (t, 4H, J = 7.4 Hz, ArCH), 2.34-2.20 (m, 8H, CH₂CH₂CH₃), 1.41 (m, 8H, CH₂CH₂CH₃), 1.04 (t, 12H, J = 7.4 Hz, CH₂CH₂CH₃). ³¹P NMR (162 MHz, CDCl₃) δ (ppm): 4.02 (s, 4P). ESI-MS: m/z 1167.3 [M+Na]⁺.

Cavitand TSiiii[C₃H₇, H, Ph].

To a solution of resorcinarene Res[C₃H₇, H] (2.26 g, 3.5 mmol) dissolved in 20 mL of freshly distilled pyridine, dichlorophenylphosphine (1.93 mL, 14.3 mmol) was slowly added at room temperature. The mixture was stirred for 3h at 80°C then cooled to room temperature. S₈ (0.72g, 2.81 mmol) was added and left stirring for 1h at 50°C. The solvent was removed in vacuum followed by addition of 50 mL of water and the yellow suspension was filtered. Purification by column chromatography on silica gel with CH₂Cl₂/hexane (9/1 v/v) yielded the product (2.62 g, 62%).

¹H NMR (300 MHz, CDCl₃): δ (ppm) 8.19 (m, 8H, POArH_o); 7.60 (m, 4H, POArH_p); 7.51 (m, 8H, POArH_m); 7.21 (s, 4H, ArH_{down}); 6.50 (s, 4H, ArH_{up}); 4.72 (t, 4H, J=7.8 Hz, ArCH); 2.31 (m, 8H, CH₂CH₂CH₃); 1.40 (m, 8H, CH₂CH₂CH₃); 1.02 (t, 12H, J=7.2 Hz, CH₂CH₂CH₃). ³¹P NMR (172 MHz, CDCl₃): δ (ppm) 72(s, 4P). ESI-MS: m/z: 1231.3 [M+Na]⁺.



Scheme 3. Synthesis of guest 1.

2-(Hydroxymethyl)-2-(pyridin-4-yl)-1,3-propanediol (I).

The following procedure (scheme 3) improves the method proposed by Koenigs and Happe.²¹ 4-Picoline (2.00 g, 21.5 mmol) was refluxed in 37% aqueous formaldehyde (27 mL, 360 mmol) for 24 h. The solvent and excess formaldehyde were removed under reduced pressure at 50°C. Methanol (50 mL) was added to the residue and removed under vacuum at 50°C and the procedure was repeated. The crude product was subject to prolonged vacuum pumping (1 mmHg, 3 hours) and purified by column chromatography (CH₂Cl₂/CH₃OH 8/2 v/v) to afford the desired compound as a white crystalline solid (2.25 g, 57%).

¹H-NMR (200 MHz, CD₃OD): δ (ppm) 8.45 (m, 2H, **aromatic**), 7.54 (m, 2H, **aromatic**), 3.93 (s, 6H, CH₂OH).

4-[1,3-Dihydroxy-2-(hydroxymethyl)propan-2-yl]-1-methylpyridinium iodide (1).

Compound I (0.100 g, 0.546 mmol) was suspended in acetone (3 mL) and MeI (50 μL, 0.80 mmol) was added. The mixture was stirred overnight at 40-45°C in a closed glass tube, cooled down to room temperature and concentrated. The off-white solid so obtained was separated by filtration and dried under vacuum (163 mg, 92%).

¹H-NMR (200 MHz, CD₃OD): δ (ppm) 8.80 (m, 2H, **aromatic**), 8.23 (m, 2H, **aromatic**), 4.38 (s, 3H, CH₃), 3.97 (s, 6H, CH₂OH).

Crystal structure determination of the Tiii[C₃H₇, CH₃, Ph] (C₁₀H₁₆INO₃) 5CH₃CN complex

The molecular structure of the inclusion compound Tiii[C₃H₇, CH₃, Ph] (C₁₀H₁₆INO₃) 5CH₃CN was determined by single-crystal X-ray diffraction methods.

Crystallographic and experimental details are summarized in table 2.

Intensity data and cell parameters were recorded at 173 K on a Bruker AXS Smart 1000 single-crystal diffractometer (employing a MoK_α radiation and a CCD area detector).

The raw frame data were processed using SAINT and SADABS to yield the reflection data file.²²

The structure was solved by Direct Methods using the SIR97 program²³ and refined on F_o^2 by full-matrix least-squares procedures, using the SHELXL-97 program.²⁴

The PLATON SQUEEZE procedure²⁵ was used to treat regions of diffuse solvent which could not be sensibly modeled in terms of atomic sites. Their contribution to the diffraction pattern was removed and modified F_o^2 written to a new HKL file.

The 275 electrons per unit cell thus located are included in the formula, formula weight, calculated density, μ and F(000). This residual electron density was assigned to twelve molecules of acetonitrile per unit cell.

All non-hydrogen atoms were refined with anisotropic atomic displacements with the exception of one acetonitrile molecule. The hydrogen atoms were included in the refinement at idealized geometry (C-H 0.95 Å) and refined "riding" on the corresponding parent atoms.

<i>Tiii</i> [C ₃ H ₇ , CH ₃ , Ph] (C ₁₀ H ₁₆ INO ₃) • 5CH ₃ CN	
Formula	C ₈₈ H ₉₉ IN ₆ O ₁₅ P ₄
Formula weight	1731.51
Crystal system	Monoclinic
Space group	<i>P</i> 21/ <i>c</i>
<i>a</i> /Å	15.479(3)
<i>b</i> /Å	37.943(6)
<i>c</i> /Å	16.352(3)
β /°	113.988(2)
<i>V</i> /Å ³	8775(2)
<i>Z</i>	4
<i>D_c</i> /g cm ⁻³	1.311
<i>F</i> (000)	3608
μ /mm ⁻¹	0.504
$\theta_{\min, \max}$ /°	1.07, 28.56
Reflections collected	71985
Independent reflections	19711 (<i>R</i> _{int} = 0.0384)
Obs. refl. [<i>I</i> > 2 σ (<i>I</i>)]	13715
Data / restr. / param	19711 / 0 / 950
R indices [<i>I</i> > 2 σ (<i>I</i>)] ^a	<i>R</i> ₁ = 0.0484, <i>wR</i> ₂ = 0.1296
R indices (all data)	<i>R</i> ₁ = 0.075, <i>wR</i> ₂ = 0.1420
$\Delta\rho_{\min, \max}$ /e Å ⁻³	-1.097, 0.827
<i>S</i> ^b	1.002

^a*R*₁ = $\Sigma ||F_o| - |F_c|| / \Sigma |F_o|$, *wR*₂ = $[\Sigma w(F_o^2 - F_c^2)^2 / \Sigma wF_o^4]^{1/2}$. ^bGoodness-of-fit *S* = $[\Sigma w(F_o^2 - F_c^2)^2 / (n - p)]^{1/2}$, where *n* is the number of reflections and *p* the number of parameters.

Table 2. Crystallographic data and refinement details for compound *Tiii*[C₃H₇, CH₃, Ph] • (C₁₀H₁₆INO₃) • 5CH₃CN.

The weighting schemes used in the last cycle of refinement was $w = 1/[\sigma^2 F_o^2 + (0.0848P)^2 + 1.4464P]$, where $P = (F_o^2 + 2F_c^2)/3$. Molecular geometry calculations were carried out using the PARST97 program.²⁶

Drawings were obtained using ORTEP3 in the WinGX suite²⁷ and Mercury.²⁸

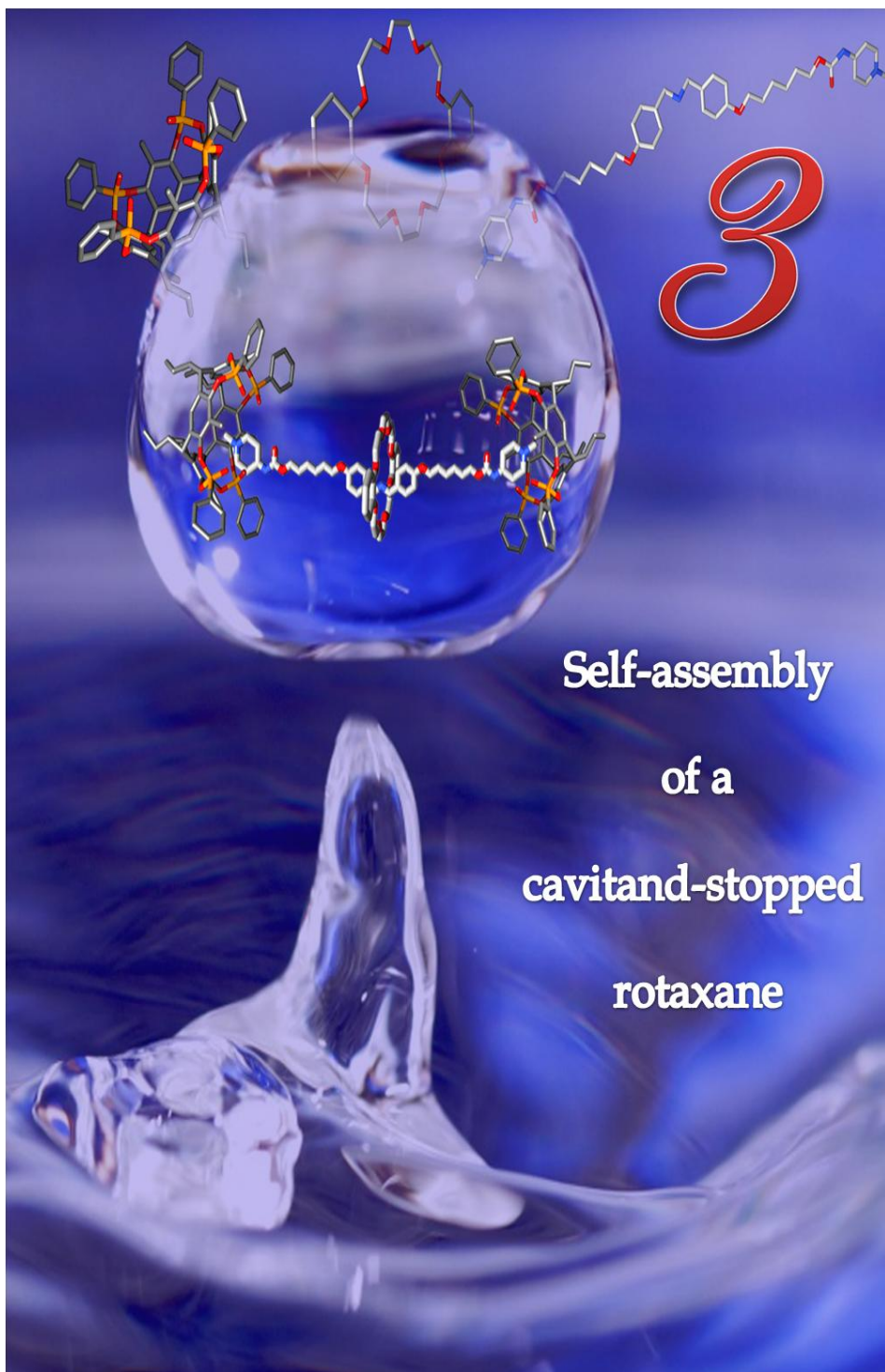
Crystallographic data (excluding structure factors) for the structure reported have been deposited with the Cambridge Crystallographic Data Center as supplementary publication no. CCDC-777331 and can be obtained free of charge on application to the CCDC, 12 Union Road, Cambridge CB2 1EZ, U.K. [Fax: (internat.) + 44-1223/336-033; E-mail: deposit@ccdc.cam.ac.uk]

2.5 REFERENCES

- ¹ Dutasta, J.-P. *Top. Curr. Chem.* **2004**, 232, 55-91.
- ² Biavardi, E.; Favazza, M.; Motta, A.; Fragalà, I. L.; Massera, C.; Prodi, L.; Montalti, M.; Melegari, M.; Condorelli, G. G.; Dalcanale, E. *J. Am. Chem. Soc.* **2009**, 131, 7447-7455.
- ³ Tancini, F.; Genovese, D.; Montalti, M.; Cristofolini, L.; Nasi, L.; Prodi, L.; Dalcanale, E. *J. Am. Chem. Soc.* **2010**, 132, 4781-4789.
- ⁴ Yebeutchou, R. M.; Tancini, F.; Demitri, N.; Geremia, S.; Mendichi, R.; Dalcanale, E. *Angew. Chem. Int. Ed.* **2008**, 47, 4504-4508.
- ⁵ Lippmann, T.; Mann, G.; Dalcanale, E. *Tetrahedron Lett.* **1994**, 35, 1685-1688.
- ⁶ Delangle, P.; Dutasta, J.-P. *Tetrahedron Lett.* **1995**, 36, 9325-9328.
- ⁷ For the nomenclature adopted for phosphonate cavitands see Pinalli, R.; Suman, M.; Dalcanale, E. *Eur. J. Org. Chem.* **2004**, 451-462.
- ⁸ Delangle, P.; Mulatier, J.-C.; Tinant, B.; Declercq, J.-P.; Dutasta, J.-P. *Eur. J. Org. Chem.* **2001**, 66, 3695-3704.
- ⁹ Kalenius, E.; Moiani, D.; Dalcanale, E.; Vainiotalo, P. *Chem. Commun.* **2007**, 3865-3867.
- ¹⁰ Melegari, M.; Suman, M.; Pirondini, L.; Moiani, D.; Massera, C.; Ugozzoli, F.; Kalenius, E.; Vainiotalo, P.; Mulatier, J.-C.; Dutasta, J.-P.; Dalcanale, E. *Chem. Eur. J.* **2008**, 14, 5772-5779.
- ¹¹ Biavardi, E.; Battistini, G.; Montalti, M.; Yebeutchou, R. M.; Prodi, L.; Dalcanale, E. *Chem. Commun.* **2008**, 1638-1640.
- ¹² Sessler, J.L.; Gross, D.E.; Cho, W.-S.; Lynch, V. M.; Schmidtchen, F.-P.; Bates, G. W.; Light, M. E.; Gale, P.A. *J. Am. Chem. Soc.* **2006**, 128, 12281-12288.

- ¹³Schmidtchen, F.-P. in *Analytical Methods in Supramolecular Chemistry*; Shalley, C. A., Ed. WILEY-VCH; Verlag GmbH & Co. KGaA, Weinheim, Germany, **2007**, 55-78.
- ¹⁴De Zorzi, R.; Dubessy, B.; Mulatier, J.-C.; Geremia, S.; Randaccio, L.; Dutasta, J.-P. *J. Org. Chem.* **2007**, *72*, 4528-4531.
- ¹⁵For selected references of CH- π interactions see: (a) Nishio, M.; Hirota, M.; Umezawa, Y. *The CH- π Interactions*, Wiley-VCH, New York, **1998**; (b) Dougherty, D. A.; Stauffer, D. A. *Science* **1990**, *250*, 1558-1560; (c) Kim, E.-I.; Paliwal, S.; Wilcox, C. S. *J. Am. Chem. Soc.* **1995**, *120*, 11192-11193; (d) Piatnitski, E. L.; Flowers II, R. A.; Deshayes, K. *Chem. Eur. J.* **2000**, *6*, 999-1006.
- ¹⁶Hawkins, N. J.; Cohen, V. W. *J. Chem. Phys.* **1952**, *20*, 528.
- ¹⁷The crystal structure of **TSiii[C₃H₇, H, Ph]•CH₃CN** with acetonitrile included in the cavity has been determined (Geremia, S.; Melegari, M.; Dalcanale, E. unpublished results).
- ¹⁸Moghaddam, S.; Inoue, Y.; Gilson, M. K. *J. Am. Chem. Soc.* **2009**, *131*, 4012-4021.
- ¹⁹Schmidtchen, F.-P. *Coord. Chem. Rev.* **2006**, *250*, 2918-2928.
- ²⁰Tunstad, L. M.; Tucker, J. A.; Dalcanale, E.; Weiser, J.; Bryant, J. A.; Sherman, J. C.; Hegelson, R. C.; Knobler, C. B.; Cram, D. J. *J. Org. Chem.* **1989**, *54*, 1305-1312.
- ²¹Koenigs, W.; Happe, G. *Ber. Dtsch. Chem. Ges.* **1903**, *36*, 2904-2912.
- ²²SADABS Bruker AXS; Madison, Wisconsin, USA, **2004**; SAINT, Software Users Guide, Version 6.0; Bruker Analytical X-ray Systems. In Software Users Guide, Version 6.0; Bruker Analytical X-ray Systems, Madison, WI, **1999**. Sheldrick, G. M.; SADABS v2.03: Area-Detector Absorption Correction. University of Göttingen, Germany, **1999**.

- ²³Altomare, A.; Burla, M. C.; Camalli, M.; Cascarano, G. L.; Giacovazzo, C.; Guagliardi, A.; Moliterni, A. G. G.; Polidori, G.; Spagna, R. *J. Appl. Crystallogr.* **1999**, *32*, 115-119.
- ²⁴Sheldrick, G. M.; *SHELXL97. Program for Crystal Structure Refinement*, University of Göttingen: Göttingen, Germany, **1997**; Sheldrick, G. M. *Acta Cryst.* **2008**, *A64*, 112-122.
- ²⁵SQUEEZE-v.d Sluis P., Spek A. L. *Acta Crystallogr., Sect A* **1990**, *46*, 194-201.
- ²⁶PARST-(a) Nardelli, M. *Comput. Chem.*, 1983, **7**, 95-97; (b) Nardelli, M. *J. Appl. Crystallogr.* **1996**, *29*, 296-300.
- ²⁷ORTEP3 for Windows-Farrugia, L. J. *J. Appl. Crystallogr.* **1997**, *30*, 565-566.
- ²⁸Mercury CSD 2.2 (Build RC5).



3.1 INTRODUCTION

Top-down versus bottom-up approach. Novel devices and machines have always come along with the human progress. Depending on their aim, these machines can be "big" or "small". The trend of the last decades, especially in the field of information technology, is to reach the smallest miniaturization possible in order to confer more handiness, more portability and to store more information. Two possible approaches can be used:

- ∅ *top-down*; it consists in the manipulation of smaller and smaller pieces of matter. Despite the presence of semiconductor devices of 65 nm on the market¹ and reports of even 45 nm devices,² this method has its own limitations due to physical and engineering limits and cost escalation once the nanometer dimension has been reached.
- ∅ *Bottom-up*; chemistry plays the pivotal role in this approach, translating the notion of macroscopic machine to the molecular level. This method provides the assembly of atoms and/or molecules in order to build nanostructures.

Bottom-up approach: atoms or molecules? In the late seventies supramolecular chemistry (see chapter 1 for more details on supramolecular chemistry and its birth) started to answer to this question. Molecules are more suitable building blocks than atoms for the construction of nanostructures, the reasons are listed below:

- ∅ molecules are stable, atoms are more difficult to handle;
- ∅ nature itself uses molecules and not atoms to construct devices that are the foundation of life;³
- ∅ chemical processes deal largely with molecules, not atoms;
- ∅ molecules are characterized by shapes and properties like manipulation with electrochemical inputs, opposite of atoms;
- ∅ molecules can self-assemble to reach larger structures.⁴

It was Richard Feynman,⁵ in December of 1959, that used for the first time the terms "bottom-up approach" in his historic lecture "*There is Plenty of Room at the Bottom*" to the American Physical Society, but it was just in the early 1980's that the first examples of molecular machines based on photoisomerization of azobenzene were reported.⁶ In the last three decades the interest on this approach has arisen due to several breakthroughs in the scientific field, comprising: the rapid development in probe microscopies (that followed the

Nobel Prize in Physics to Binnig and Rohrer in 1986),⁷ the flourishing interest in the supramolecular field (after the Nobel Prize given to Pedersen, Cram and Lehn in 1987),⁸ the clarification and the understanding of the working mechanism of some key biological devices and machines,⁹ the advances in comprising the mechanism of homogeneous and heterogeneous thermal and photoinduced electron transfer reactions,¹⁰ and finally the realization that the physical top-down approach had its own intrinsic limitations and it could be replaced by the more efficient chemical bottom-up approach.¹¹

One of the aim of supramolecular chemistry is to create organized molecular-scale devices which are able to interpret, store and process information like the corresponding macroscopic devices. In particular, creation of the so-called rotaxane¹² was achieved using supramolecular synthesis under thermodynamic control, while for the construction of structure like catenane¹² (as well as rotaxane) under kinetic and thermodynamic control,¹³ supramolecular assistance to molecular synthesis was needed.

Synthetic supramolecular chemistry¹⁴ for the construction of these type of structure has relied mostly both on self-assembly in its strict sense and with its covalent modifications.¹⁵

Catenanes, rotaxanes, pseudorotaxanes. Attention on interlocked molecular species⁴ has grown in the last decades since interesting applications in topology and nanotechnology have been reported.¹⁶ In this chapter the attention will be focused on three different types of molecular machines, namely catenanes, rotaxanes and pseudorotaxanes (see figure 1 for the generic structures).

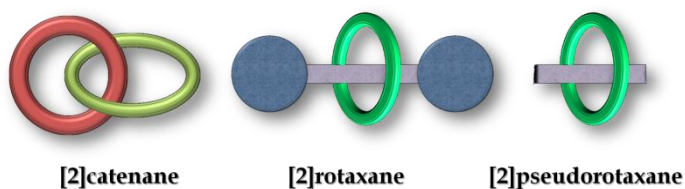


Figure 1. *Generic representation of three classes of molecular machines: catenanes, rotaxanes and pseudorotaxanes. The number comprised in the square brackets corresponds to the number of components that take part in the construction of the supramolecular structure.*

A [2]catenane¹² is a molecule composed of two interlocked macrocyclic components that are not covalently linked one to the other but is rather the presence of a mechanical bond that holds them together preventing their dissociation. When one of the two macrorings bears two different recognition sites then there is the possibility to control the dynamic process involving the two interlocked components. In figure 2 the working principle of a [2]catenane is explained.¹⁷ The catenane contains two interlocked macrocycles: both contain a phenantroline unit, but just one of them contains a terpyridine unit. Changing the oxidation state of the central metal ion causes a change in the coordination geometry preferences of the copper ion: Cu^{I} prefers a tetracoordination geometry therefore it interacts preferentially with the two phenantroline moieties, while Cu^{II} prefers a pentacoordination geometry and it forces the circumrotation of one of the macrocycle until the terpyridine moiety is exposed to the metal ion.

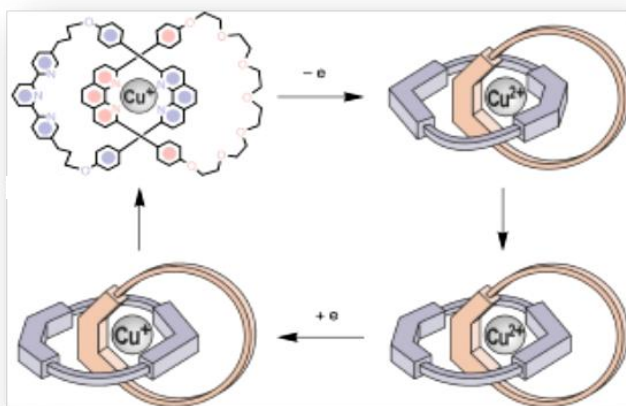


Figure 2. Circumrotation of the terpyridine containing macrocycle can be controlled by oxidizing/reducing the central metal. The change in its oxidation state changes the preferred coordination geometry.

A [2]rotaxane¹² is a molecule composed of a macrocycle that encircles a dumbbell-shaped component. Dethreading of the macrocycle from the axle is prevented by the presence of two bulky groups at both ends of the axle. Therefore the two components cannot dissociate from one another even if they are not linked covalently together.

Presence of two identical recognition sites on the axle results in a degenerate co-conformational equilibrium state in which the ring can shuttle back and forth from one site to another, creating what is called a molecular shuttle.¹⁸ In the case in which those two sites are not identical, the rotaxane can exist in two different co-conformations. These two states are distinctly populated depending on the relative free energies related to the strengths of the two different sets of non-covalent interactions. By switching on and off the non-covalent interactions present between the ring and the axle results in a reversible control of the relative population of the two states. In figure 3 a sophisticated example of the latter situation is described.¹⁹

The rotaxane is formed by a trifurcated guest containing two different recognition sites, a dialkylammonium ion ($\text{CH}_2\text{NH}_2^+\text{CH}_2$) and a bipyridinium dication (BIPY^{2+}), and a tritopic host that consists of a tris-crown ether derivative. In the guest protonated form, the dibenzo[24]crown-8 (DB24C8) resides exclusively around the $^+\text{NH}_2$ centre because of the combination of strong $[\text{N-H}\cdots\text{O}]$ hydrogen bonding and weak $[\text{C-H}\cdots\text{O}]$ interactions, helped by some stabilizing π - π stacking between host and guest. Addition of a base results in the deprotonation of the ammonium moiety with removal of the hydrogen bonding, promoting the shuttling of the trifurcated host from the first recognition site to the BIPY^{2+} as a consequence of Brownian motion.²⁰ The system can be restored by adding acid in order to reprotonate the ammonium groups and force the crown ethers to shuttle back to the original position guided by the hydrogen bonding. Nanoelevators are an example of rotaxane-based molecular shuttles.

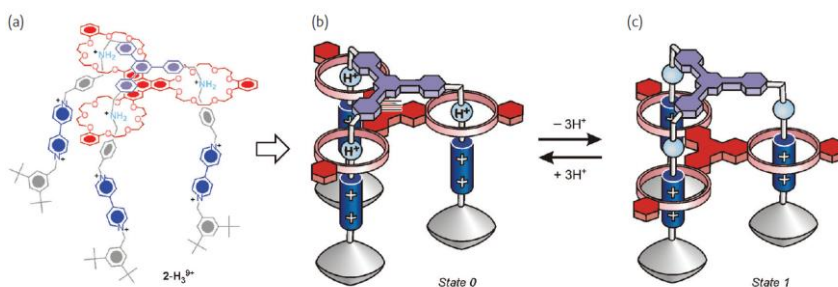


Figure 3. Working principle of the molecular elevators. a) chemical structure of the nano-elevator; b) state 0 of the nanostructure: the crown ethers reside exclusively around the ammonium sites; c) after deprotonation, the shuttling of the macrocycles from the ammonium moiety to the bipyridyl ion is observed. The system is completely reversible.

Rotaxane-based molecular shuttles have been extensively studied and they have been used for different tasks like information storage,²¹ mechanical work,²² gel formation,²³ fluorescence²⁴ and chiroptical²⁵ switching, to control binding events,²⁶ in various controlled-release²⁷ systems and for catalytic purposes (figure 4).²⁸ The rotaxane shown herein consists of a dumbbell component that bears two different recognition sites for the DB24C8: a central dibenzylammonium moiety and two triazolium rings. When the central ammonium group is protonated, the crown resides exclusively around it, guided by the strong hydrogen bonds. When the central site is deprotonated, the crown is able to shuttle toward the electron acceptors triazolium rings. In principle a secondary amine/ammonium group is able to carry out iminium catalysis, therefore this molecular shuttle can be exploited to reveal or conceal an organocatalytic site.

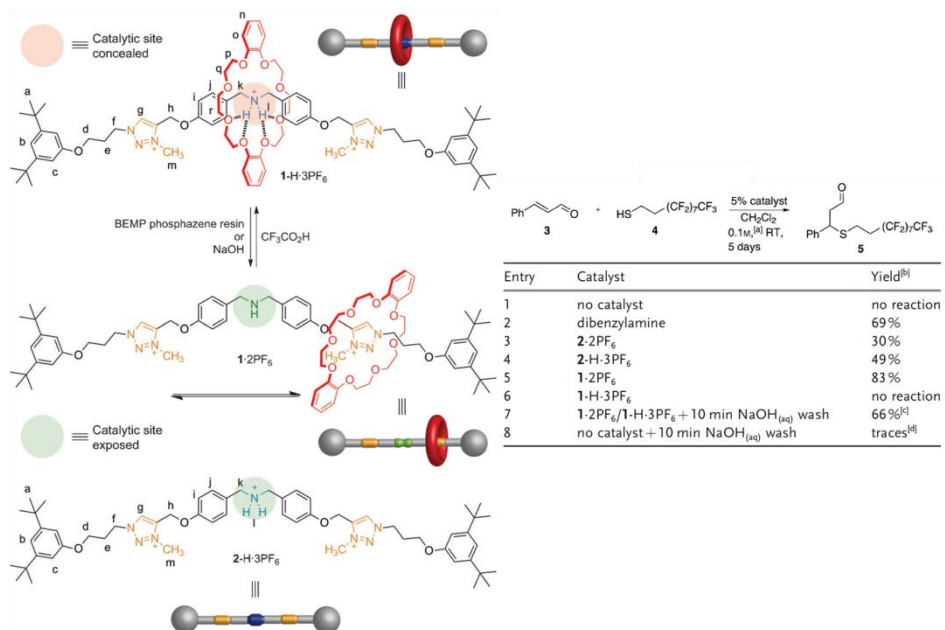


Figure 4. Working principle of the molecular shuttle (on the left). Investigation of the catalytic properties of threads **2** **2PF₆** (deprotonated form of the thread, not shown in figure), **2-H 3PF₆** and rotaxanes **1** **2PF₆**, **1-H 3PF₆** on the Michael addition of thiol **4** to trans-cinnamaldehyde **3** (table on the right).

A [2]pseudorotaxane²⁹ is an interwoven inclusion complex in which a molecular thread is encircled by one or more macrorings and at least one of the final moieties does not possess a bulky stopper group, therefore the components are free to dissociate in different single species. Unlike rotaxane and catenane, there is no mechanical bond that holds the system's integrity. Moreover, also the presence of two final bulky groups that are not covalently linked to the dumbbell-shaped component but that are rather interacting via non-covalent bonding is a feature of a pseudorotaxane-like structure. In figure 5 an example of a pseudorotaxane machine is described.³⁰ In this case a "light-fueled" motor has been incorporated in the axle. The working principle resides in the irradiation of the ruthenium complex by UV-visible light and the subsequent transfer of an electron from the complex to the BIPY²⁺ unit. This transfer causes a destabilization of the charge-transfer interaction (that were responsible for the threading of the 1,5-dioxynaphthalene) that then leads to the disassembly of the intercomponents.

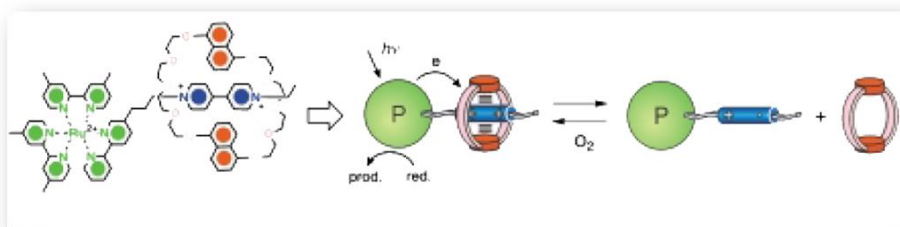


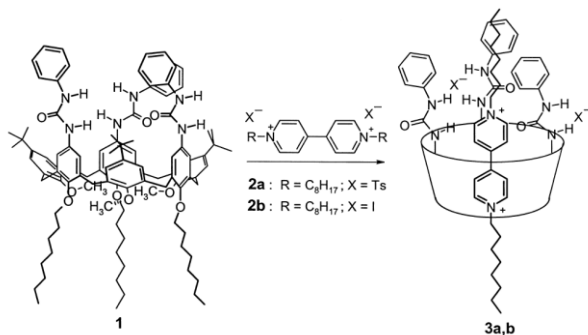
Figure 5. Working principle of a pseudorotaxane-based machine. The electron transfer from the metal complex to the BIPY²⁺ unit leads to the disassembly of the axle-crown threaded structure.

Non-covalent interactions in rotaxanes. Large variety of recognition motif and non-covalent interactions have been extensively studied for the synthesis of rotaxanes: a) cyclodextrins that bind organic molecules in water;⁴ b) crown ethers that can bind metal cations or secondary dialkylammonium sites⁴ or c) amide groups that can establish hydrogen bonds.⁴

The most appealing structures for the synthesis of molecular machines are the ones that carry redox and/or photo active units and/or acid-base sensitive sites in one or both or all the components, this because the control over them is reached respectively electrochemically, photochemically or via acid-base stimuli.

Transition metals that can bind organic ligands were largely exploited (see figure 2 for an example), bipyridinium moieties that can sustain π - π interactions and $\text{CH}\cdots\text{O}$ interactions with polyethers (see figure 4) have also been extensively employed to guide the self-assembly of catenanes and rotaxanes. Majority of complexes studied, especially in the case of pseudorotaxanes, relies on the $^+\text{NH}\cdots\text{O}$ and $\text{CH}\cdots\text{O}$ hydrogen bonding and π -electron donor/acceptor (charge transfer) interactions. This recognition site can be easily destroyed by addition of a suitable base able to deprotonate the ammonium moiety and also easily restored by mean of a proper acid stimuli that can reprotonate the amine. Hydrogen bonds-based system can therefore be easily controlled by acid/base stimuli (see figure 3 for an example).

Aim of the work. The purpose of the present work is the synthesis of a novel type of pseudorotaxane in which the stopping groups are tetraphosphonate cavitands non covalently linked to the axle via host-guest complexation. Calixarene-based structures were already used in the synthesis of pseudorotaxanes exploiting their ability to bind cationic species both at the upper and lower rim, acting as wheels capable to encapsulate positively charged axles (scheme 1).³¹



Scheme 1. Synthesis of a calixarene-based pseudorotaxane in which the calixarene acts as a wheel encapsulating the discharged guest.

In figure 6 the structure of a calixarene-based pseudorotaxane in which the macrocycle acts like a wheel capable to bind chloride anions is shown.³²

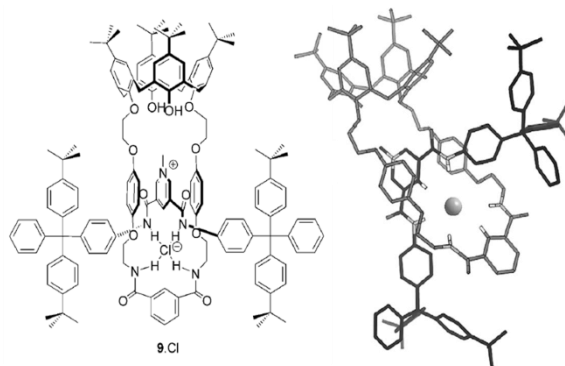
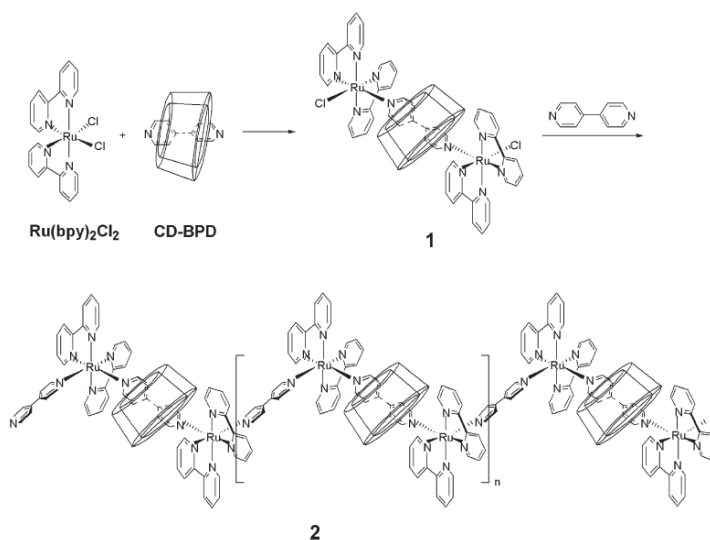


Figure 6. Chemical structure (left) and X-ray structure (right) of the $9 \cdot Cl$ complex for chloride anion recognition.

Regarding the non-covalent interaction modes exploited to connect the stopping groups to the axle of a pseudorotaxane, metal ligand complexation was mainly reported (scheme 2).^[26, 33] As alternative, photoswitchable capping groups were used like stilbene³⁴ or azobenzene.³⁵



Scheme 2. Use of a ruthenium-based complex for luminescent purposes and for stopping group.

Herein we propose host-guest complexation to connect stoppers to the axle.

The remarkable complexation properties of tetraphosphonate cavitands towards methylpyridinium salts (see chapter 2 for details about the thermodynamics of the recognition process) will be explored to connect the stopping groups to the axle.

The dumbbell component of this new pseudorotaxane consists of a two-recognition-sites based molecule: the central is the known dialkylammonium/crown ether recognition motif, the second one is a methylpyridinium terminal group capable to interact with the tetraphosphonate cavitands, that act as hindered stoppers, via CH- π and cation dipole interactions.

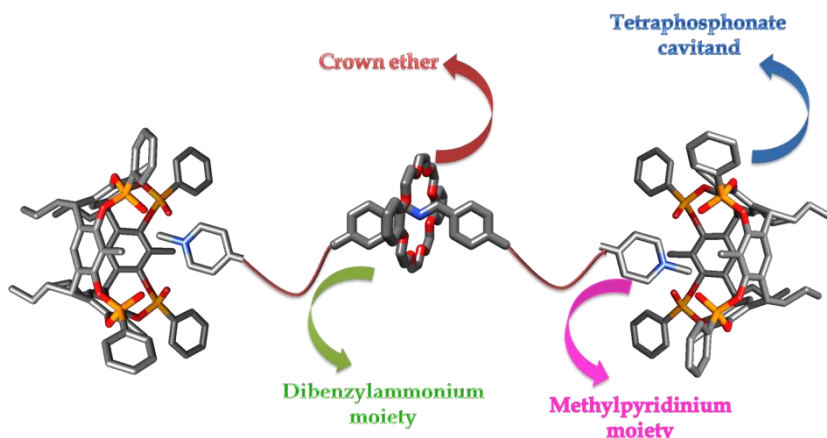
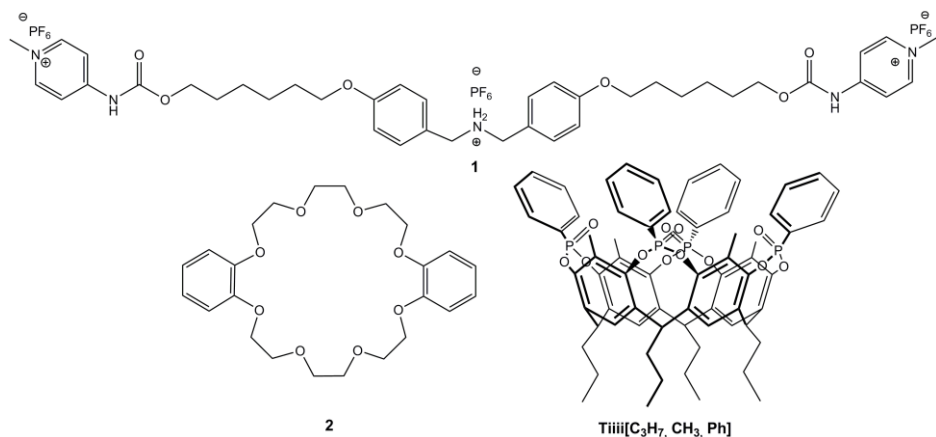


Figure 7. Design of the cavitand-based pseudorotaxane. The central ammonium moiety is able to interact with the crown ether, while the terminal methylpyridinium moieties are recognized by the tetraphosphonate cavitands and inserted in the cavity. The cavitands can be considered as bulky stoppers linked via host-guest interactions to the axle.

3.2 RESULTS AND DISCUSSION

Axle, cavitand and crown. The pseudorotaxane components used in the present work are shown in scheme 3. Crown ether **2** was used as received, while the synthesis of **Tiii**[C₃H₇, CH₃, Ph] (from now on referred to as **Tiii**) follows a reported procedure.³⁶

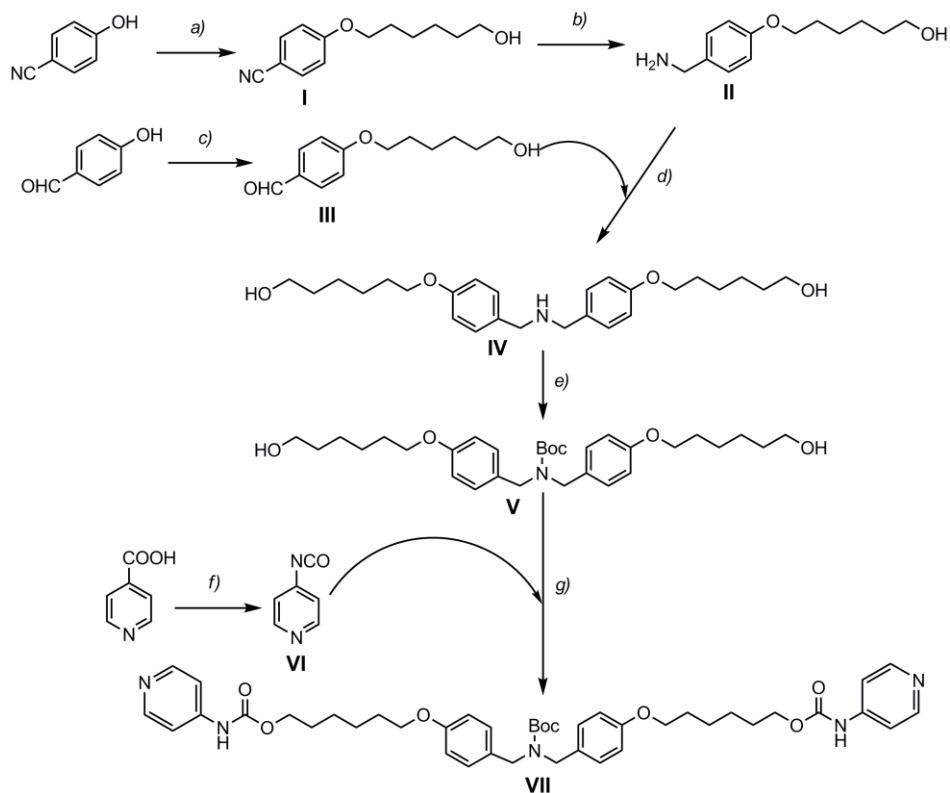


Scheme 3. Compounds used in the present work.

The synthesis of compound **1** is presented in schemes 4 and 5 (for details see experimental section).

Compound **1** was obtained by a 12-steps synthesis starting from two Williamson on 4-hydroxybenzonitrile and *p*-hydroxybenzaldehyde with 6-bromo-1-hexanol (compounds **I** and **III**, scheme 4), followed by conversion of the cyano into an amino group (compound **II**) by reduction with lithium aluminum hydride. The core of the final axle was then formed by a two step reductive amination of compounds **II** and **III** (for these first steps a modified literature procedure was used).³⁷ The choice of the connector group between the axle and the final pyridine moiety was not trivial. The first choice was an ester group, but its facility to hydrolyze both under acidic and basic conditions made this group not suitable for the axle. Isocyanate **VI** was then synthesized starting from the isonicotinic acid and diphenylphosphoryl azide following a published procedure.³⁸ The product was used as a crude (after testing its reactivity with a model of the axle, see experimental procedure for details) and reacted with the

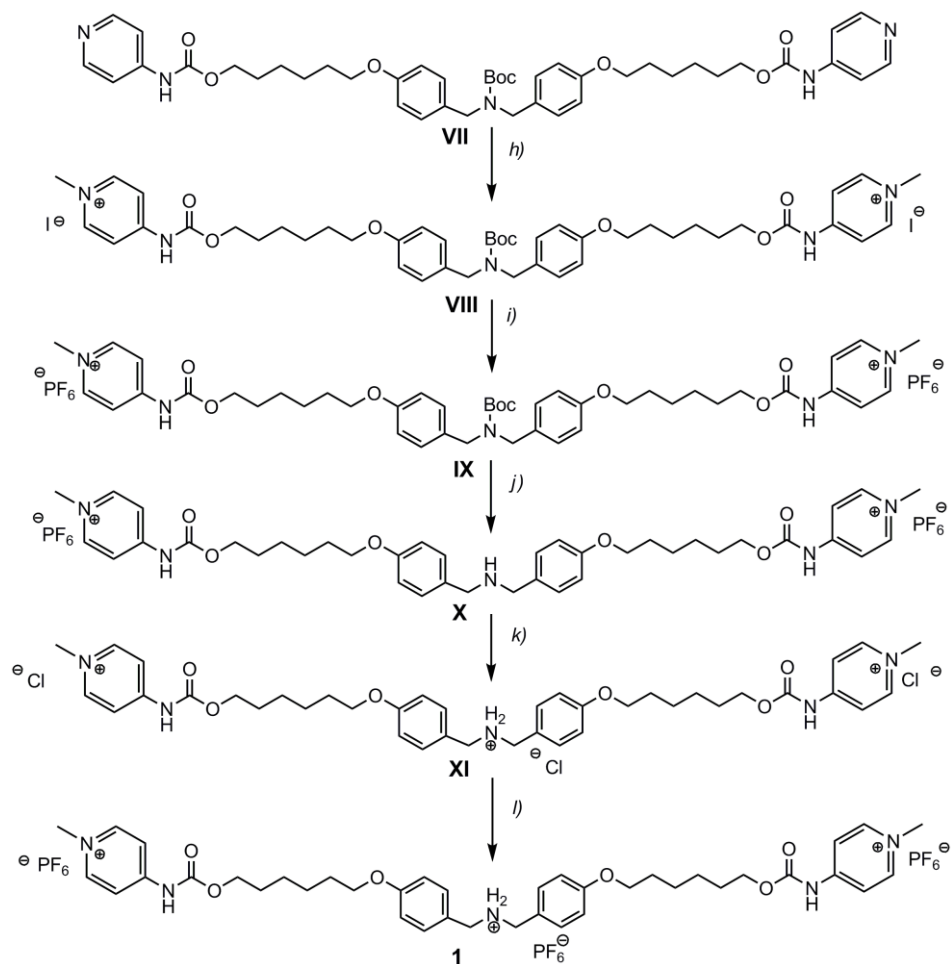
Boc protected axle (compound **V**) to form the carbamate **VII**. This group demonstrated to be stable under both acidic and basic conditions.



Scheme 4. Synthesis of the axle, first part. a) 6-bromo-1-hexanol, K_2CO_3 , dry CH_3CN , reflux, overnight, yield 85%; b) $LiAlH_4$, dry THF , r.t., from $0^\circ C$ to r.t., yield 73%; c) 6-bromo-1-hexanol, K_2CO_3 , dry DMF , $80^\circ C$, overnight, yield 93%; d) 1_compound **III**, $CHCl_3$, r.t., 2 h; 2_dry $MeOH$, r.t., 3 h, yield 75%; e) $(Boc)_2O$, NEt_3 , dry CH_2Cl_2 , r.t., overnight, yield 80%; f) diphenylphosphoryl azide (*dppa*), NEt_3 , CH_3CN , from $0^\circ C$ to $75^\circ C$, 2.5 h; yield not calculated since the product was used as a crude; g) compound **VI**, CH_2Cl_2 , NEt_3 , r.t., yield 61%.

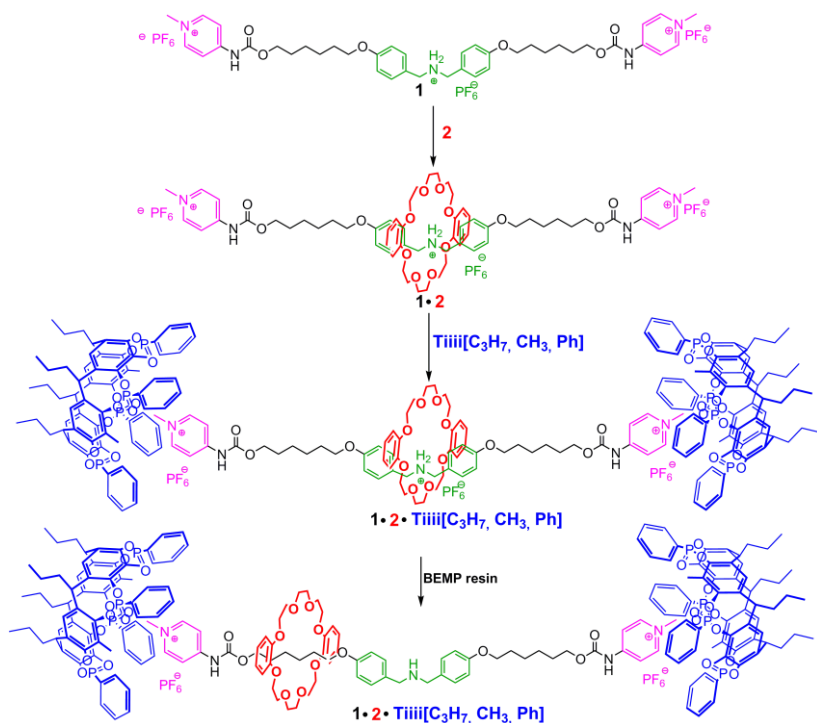
Pyridine methylation, counterion exchange, Boc deprotection, protonation and again counterion exchange to give the axle in the PF_6^- salt form were the last steps of the synthesis that gave all quantitative yields (see scheme 5 and experimental part for details). The iodide/ PF_6^- exchange (passage *i*) is necessary

because I⁻ undergoes easily to disproportionation and to enhance solubility of the axle.



Scheme 5. Synthesis of the axle, second part. h) CH_3I , CH_2Cl_2 , 40°C , overnight; quantitative yield; i) KPF_6 , $\text{H}_2\text{O}/\text{MeOH}/\text{acetone}$, r.t., overnight, quantitative yield; j) trifluoroacetic acid (TFA) 20%, $\text{CH}_2\text{Cl}_2/\text{CH}_3\text{CN}$, r.t., 1.5 h, quantitative yield; k) HCl 36%, $\text{CH}_2\text{Cl}_2/\text{CH}_3\text{CN}$, r.t., 0.5 h, quantitative yield; l) KPF_6 , $\text{H}_2\text{O}/\text{MeOH}/\text{acetone}$, r.t., overnight, quantitative yield.

Working principle. The working principle of the architecture-like rotaxane is presented in scheme 6. The axle is composed by an internal dibenzylammonium and two terminal methylpyridinium groups. Both recognition sites are able to interact with the dibenzo-24-crown-8 component (**2**) that acts like an electron donor, respectively via hydrogen bonding and charge transfer (CT) interactions. Since hydrogen bonding is stronger than CT interactions the pseudorotaxane should exist just as one of the two possible translational isomers. The terminal methylpyridinium moieties of **1** are recognition sites for tetraphosphonate cavitant **Tiiii**[C₃H₇, CH₃, Ph] via cation-dipole interactions and, to a less extent, CH- π interactions (see chapter 2 for details). After deprotonation, the absence of hydrogen bonding between the internal amino group and the crown ether should lead to the translation of the crown ether from the internal amine towards the methylpyridinium moieties, but the presence of the terminal cavitants should influence the shuttling of the crown ether, avoiding its dethreading and hindering its interaction with the methylpyridinium ending moieties.



Scheme 6. Assembly and working principle of the cavitant-capped rotaxane.

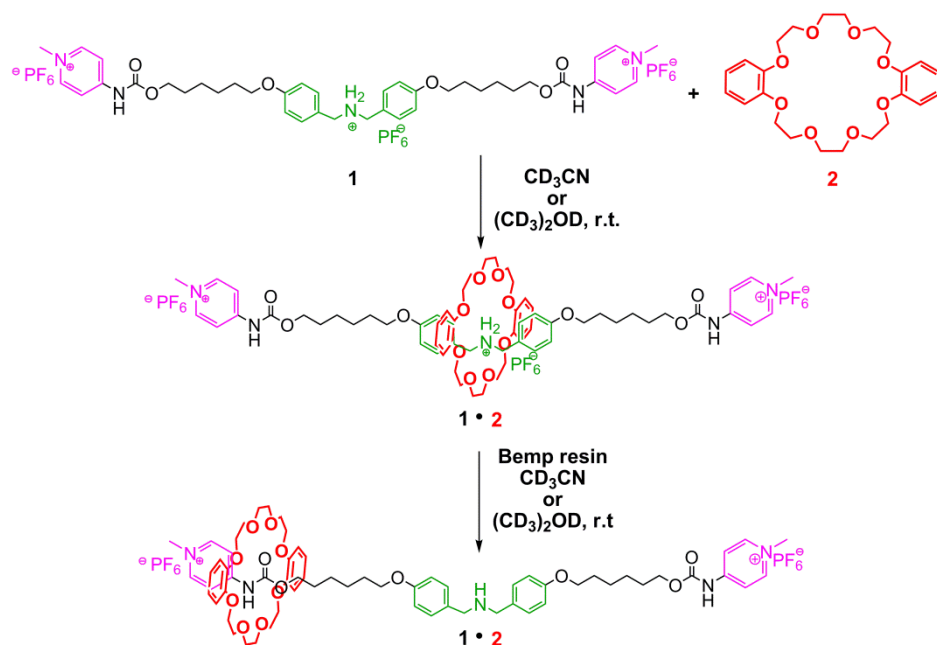
Titration experiments. Due to the complexity of the four components system, we tried to separate and evaluate the contributions belonging to the crown ether and the cavitand.

Crown-axle interaction. From a theoretical point of view nor polar neither protic solvent should be used to study the threading process of the crown ether **2** into the axle **1** since the thermodynamic stabilization of hydrogen bonding is needed as driving force of the process.³⁹ In reality, the choice of an apolar aprotic solvent is not feasible, due to the presence of three positive charges on the axle, that render **1** not sufficiently soluble in this type of solvents. The best solvent compromises are acetone and acetonitrile, two polar but not protic solvents that don't suppress the hydrogen bonding between **1** and **2** and present good solubility properties towards both components. Their properties are summarized in table 1.

Solvent	b.p. (°C)	d (g/mL)	Relative polarity ^a	Eluant strength ^b	Vapor pressure 20°C (hPa)	Protic/ Aprotic
Acetonitrile	81.6	0.786	<u>0.460</u>	0.66	97	<u>Aprotic</u>
Acetone	56.2	0.786	<u>0.355</u>	0.56	240	<u>Aprotic</u>

Table 1. Significant physical properties of acetonitrile and acetone. ^aThe values for relative polarity are normalized from measurements of solvent shifts of absorption spectra and were extracted from Christian Reichardt, *Solvents and Solvent Effects in Organic Chemistry*, Wiley-VCH Publishers, 3rd ed., **2003**. ^bSnyder's empirical eluant strength parameter for alumina. Extracted from Reichardt, page 495.

In scheme 7 the titration experiment is reported: to a solution of the free axle, the crown ether was added into portions and the interaction mode was monitored via ¹H NMR. The titrations were performed both in acetonitrile and in acetone.



Scheme 7. Axle-crown titration. Crown **2** was added in portions into a solution of axle **1**, then the benzylic ammonium was deprotonated via BEMP resin. Experiments were performed both in acetonitrile and acetone.

Acetonitrile titration. Entry **a** of figure 8 shows the spectra of the free axle in CD_3CN solution.

Upon addition of 1.0 equivalent of the crown **2**, the threading process was monitored (spectrum **b**). The threading of the crown inside the axle is demonstrated by the shift and the shape change of signal of methylenes *a*²⁴ that is subjected to a downfield shift and a broadening of the shape due to the formation of strong hydrogen bonding of the nearby ⁺NH₂. The aromatic protons *b* and *b*' of the dibenzylammonium (signals labeled with the green color) partially undergo to a downfield shift due to the shielding effect of the electron rich crown ether. The presence of two set of resonances to attribute to the complexed and non-complexed axle indicate a slow exchange process on the NMR time scale, that, after the addition of 1.0 equivalent of **2**, leads to the complexation of 50% of the axle. This partial threading has been already observed in similar systems and rationalized as slow exchange of the crown ether between the axle and the free solution.⁴⁰ The same effect of the contemporary existence of the two resonances is also present in the case of the

crown ether, in which an upfield splitting of the red labeled signal belonging to the complexed and non complexed species in spectrum **b** is evident. In the case of the carbamate proton *e* on the NH a slight downfield shift (+0.10) and a signal splitting were visible. This might be due to the interaction of the crown ether not only with the internal station but also with the methylpyridinium groups via CT interactions.

Upon addition of other 2.0 equivalents of **2** (entry **c**) the percentage of complexed axle increased to 80%. For the carbamate NH group the signal splitting became more evident, meaning that some interaction with the crown ether is occurring, as testified also from the upshield shift of the neighboring protons on the pyridinium moiety *f* and *f'* (-0.12 ppm).

The final addition of 3.0 equivalents of **2** (6.0 equivalents in total, shown in entry **d**) caused the increase of complexation to a 92%, but a 1:1 complex between **1** and **2** is not reached even in the presence of a large excess of the crown ether. From the ¹H NMR it appeared that more than one translational isomer is present. This hypothesis was also confirmed by the ESI-MS, that showed three different type of complexes between **1** and **2** as main signals:

⊘ 1:1 ratio;

⊘ 1:2 ratio;

⊘ 1:3 ratio.

To study the dethreading process, the pseudorotaxane solution was then subjected to deprotonation of the ammonium salt by BEMP resin, a very strong but low nucleophilic base that belongs to the phosphazine class. As a result, the intercomponent hydrogen bonds are destroyed and the crown ether is able to move away. This shuttling movement is testified by the NMR of entry **e**. Diagnostic signal *a* disappears and the original signal of entry **a** is restored, meaning that the crown ether does not interact anymore via hydrogen bonds with the axle. However, the aromatic protons of the dibenzylamine do not regain the exact initial position, most probably due to the loss of the deshielding effect of the deprotonated amino group. Dethreading process seems complete, based on the lack of any other shift signals of the axle.

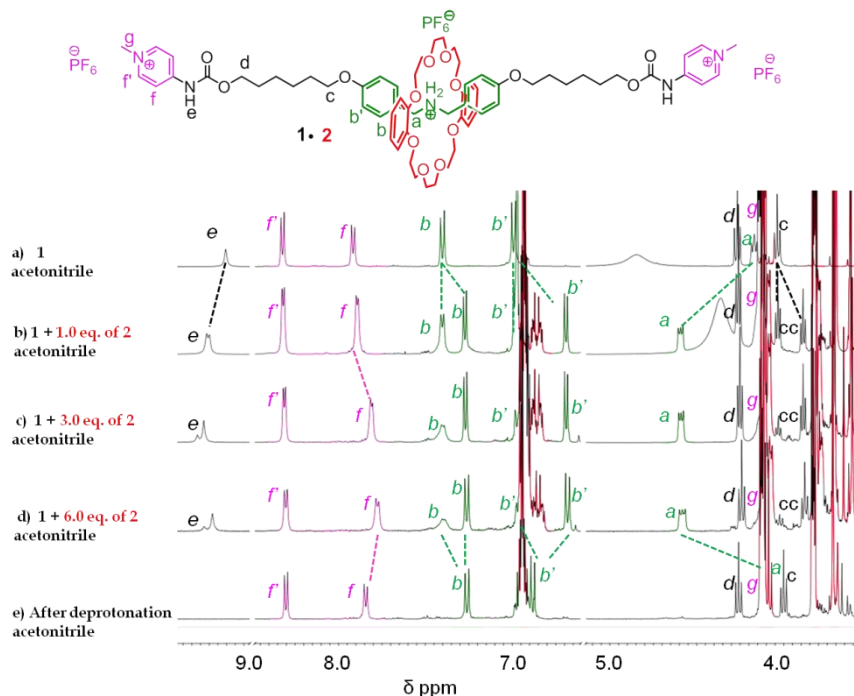


Figure 8. Relevant portions of the ^1H NMR spectra of a) the free axle **1**; b) **1** upon addition of 1.0 equivalent of **2**; c) **1** after the addition of 3.0 equivalents of **2**; d) **1** upon addition of 6.0 equivalents of **2**; e) after deprotonation of the internal ammonium group.

Acetone titration. The same experiment was then repeated in acetone (figure 9) to evaluate if any difference in the threading behavior could be observed and related to the change of the buffer. Upon addition of 1.0 equivalent of **2** (entry b) the diagnostic signal at 4.7 ppm of the methylene groups in α to the ammonium moiety is upfield shifted, indicating that also in acetone we have threading of the crown ether into the axle. The same upfield shifts already reported in the acetonitrile NMR of the aromatic protons of the dibenzylammonium are present (green labeled signals b and b'). What emerged from the comparison between entry b of figure 8 and entry b of figure 9 was that in both cases the insertion process is slow on the NMR time-scale. From the signals integration of the complexed and non complexed axle the threading process in acetonitrile is favored with respect to acetone. In fact, after the addition of one equivalent in the case of acetonitrile the complexed axle reached 50%, while in the case of acetone just 34%. This is most probably due to the reduced separation of the ionic couple (axle- PF_6^-) in acetone with respect to

acetonitrile. Upon addition of 3.0 equivalents (compare entry **c** of figure 8 with entry **d** of figure 9) the threading in acetonitrile reached 80%, while in acetone was 62%. The addition of **2** caused also the upfield shift of the *f* aromatic protons of the pyridinium moieties (labeled with fuchsia): after the addition of 3.0 equivalents of **2** the shift was -0.10 ppm, comparable with the one obtained in the case of the complexation in acetonitrile. Also in acetone more than one translational isomer is present.

The main difference between the two spectra resides in the behavior after deprotonation of the dibenzylammonium with BEMP resin (entry **f**). Signal *a* disappeared, denoting the absence of hydrogen bonding between the two components, while the aromatic signals of the methylpyridinium moiety underwent to a huge upfield shift, caused by the presence of the electron donor species that shields the electronic environment.

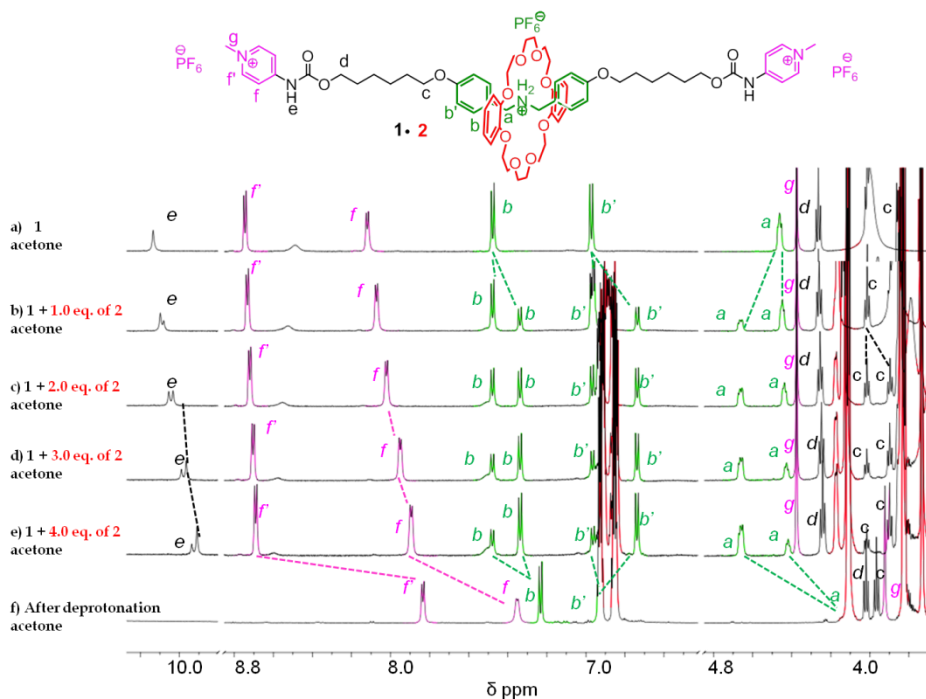
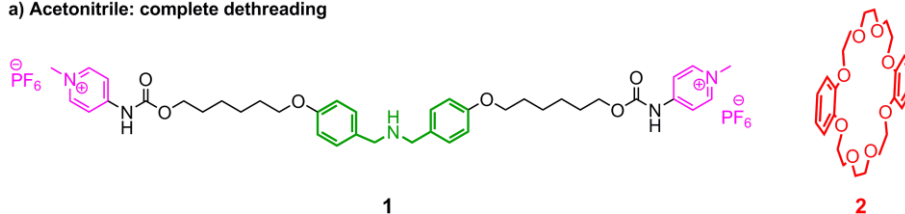


Figure 9. Relevant portions of the ^1H NMR spectra of *a*) the free axle **1**; *b*) **1** upon addition of 1.0 equivalents of **2**; *c*) **1** after the addition of 2.0 equivalent of **2**; *d*) **1** upon addition of 3.0 equivalents of **2**; *e*) **1** upon addition of 4.0 equivalents of **2**; *f*) after deprotonation of the internal ammonium group.

In acetonitrile the dethreading of the crown ether was observed, while in the case of acetone the dethreading process is translated into a shuttling from the dibenzylammonium to the ending methylpyridinium groups (figure 10).

a) Acetonitrile: complete dethreading



b) Acetone: crown shuttling

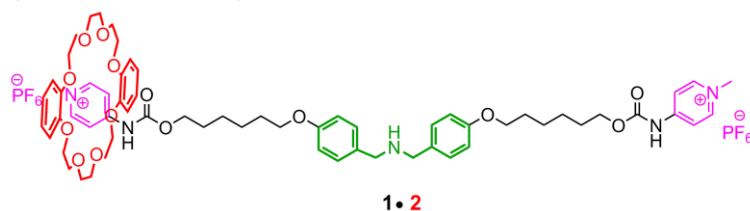
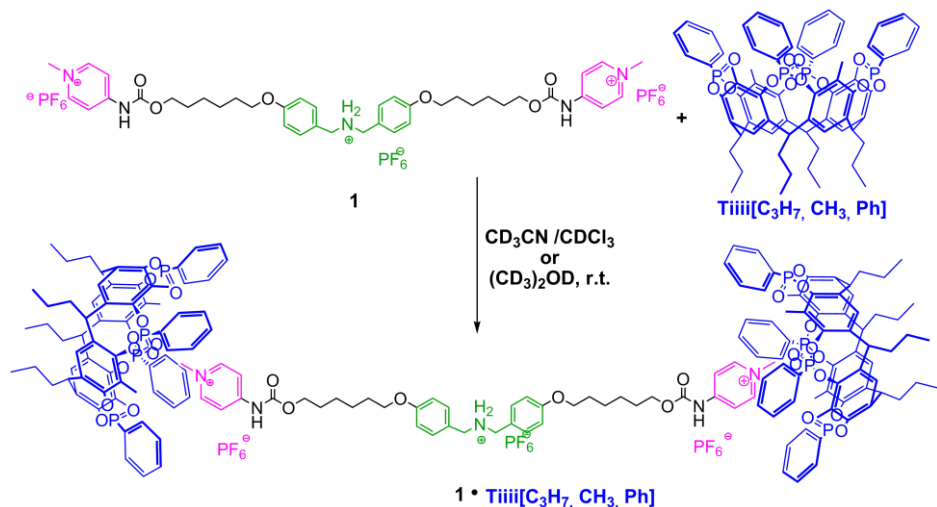


Figure 10. Representation of the two different processes that occur in solution after deprotonation of the internal ammonium group. a) In acetonitrile the disassembly of the pseudorotaxane is observed; b) in acetone the shuttling of the crown ether from the central station to the terminal recognition site is observed.

Cavitand-axle titrations. Next, the interaction of cavitand **Tiiii** with the axle was evaluated.

In scheme 8 the experiment is shown: to a solution of the free axle in acetonitrile or acetone the cavitand was added in portions dissolved respectively in a chloroform or in an acetone solution to evaluate the complexation mode.

Both experiments are herein described.



Scheme 8. Axle-**TiIII** titration. Cavitand was added in portions into a solution of axle **1**. Experiments were performed both in a mixture of acetonitrile/chloroform and acetone.

Acetonitrile/chloroform experiment. In figure 11 the ^1H NMR titration of **1** and **TiIII** in the mixture acetonitrile/chloroform is reported.

In entry **a** the spectra of the free axle in solution of acetonitrile is shown. The receptor was added in a chloroform solution, since its solubility in acetonitrile at room temperature is very limited.

Upon addition of 1.0 equivalent of **TiIII** the NMR showed a substantial upfield shift of the aromatic protons of the methylpyridinium moiety. This is a typical effect of the shielding effect due to the presence of the cavity surrounding the guest part. Major proof of the host-guest interaction was given by the large upfield shift of the methyl signal of the pyridinium groups *g* that moved from 4.2 ppm to the alkyl part of the NMR spectra, around 2 ppm. Unfortunately even from NOESY NMR no univocal assignment could be done to the shift of the methyl group. The shift is larger in the case of the methyl *g* with respect to the aromatic protons of the terminal pyridinium moiety *f* and *f'* because the CH_3 , upon complexation, is inserted deeper in the cavity and therefore the shielding effect of the receptor is stronger.

The small shifts observed in the case of signals *b*, *b'*, *d*, *a*, and *c* belonging to the axle are due to the new solvent mixture after the addition of the cavitand.

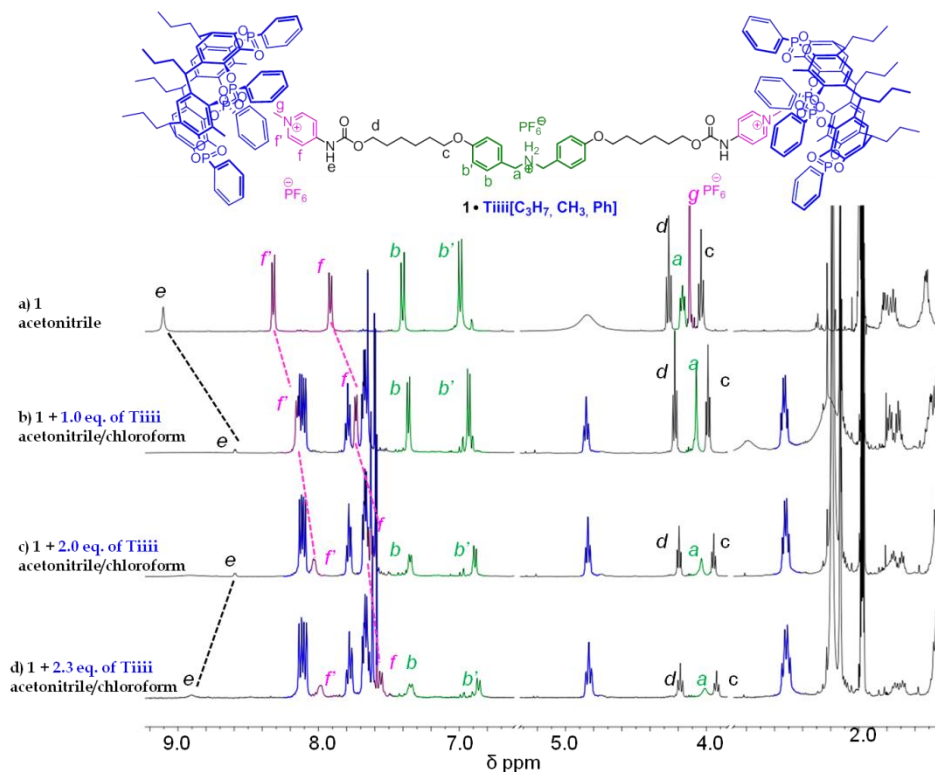


Figure 11. Relevant portions of the ^1H NMR spectra of a) the free axle **1**; b) **1** upon addition of 1.0 equivalent of Ti^{III} ; c) **1** after the addition of 2.0 equivalents of Ti^{III} ; d) **1** upon addition of 2.3 equivalents of Ti^{III} .

The final proof for complexation came from ^{31}P NMR (figure 12). In entry **a** the peak of the phosphorus of the free cavitaand in a chloroform/acetonitrile solution is shown.

Upon addition of 1.0 equivalent of the host in chloroform to the axle solution in acetonitrile an upfield shift of +1.17 ppm of the phosphorus peak was observed (entry **b**). The final methylpyridinium moieties of the axle can establish two synergistic interactions with the cavity, that are CH- π interactions and cation-dipole interactions. These are the driving forces for the host-guest recognition. The large downfield shift observed in this case is due to the major deshielding effect of the phosphorus electron cloud due to the presence of a positive charged guest inside the receptor.

In entry **c** the change of the signal shift after the addition of 2.3 equivalents of cavitaand is shown. In this case the peak underwent to a slight upfield shift of

-0.17 ppm, related to the presence of an excess of the host with respect to the guest: since the complexation process is in fast exchange at room temperature the peak represents the average situation between the two different cavitant states, complexed and free.

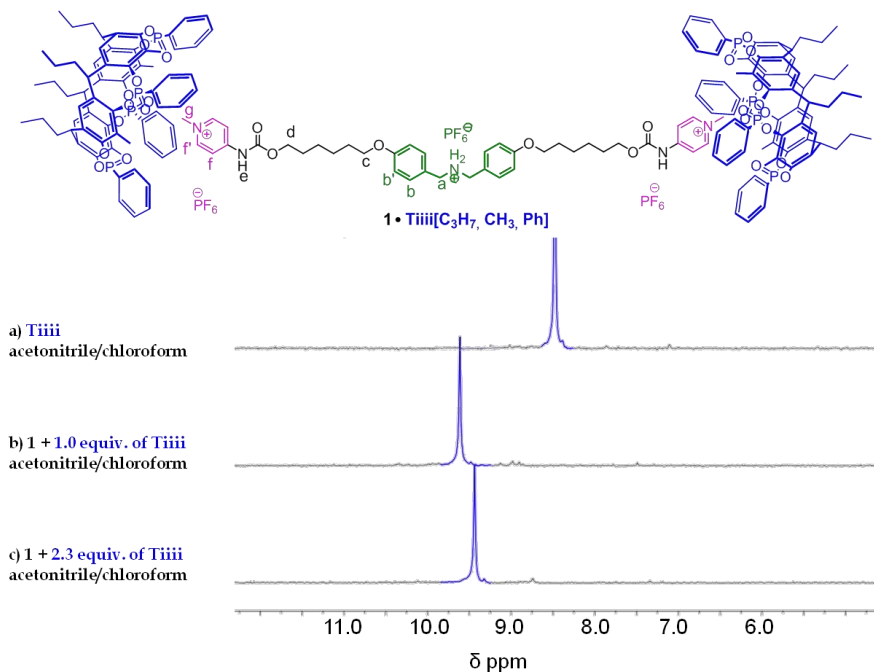


Figure 12. ^{31}P NMR of *TiIII*: a) free *TiIII*; b) axle + 1.0 equivalents of *TiIII*; c) axle + 2.3 equivalents of *TiIII*.

Acetone experiment. Host-guest recognition was then monitored in acetone (figure 13).

The use of a unique solvent instead of a mixture will unambiguously show the contributions related to the complexation process. Solubility of the free cavitant in acetone at room temperature is not sufficient to obtain a clear solution but just a suspension. Once that the cavitant is added to the axle solution, the complex is completely soluble in acetone.

In entry **a** the spectra of the free axle in solution is presented.

After the addition of 1.0 equivalent of *TiIII* (entry **b**) the shifts already monitored in the case of the acetonitrile/chloroform mixture were again observed: the aromatic protons of the methylpyridinium moieties underwent to

an upfield shift due to the shielding effect of the host electron rich cavity and the signal of the methyl *g* underwent again to a significant upfield shift moving to the alkyl part of the spectra, even if, also in acetone, an unambiguous assignment was not possible even with the NOESY NMR. Upfield shift of the proton of the carbamate was also monitored.

Signals of benzylammonium protons *b*, *b'*, of protons *d*, *a* and *c* did not move, meaning that there is no interaction between the central part of the axle and the cavitand and that the shift previous monitored in the case of the acetonitrile/chloroform mixture (figure 11) were just to ascribe to the change of the solvent environment.

Upon addition of 1.5 and 1.9 equivalents of the cavitand (entry **c** and **d**) the only signals affected are the aromatic protons of the methylpyridinium and the protons of the internal ammonium group. The presence of the cavitand sharpens the peak belonging to the central $^+\text{NH}_2$ protons at ~ 3.3 ppm (exchanging with water).

One plain difference from the previous titrations experiments conducted in the acetonitrile/chloroform mixture (figure 11) is the shape broadening of **Tiiii** signals involved in the complexation process, namely the protons belonging to the upper phenyl groups and the CH bridging groups. The broadening of the shape is a signal of an intermediate exchange process. A fast exchange process provides sharp signals that are the average of the two different states of the molecule, while in the case of a slow exchange the presence of two different signals for the two different states are present. In our case neither slow exchange nor fast exchange are satisfied. The broadening of the signal is a clear sign of an intermediate situation between fast and slow exchange that is solvent dependent.

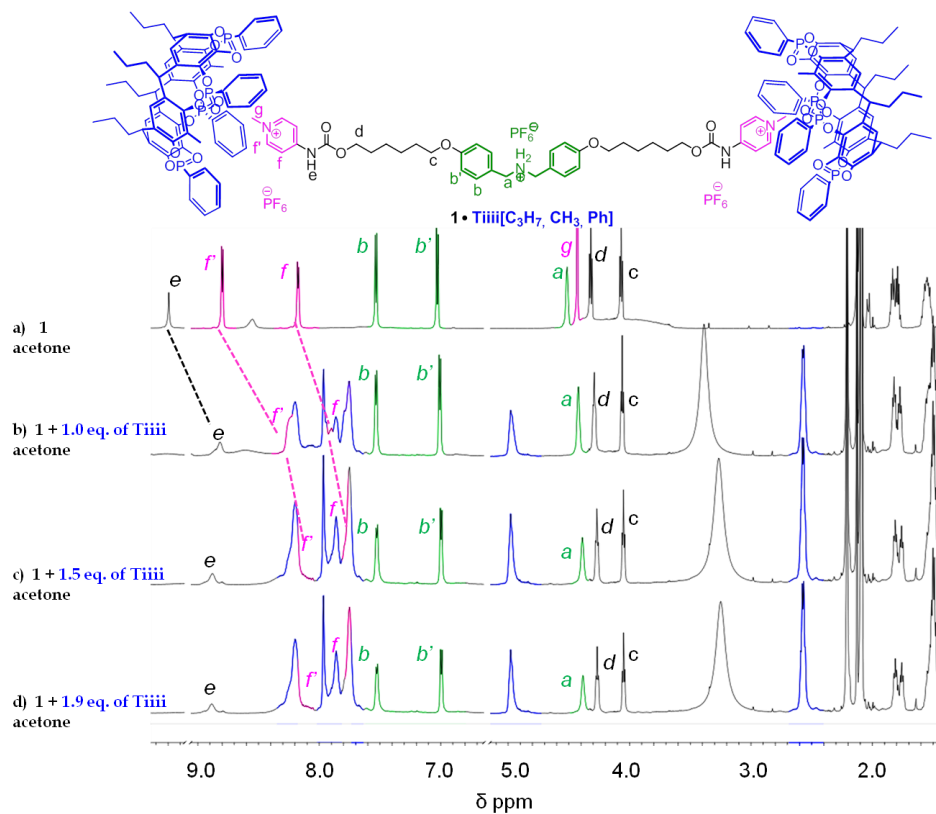


Figure 13. Relevant portions of the ^1H NMR spectra of a) the free axle **1**; b) **1** upon addition of 1.0 equivalent of **TiIII**; c) **1** after the addition of 1.5 equivalents of **TiIII**; d) **1** upon addition of 1.9 equivalents of **TiIII**.

In figure 14 the complexation process monitored via ^{31}P NMR is shown.

Again, upon complexation of the axle with the cavitant (entry **b**, **c**, and **d**) the downfield shift of the phosphor peak diagnostic of the complexation is observed.

In conclusion, the same complexation is observed both in acetonitrile/chloroform and in acetone, with the only difference that in acetone the process is slower.

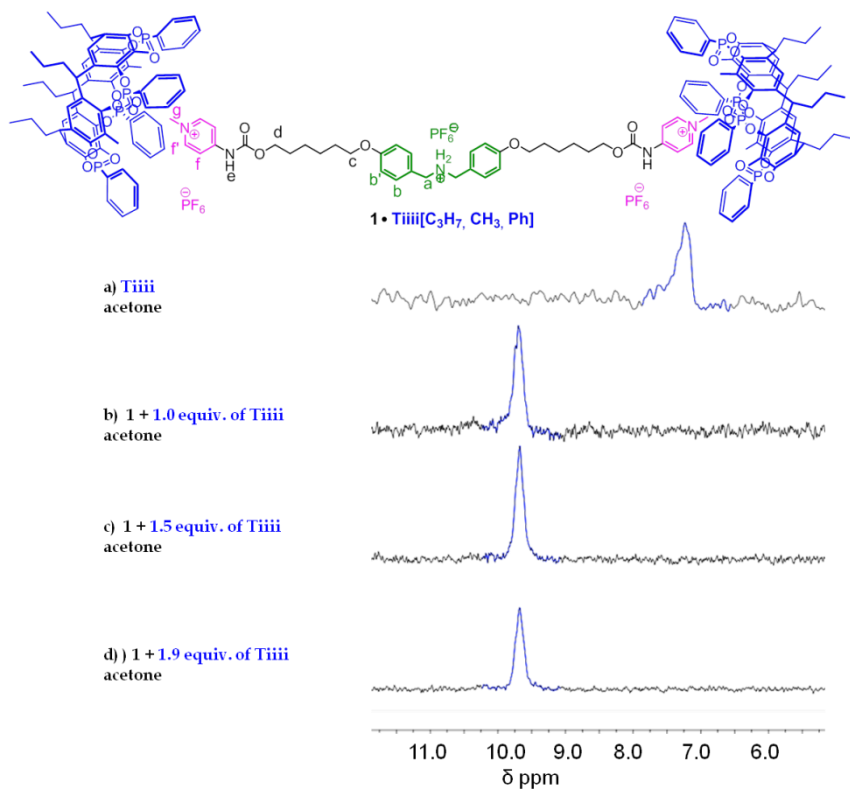
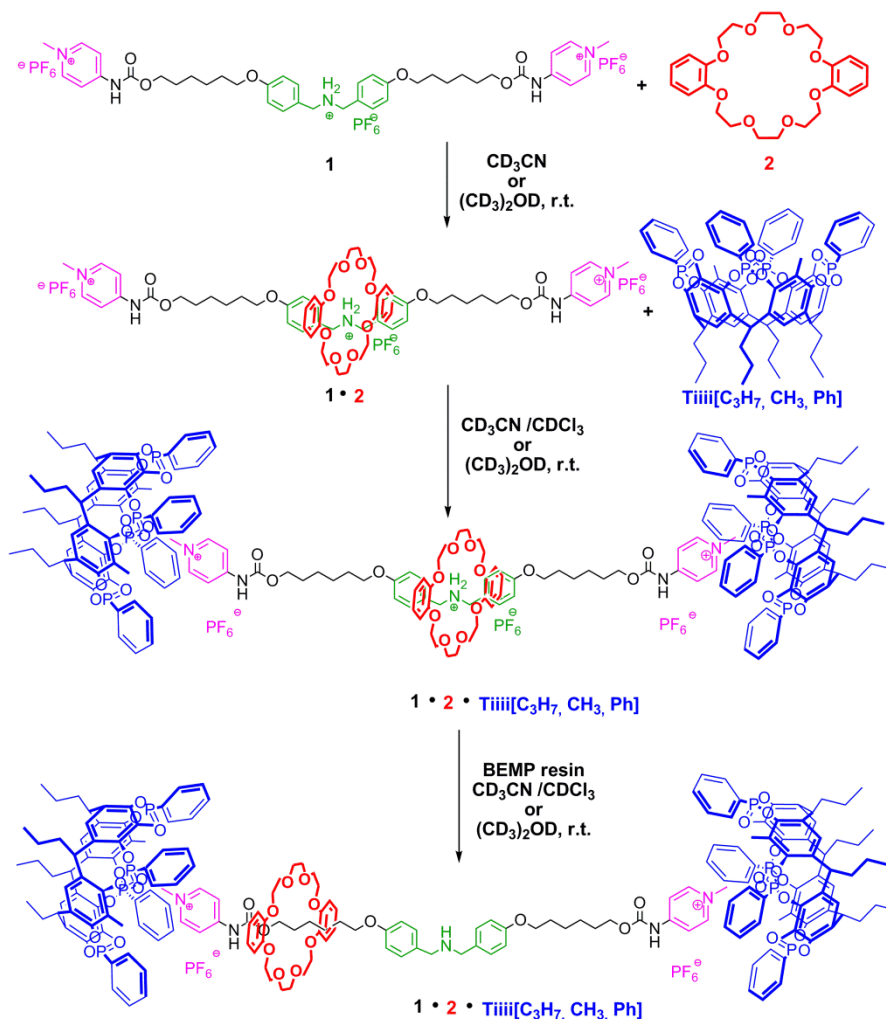


Figure 14. ³¹P NMR of **TiIII**: a) free **TiIII** in acetone; b) **axle** + 1.0 equivalents of **TiIII** in acetone; c) **axle** + 1.5 equivalents of **TiIII**; d) **axle** + 1.9 equivalents of **TiIII**.

Pseudorotaxane assembly. Next step was the assembly of the four components rotaxane. In scheme 9 the titration principle is shown: first the axle was titrated with the crown **2** until the 1:1 ratio was reached. Then the pseudorotaxane **1•2** was titrated with the cavitand host until the complex **TiIII•1•2** was formed in a 2:1:1 ratio. Experiments were performed both in a mixture acetonitrile/chloroform and in acetone.

Self-assembly of a cavitand-stopped rotaxane



Scheme 9. Cavitand-stopped rotaxane: first the free axle was titrated with **2**. Then **Tiii** was added to the preformed pseudorotaxane in portions and the architecture-like rotaxane was then subjected to deprotonation of the internal ammonium salt. The experiments were performed both in a mixture of $\text{CD}_3\text{CN}/\text{CDCl}_3$ and in acetone.

Acetonitrile/chloroform experiment. First, the assembly of the pseudorotaxane in acetonitrile/chloroform was performed (figure 15). The axle was dissolved in an acetonitrile solution and one equivalent of the crown ether **2** was added (entry **b**), showing the same behavior and the same signals shifts already observed in figure 8.

Then 1.2 (entry **c**) and 2.2 (entry **d**) equivalents of **Ti**iii were added to the preformed complex. Signals belonging to the axle-crown interaction remained unchanged, while the signal belonging to the methylpyridinium groups underwent to an upfield shift due to the host-guest recognition process.

Upon deprotonation of the dibenzylammonium via BEMP resin and consequent removal of the hydrogen bonds, the signal associated with the interaction between **1** and **2** disappeared, restoring the initial shift of the axle. Unlike figure 8 entry **e**, in this case we observe a slight upfield shift of the protons of the methylpyridinium meaning that the crown ether resides in the axle and that no dethreading process is occurring. The presence of the tetraphosphonate cavitands prevents the dissociation of the two components **1** and **2**.

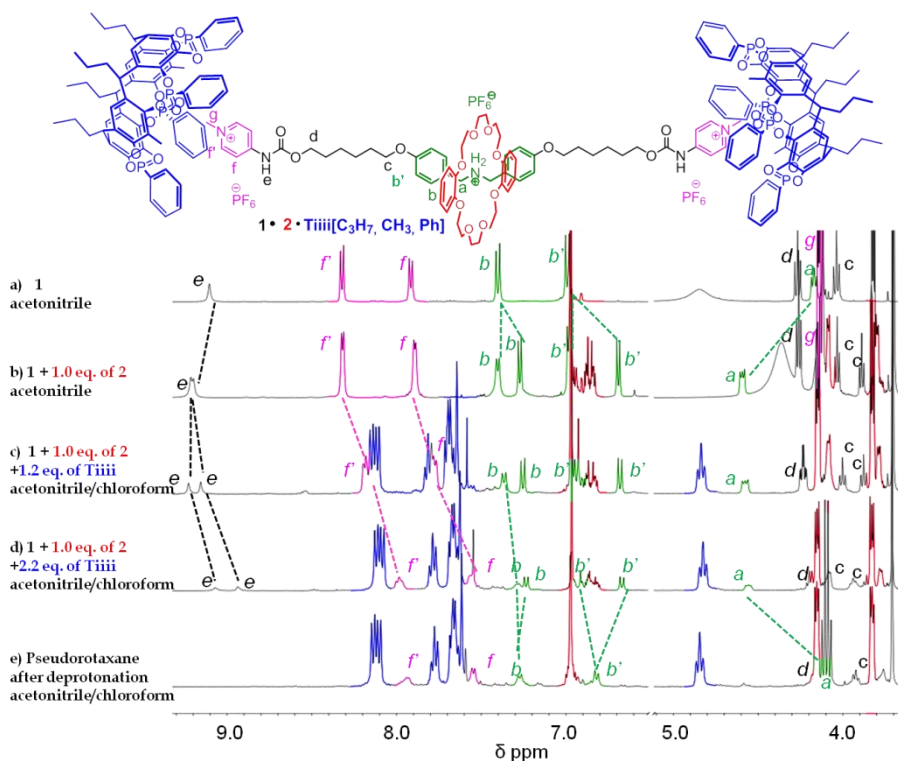


Figure 15. Relevant portions of the ^1H NMR spectra of a) the free axle **1**; b) **1** upon addition of 1.0 equivalent of **2**; c) after the addition of 1.2 equivalents of **Ti**iii; d) upon addition of 2.2 equivalents of **Ti**iii; e) upon deprotonation of the dibenzylammonium group.

Each step of the pseudorotaxane assembly was monitored also via ^{31}P NMR (figure 16), showing that the hosts-guest complexation is maintained also after the deprotonation of the central ammonium moiety (as shown comparing entry **a** with entry **d**).

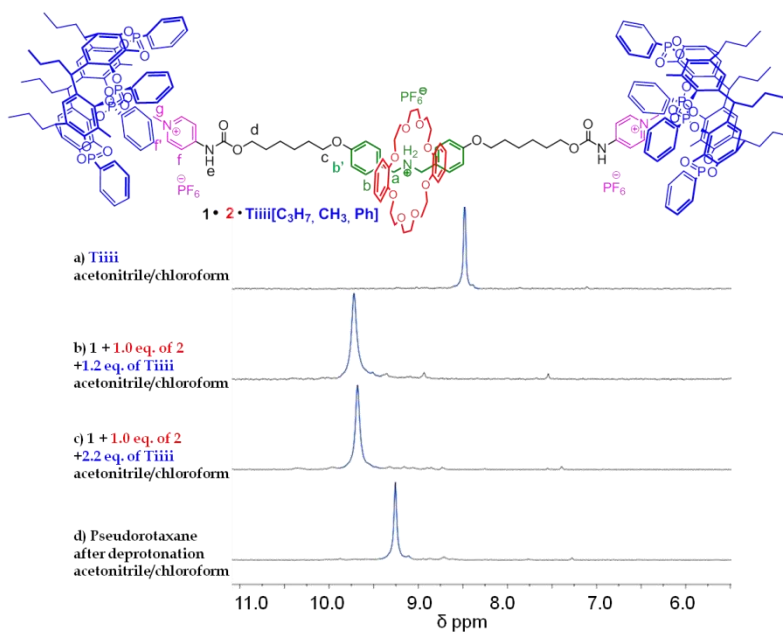


Figure 16. ^{31}P NMR of *Tiiii*: a) free *Tiiii*; b) axle + 1.0 equivalent of crown + 1.2 equivalents of *Tiiii*; c) axle + 1.0 equivalent of crown + 2.2 equivalents of *Tiiii*; d) pseudorotaxane after deprotonation.

Acetone experiment. The cavitand-stopped rotaxane assembly was then performed also in acetone (figure 17). To the free axle in solution (entry **a**), 1.0 equivalent of crown ether was added (entry **b**). The same spectra already discussed in figures 9 and 15 were obtained: threading of the axle occurs in a slow-exchange NMR time scale originating two sets of resonances for both axle and crown ether.

The addition of the *Tiiii* (entries **c** and **d**) caused an expected upfield shift of the aromatic protons of the methylpyridinium moiety and a huge shift toward the alkyl part of the spectra to the methyl *g* of the pyridinium groups,

typical shifts already observed in the pure host-guest assembly processes (figures 9 and 15).

After the deprotonation of the dibenzylammonium group the behavior monitored in entry **e** is quite different from the one observed in the case of the deprotonation of the axle in the presence of the crown ether alone (figure 9): in this case the huge shift of the methylpyridinium protons is not observed meaning that **2**, once deprived of the interaction via hydrogen bonds with the central recognition site, does not shuttle to the methylpyridinium units, but instead, it seems to stop in a intermediate position between the two recognition sites. This difference from the NMR of figure 9 depends from the presence of the cavitands: the complex between the hosts and the terminal guest units is strong enough to suppress the interaction between the crown and the methylpyridinium and relegate the macroring in an intermediate position in the axle, avoiding the dethreading process.

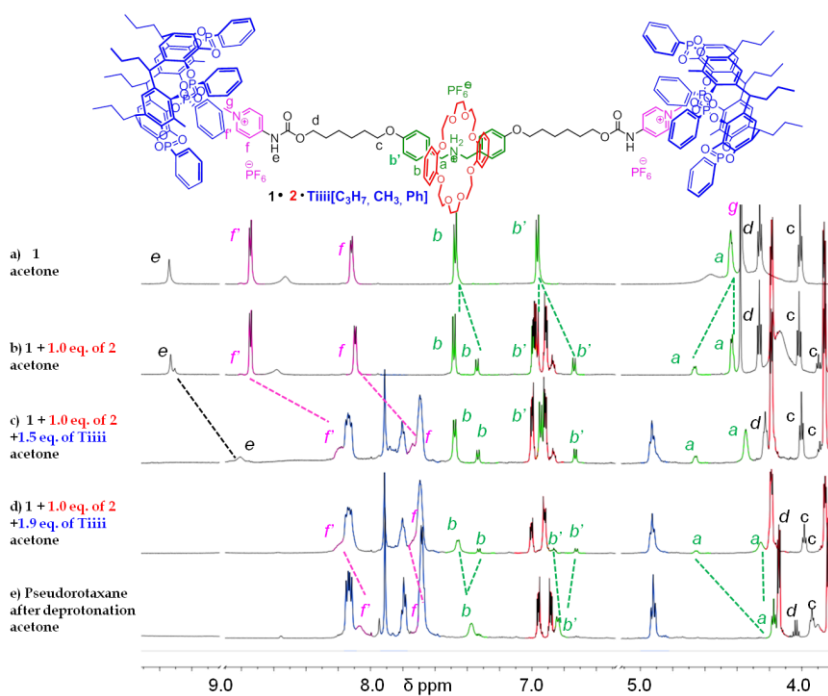


Figure 17. Relevant portions of the ^1H NMR spectra of a) the free axle **1**; b) **1** upon addition of 1.0 equivalent of **2**; c) after the addition of 1.5 equivalents of **Tiiiif**; d) upon addition of 1.9 equivalents of **Tiiiif**; e) upon deprotonation of the dibenzylammonium group.

^{31}P NMR (figure 18) confirmed the complexation properties of the tetraphosphonate cavitants also after the deprotonation of the internal ammonium group.

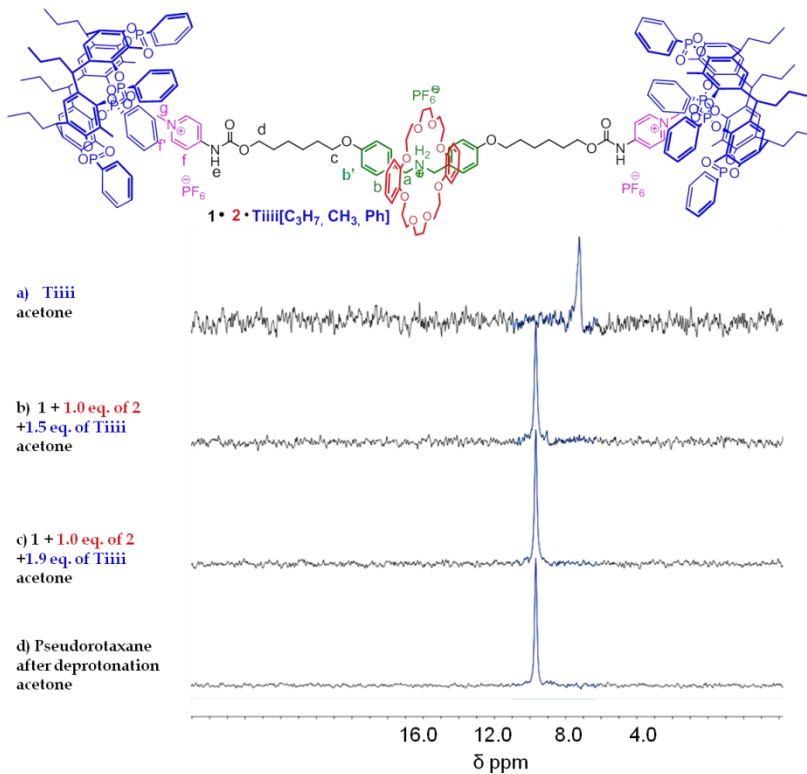


Figure 18. ^{31}P NMR of **Tiiii**: a) free **Tiiii**; b) axle + 1.0 equivalent of crown + 1.5 equivalents of **Tiiii**; c) axle + 1.0 equivalent of crown + 1.9 equivalents of **Tiiii**; d) pseudorotaxane after deprotonation.

3.3 CONCLUSIONS

This chapter reports the synthesis of a new axle and the assembly of a new type of cavitand-stopped rotaxane in which the stopping groups are linked to the axle by molecular recognition interactions.

The recognition processes of the axle with the crown ether and the cavitand were monitored by ^1H NMR and ^{31}P NMR, showing that the presence of the cavitand stoppers blocks the crown ether within the axle both in a acetonitrile/chloroform mixture and in acetone.

Studies performed in the acetonitrile/chloroform solution demonstrated that the deprotonation of the internal ammonium moiety and the consequent removal of the hydrogen bonding causes the complete dethreading of the crown ether when the stopping groups are absent. Instead, the presence of the cavitands bulky groups interacting via cation-dipole and CT interactions with the terminal methylpyridinium moieties prevents the dissociation of the pseudorotaxane intercomponents.

Studies performed in acetone showed that, without any stopping group, the treatment of the axle with a phosphazine base causes the shuttling of the crown ether from the central amino group to the ending methylpyridinium moiety, while the presence of the host stopping groups forces the macrocycle in an intermediate position between the two recognition sites.

This work demonstrated that a supramolecular pseudorotaxane can be assembled exclusively via host-guest interactions. The site specific recognition of cavitand hosts with the terminal groups of the axle overcomes not specific crown ether binding, relegating crown **2** on the central dibenzylammonium station, suppressing at the same time its dethreading.

Acknowledgements

This work has been carried out in the group of Prof. Leigh at the University of Edinburgh.

3. 4 EXPERIMENTAL SECTION

General Methods. Unless otherwise stated, all reagents were purchased from commercial sources and used without further purification. Dry CH_2Cl_2 , CD_3CN , and THF were obtained by passing the solvent (HPLC grade) through an activated alumina column on a PureSolv™ solvent purification system (Innovative Technologies, Inc., MA). Dry DMF and MeOH were purchased from Sigma-Aldrich. Flash column chromatography was carried out using Kieselgel C60 (Merck, Germany) as the stationary phase. All commercial reagents were ACS reagent grade and used as received. Analytical TLC was performed on precoated silica gel plates (0.25 mm thick, 60F254, Merck, Germany) and observed under UV light. All ^1H and ^{13}C NMR spectra were recorded on Bruker AV 400, AV 500 (cryoprobe), at a constant temperature of 298 K. Titrations experiments were recorded on Bruker and Varian 600. Chemical shifts are reported in parts per million and referenced to residual solvent. Coupling constants (J) are reported in Hertz (Hz). Mass spectrometric analysis was carried out by the mass spectrometry services at the University of Edinburgh.

Compound I

4-Hydroxybenzonitrile (0.8 g, 6.72 mmol) and K_2CO_3 (1.86 g, 13.43 mmol) were dissolved in 50 mL of dry acetonitrile and put on reflux for 30 minutes. 6-bromo-1-hexanol (1.10 mL, 8.06 mmol) was then added and the resulting mixture was stirred overnight at reflux. The solvent was removed under reduced pressure, the crude was extracted with CH_2Cl_2 and washed 3 times with water. The organics were collected, dried over Na_2SO_4 , filtrated and evaporated under reduced pressure. The crude was then subjected to flash chromatography on silica gel (9:1 $\text{CH}_2\text{Cl}_2/\text{Et}_2\text{O}$ v/v), to give the desired compound as an oily substance prone to crystallize in 85% yield.

$^1\text{H-NMR}$ (CDCl_3 , 400 MHz): δ (ppm) 7.60 (d, 2H, **aromatic**, $J = 8.9$ Hz), 6.96 (d, 2H, **aromatic**, $J = 8.9$ Hz), 4.04 (t, 2H, CH_2OAr , $J = 6.5$ Hz), 3.71 (m, 2H, CH_2OH), 1.87-1.81 (m, 2H, $\text{CH}_2\text{CH}_2\text{OAr}$), 1.66-1.59 (m, 2H, $\text{CH}_2\text{CH}_2\text{OH}$), 1.54-1.44 (m, 4H, $\text{CH}_2\text{CH}_2\text{CH}_2\text{CH}_2\text{OAr}$). **ESI-MS**: m/z 242.4 [$\text{M}+\text{Na}$] $^+$.

Compound II

To a stirring solution of derivative **I** (890 mg, 4.05 mmol) in dry THF (25 mL), LiAlH_4 (770 mg, 20.27 mmol) was added at 0°C and the resulting mixture was stirred overnight at room temperature under N_2 . After another addition of

3 equivalents of LiAlH_4 at 0°C , the reaction was allowed to stir at room temperature for 24 hours more. Water saturated crystals of Na_2SO_4 were then added and the resulting mixture was stirred at room temperature for 20 minutes, until all the LiAlH_4 turned into a white color. Then more Na_2SO_4 (powder) was added to get rid of the water in excess. The salts were filtered off and washed several times with THF. The organics were collected and evaporated. The product was purified by column chromatography on silica gel, eluting with MeOH/ NH_3 99/1 (v/v). Product was isolated as a white powder with a 73% yield.

$^1\text{H-NMR}$ (CDCl_3 , 400 MHz): δ (ppm) 7.24 (d, 2H, **aromatic**, $J = 8.6$ Hz), 6.89 (d, 2H, **aromatic**, $J = 8.6$ Hz), 3.99 (t, 2H, CH_2OAr , $J = 6.5$ Hz), 3.82 (s, 2H, CH_2NH_2), 3.69 (t, 2H, CH_2OH , $J = 6.5$ Hz), 1.85-1.78 (m, 2H, $\text{CH}_2\text{CH}_2\text{OAr}$), 1.66-1.59 (m, 2H, $\text{CH}_2\text{CH}_2\text{OH}$), 1.54-1.45 (m, 4H, $\text{CH}_2\text{CH}_2\text{CH}_2\text{CH}_2\text{OAr}$). **ESI-MS:** m/z 224.5 $[\text{M}+\text{H}]^+$.

Compound III

p-Hydroxybenzaldehyde (1 g, 8.19 mmol) was dissolved in 20 mL of dry DMF, then K_2CO_3 (1.70 g, 12.28 mmol) was added. The resulting solution was stirred at 80°C for 15 minutes, then cooled down to room temperature. 6-Bromo-1-hexanol (1.180 mL, 9.01 mmol) was then added dropwise and the mixture was heated again at 80°C . After 4 hours other 0.7 equivalents of base were added and the solution was stirred overnight at 80°C . The reaction was cooled to room temperature and 30 mL of ice cold water were added to the reaction mixture. The crude was extracted with diethyl ether, washed with NaOH 1 M, then twice with water and dried over Na_2SO_4 . After filtration and evaporation of the organics, crude product was then purified by column chromatography eluting with dichloromethane/diethyl ether 9/1 (v/v) to afford the 4-(6-hydroxyalkyl-1-oxy)benzaldehyde as an oily substance with a 93% yield.

$^1\text{H-NMR}$ (CDCl_3 , 400 MHz): δ (ppm) 9.91 (s, 1H, ArCHO), 7.87 (d, 2H, **aromatic**, $J = 8.8$ Hz), 7.03 (d, 2H, **aromatic**, $J = 8.7$ Hz), 4.10 (t, 2H, CH_2OAr , $J = 6.5$ Hz), 3.72 (t, 2H, CH_2OH , $J = 6.5$ Hz), 1.90-1.84 (m, 2H, $\text{CH}_2\text{CH}_2\text{OAr}$), 1.68-1.61 (m, 2H, $\text{CH}_2\text{CH}_2\text{OH}$), 1.57-1.44 (m, 4H, $\text{CH}_2\text{CH}_2\text{CH}_2\text{CH}_2\text{OAr}$). **ESI-MS:** m/z 223.4 $[\text{MH}^+]$, 245.4 $[\text{M}+\text{Na}]^+$.

Compound IV

Compounds **II** (720 mg, 3.22 mmol) and **III** (716 mg, 3.22 mmol) were dissolved in 14 mL of CHCl_3 and stirred for 2 hours at room temperature. The

solution was concentrated and dried under reduced pressure to give the imine intermediate as a yellowish spongy solid without further purifications. To a stirring solution of imine in 8 mL of dry methanol, NaBH₄ (365 mg, 9.66 mmol) was added in portions under N₂. The reaction was allowed to stir at room temperature for other 3 hours. The solvent was removed under reduced pressure and ammonia (35% v/v) was added. Crude was extracted with ethyl acetate (3 times) and washed with water (2 times). Organics were collected, dried over Na₂SO₄, filtrated and concentrated under vacuum. Crude was then subjected to column chromatography on silica gel eluting 9/1 CH₂Cl₂/MeOH v/v, affording the pure product as a white powder with a 75% yield.

¹H-NMR (CDCl₃, 400 MHz): δ (ppm) 7.25 (d, 4H, **aromatic**, J = 8.6 Hz), 6.90 (d, 4H, **aromatic**, J = 8.6 Hz), 4.0 (t, 4H, CH₂OAr, J = 6.4 Hz), 3.69 (s, 4H, CH₂NH₂), 3.59 (t, 4H, CH₂OH, J = 6.5 Hz), 1.81-1.78 (m, 4H, CH₂CH₂OAr), 1.61-1.51 (m, 12H, CH₂CH₂OH; CH₂CH₂CH₂CH₂OAr). **ESI-MS:** m/z 430.7 [M+H]⁺.

Compound V

To a stirring solution of compound **IV** (900 mg, 2.09 mmol) in 20 mL of dry dichloromethane, a BOC solution (502 mg, 2.30 mmol in 5 ml of CH₂Cl₂) and triethylamine (440 μL, 3.15 mmol) were added. The reaction was allowed to stir overnight at room temperature under N₂. The solution was concentrated under vacuum to afford the pure product as an oil with a 80% yield without further purification.

¹H-NMR (CDCl₃, 400 MHz): δ (ppm) 7.14 (bd, 4H, **aromatic**), 6.87 (d, 4H, **aromatic**, J = 8.6 Hz), 4.32 (bs, 4H, CH₂NH), 3.99 (t, 4H, CH₂OAr, J = 6.4 Hz), 3.65 (t, 4H, CH₂OH, J = 6.5 Hz), 1.85-1.78 (m, 4H, CH₂CH₂OAr), 1.66-1.59 (m, 4H, CH₂CH₂OH), 1.51-1.46 (m, 17H, CH₂CH₂CH₂CH₂OAr; (O)C(CH₃)₃). **ESI-MS:** m/z 530.7 [MH⁺], 552.7 [M+Na]⁺.

Compound VI

To a stirring solution of isonicotinic acid (3g, 24.37 mmol) and triethylamine (3.6 mL, 25.59 mmol) in dry acetonitrile (20 mL), diphenylphosphoryl azide (dppa, 5.43 mL, 25.59 mmol) was slowly added at 0°C under a stream of N₂. The resulting mixture was stirred at 0°C for 30 minutes, then heated at 75°C for 2 hours. The reaction was cooled down to room temperature and the resulting precipitate was collected by filtration and washed with ethyl acetate affording the product as a yellow powder without further purification.

In order to verify its structure and its reactivity, the isocyanate was reacted with compound **I**. To a stirring solution of compound **I** (182 mg, 0.83 mmol) and triethylamine (116 μ L, 0.83 mmol) in dry DMF (1 mL), isocyanate **VI** was added under nitrogen. The solution was stirred at room temperature overnight. The solvent was evaporated under reduced pressure and the crude was purified on a column chromatography on silica gel eluting with $\text{CH}_2\text{Cl}_2/\text{MeOH}$ (95/5, v/v) to give the desired carbamate product with a 60% yield.

$^1\text{H-NMR}$ (CDCl_3 , 400 MHz): δ (ppm) 8.48 (bd, 2H, **aromatic**), 7.60 (d, 2H, **aromatic**, $J = 8.0$ Hz), 7.40 (d, 2H, **aromatic**, $J = 5$ Hz), 6.96 (d, 2H, **aromatic**, $J = 8.0$ Hz), 4.25 (t, 2H, $\text{CH}_2\text{OC}(\text{O})\text{NH}$, $J = 6.7$), 4.03 (t, 2H, CH_2OAr , $J = 6.4$ Hz), 1.86-1.83 (m, 2H, $\text{CH}_2\text{CH}_2\text{OC}(\text{O})\text{NH}$), 1.77-1.75 (m, 2H, $\text{CH}_2\text{CH}_2\text{OAr}$), 1.55-1.48 (m, 4H, $\text{CH}_2\text{CH}_2\text{CH}_2\text{CH}_2\text{OAr}$). **ESI-MS:** m/z 340.36 $[\text{M}+\text{H}]^+$, 362.29 $[\text{M}+\text{Na}]^+$.

Compound VII

Compound **V** (600 mg, 1.13 mmol) and triethylamine (395 μ L, 2.80 mmol) were dissolved in 6 mL of dry dichloromethane, then isocyanate **VI** (326 mg, 2.72 mmol) was added. The solution was stirred overnight at room temperature under argon. The solvent was evaporated under reduced pressure and the crude was subjected to column chromatography on silica gel eluting with $\text{CH}_2\text{Cl}_2/\text{MeOH}$ (95/5, v/v), to give the desired compound as a white solid with a yield of 61%.

$^1\text{H-NMR}$ (CDCl_3 , 400 MHz): δ (ppm) 8.47 (d, 4H, **aromatic**, $J = 6.2$ Hz), 7.49 (d, 4H, **aromatic**, $J = 6.2$ Hz), 7.13 (bd, 4H, **aromatic**), 6.87 (d, 4H, **aromatic**, $J = 8.6$ Hz), 4.33 (bs, 4H, CH_2NH), 4.26 (t, 4H, $\text{CH}_2\text{OC}(\text{O})\text{NH}$, $J = 6.7$ Hz), 4.00 (t, 4H, CH_2OAr , $J = 6.6$ Hz), 1.86-1.79 (m, 4H, $\text{CH}_2\text{CH}_2\text{OC}(\text{O})\text{NH}$), 1.59-1.45 (m, 4H, $\text{CH}_2\text{CH}_2\text{OAr}$), (m, 17H, $\text{CH}_2\text{CH}_2\text{CH}_2\text{CH}_2\text{OAr}$; $(\text{O})\text{C}(\text{CH}_3)_3$). **ESI-MS:** m/z 770.5 $[\text{M}+\text{H}]^+$.

Compound VII

To a stirring solution of compound **VI** (250 mg, 0.32 mmol) in dichloromethane, methyl iodide (303 μ L, 4.87 mmol) was added dropwise. The resulting mixture was heated at 50°C while stirring overnight. The solution was concentrated under reduced pressure affording compound **VII** quantitatively.

$^1\text{H-NMR}$ (MeOD , 400 MHz): δ (ppm) 8.58 (d, 4H, **aromatic**, $J = 7.4$ Hz), 7.98 (d, 4H, **aromatic**, $J = 7.2$ Hz), 7.14 (bd, 4H, **aromatic**), 6.89 (d, 4H, **aromatic**, $J = 8.6$ Hz), 4.32-4.28 (m, 8H, CH_2NH ; $\text{CH}_2\text{OC}(\text{O})\text{NH}$), 4.21 (s, 6H, N^+CH_3), 4.01 (t, 4H, CH_2OAr , $J = 6.3$ Hz), 1.84-1.78 (m, 8H, $\text{CH}_2\text{CH}_2\text{OC}(\text{O})\text{NH}$; $\text{CH}_2\text{CH}_2\text{OAr}$), 1.56-1.31 (m, 17H, $\text{CH}_2\text{CH}_2\text{CH}_2\text{CH}_2\text{OAr}$; $(\text{O})\text{C}(\text{CH}_3)_3$). **ESI-MS:** m/z 399.4 $[\text{M}]^{2+}$.

Compound VIII

Compound **VII** (282 mg, 0.27 mmol) was dissolved in a 11 mL mixture of H₂O/acetone/MeOH (5/4/2, v/v/v). KPF₆ (739 mg, 4.05 mmol) was then added and the resulting mixture was stirred at room temperature overnight. The solution was concentrated under vacuum and the product was extracted with dichloromethane (5 times). The organics were evaporated under reduced pressure affording pure product **VIII** with a quantitative yield.

¹H-NMR (CD₃CN, 400 MHz): δ (ppm) 8.33 (d, 4H, **aromatic**, J = 7.3 Hz), 7.93 (d, 4H, **aromatic**, J = 7.3 Hz), 7.18 (d, 4H, **aromatic**, J = 8.7 Hz), 6.91 (d, 4H, **aromatic**, J = 8.7 Hz), 4.29-4.25 (m, 8H, CH₂NH; CH₂OC(O)NH), 4.12 (s, 6H, N⁺CH₃), 4.07 (t, 4H, CH₂OAr, J = 6.5 Hz), 1.83-1.72 (m, 8H, CH₂CH₂OC(O)NH; CH₂CH₂OAr), 1.55-1.48 (m, 17H, CH₂CH₂CH₂CH₂OAr; (O)C(CH₃)₃). ³¹P-NMR (CD₃CN, 162 MHz): δ (ppm) -131.52, -135.87, -140.21, -144.58, -148.97, -153.33, -157.70 (2P, PF₆⁻). ESI-MS: m/z 400.0 [M]²⁺.

Compound IX

To a stirring solution of compound **VIII** (295 mg, 0.27 mmol) in a mixture of 10 mL of dichloromethane and 5 mL of methanol, trifluoroacetic acid (TFA, 20% v/v) was added. The reaction was stirred at room temperature for 2.5 hours at room temperature. The solution was concentrated under reduced pressure and the product was suspended in an aqueous solution of NaHCO₃ and extracted with 4 washes of dichloromethane. The organics were collected and evaporated in vacuo affording the pure product **IX** in quantitative yield.

¹H-NMR (MeOD, 400 MHz): δ (ppm) 8.56 (d, 4H, **aromatic**, J = 7.3 Hz), 7.98 (d, 4H, **aromatic**, J = 7.1 Hz), 7.40 (d, 4H, **aromatic**, J = 8.6 Hz), 7.01 (d, 4H, **aromatic**, J = 8.6 Hz), 4.31 (t, 4H, CH₂OC(O)NH, J = 6.7 Hz), 4.20, (s, 6H, N⁺CH₃), 4.14 (s, 8H, CH₂NH), 4.04 (t, 4H, CH₂OAr, J = 6.3 Hz), 1.83-1.79 (m, 8H, CH₂CH₂OC(O)NH; CH₂CH₂OAr), 1.55-1.53 (m, 8H, CH₂CH₂CH₂CH₂OAr). ³¹P-NMR (MeOD, 162 MHz): δ (ppm) -131.48, -135.83, -140.20, -144.58, -148.94, -153.32, -157.73, (2P, PF₆⁻). ESI-MS: m/z 350.0 [M]²⁺.

Compound X

Compound **IX** (268 mg, 0.27 mmol) was dissolved in a mixture of dichloromethane (10 mL) and acetonitrile (4 mL). HCl 37% was then added dropwise, until the neutralization of the solution. The resulting mixture was stirred for 30 minutes more, and a white suspension was obtained. The solution was concentrated under reduced pressure and washed with dichloromethane, affording the pure product quantitatively.

¹H-NMR (MeOD, 400 MHz): δ (ppm) 8.58 (d, 4H, **aromatic**, $J = 7.1$ Hz), 7.99 (d, 4H, **aromatic**, $J = 7.3$ Hz), 7.43 (d, 4H, **aromatic**, $J = 8.7$ Hz), 7.01 (d, 4H, **aromatic**, $J = 8.6$ Hz), 4.32 (t, 4H, **CH₂OC(O)NH**, $J = 6.6$ Hz), 4.21, (s, 6H, **N⁺CH₃**), 4.16 (s, 8H, **CH₂NH**), 4.05 (t, 4H, **CH₂OAr**, $J = 6.3$ Hz), 1.83-1.78 (m, 8H, **CH₂CH₂OC(O)NH; CH₂CH₂OAr**), 1.56-1.55 (m, 8H, **CH₂CH₂CH₂CH₂OAr**). **ESI-MS:** m/z 350.0 **[M-H]²⁺**.

Compound 1

Compound X (278 mg, 0.27 mmol) was dissolved in a 11 mL mixture of H₂O/acetone/MeOH (5/4/2, v/v/v). KPF₆ (748 mg, 4.06 mmol) was then added and the resulting mixture was stirred at room temperature overnight. The solution was concentrated under vacuum and the product was extracted with dichloromethane (5 times). The organics were evaporated under reduced pressure affording pure product 1 with a quantitative yield.

¹H-NMR (CD₃CN, 400 MHz): δ (ppm) 9.01 (s, 2H, **OC(O)NH**), 8.33 (d, 4H, **aromatic**, $J = 7.3$ Hz), 7.93 (d, 4H, **aromatic**, $J = 7.2$ Hz), 7.41 (d, 4H, **aromatic**, $J = 8.6$ Hz), 7.00 (d, 4H, **aromatic**, $J = 8.6$ Hz), 4.28 (t, 4H, **CH₂OC(O)NH**, $J = 6.6$ Hz), 4.17, (t, 6H, **N⁺CH₃**, $J = 6.2$ Hz), 4.12 (s, 8H, **CH₂NH**), 4.05 (t, 4H, **CH₂OAr**, $J = 6.5$ Hz), 1.85-1.72 (m, 8H, **CH₂CH₂OC(O)NH; CH₂CH₂OAr**), 1.53-1.51 (m, 8H, **CH₂CH₂CH₂CH₂OAr**). **³¹P-NMR (CD₃CN, 162 MHz):** δ (ppm) -131.51, -135.87, -140.24, -144.58, -148.97, -153.33, -157.69, (2P, **PF₆**). **ESI-MS:** m/z 350.17 **[M-H]²⁺**.

3.5 REFERENCES

- ¹ a) Tullo, A. *Chem. Eng. News* **2006**, *84*, 22-23; b) Thompson, S. E.; Parthasarathy, S. *Materials Today* **2006**, *9*, 20-25.
- ² www.intel.com/pressroom/archive/releases/20060125comp.htm.
- ³ Goodsell, D. S. *Bionanotechnology—Lessons from Nature* **2004**, Wiley, New York;
- ⁴ For complete reviews and interesting articles on molecular machines and devices see: a) Balzani, V.; Credi, A.; Raymo, F. M.; Stoddard, J. F. *Angew. Chem. Int. Ed.* **2000**, *39*, 3348-3391; b) Balzani, V.; Credi, A.; Venturi, M. *Nanotoday* **2007**, *2*, 18-25; c) Balzani, V.; Credi, A.; Venturi, M. *Molecular Devices and Machines – Concepts and Perspectives for the Nanoworld*, Wiley-VCH, Weinheim, **2008**; d) Browne, W. R.; Feringa, B. L. *Nat. Nanotechnol.* **2006**, *1*, 25-35; e) Kay, E. R.; Leigh, D. A.; Zerbetto, F. *Angew. Chem. Int. Ed.* **2007**, *46*, 72-191
- ⁵ a) Feynman, R. P. *Eng. Sci.* **1960**, *23*, 22-36; b) Feynman, R. P. *Saturday Rev.* **1960**, *43*, 45-47.
- ⁶ Shinkaim S.; Manabe, T. *Top. Curr. Chem.* **1984**, *121*, 76-104.
- ⁷ Binnig, G.; Rohrer, *Angew. Chem. Int. Ed.* **1987**, *26*, 606-614.
- ⁸ a) Lehn, J.-M. *Angew. Chem. Int. Ed.* **1988**, *27*, 89-112; b) Pedersen, C. J. *Angew. Chem. Int. Ed.* **1988**, 1021-1027; c) Cram, D. J. *Angew. Chem. Int. Ed.* **1988**, *27*, 1009-1020.
- ⁹ a) Deisenhofer, J.; Michel H. *Angew. Chem. Int. Ed.* **1989**, *28*, 829-847; b) Huber, R. *Angew. Chem. Int. Ed.* **1989**, *28*, 869-882; c) Boyer, P. D. *Angew. Chem. Int. Ed.* **1998**, *37*, 2296-2307; d) Walker, J. E. *Angew. Chem. Int. Ed.* **1998**, *37*, 2308-2319; e) Skou, J. C. *Angew. Chem. Int. Ed.* **1998**, *37*, 2320-2328.
- ¹⁰ Marcus, R. A. *Angew. Chem. Int. Ed.* **1993**, *32*, 1111-1121.

- ¹¹a) *Molecular Electronics Devices* (Ed. Carter, F. L.), Dekker, New York **1982**; b) *Molecular Electronics-Science and Technology* (Ed. Aviram, A.), American Institute of Physics, Washington **1992**; c) *Chem. Rev.* **1999**, *99*, 1641-1990 (special issue on nanostructures); d) *Acc. Chem. Res.* **1999**, *32*, 387-454 (special issue on nanoscale materials).
- ¹²a) Schill, *Catenanes, Rotaxanes and Knots*, Academic Press, New York, **1971**; b) *Molecular Catenanes, Rotaxanes and Knots* (Eds.: Sauvage, J.-P.; Dietrich-Buchecker, C. O.), Wiley-VCH, Weinheim, **1999**; c) Walba, D. M. *Tetrahedron* **1985**, *41*, 3161-3212; d) Dietrich-Buchecker, C. O.; Sauvage, J.-P. *Chem. Rev.* **1987**, *87*, 795-810; e) Dietrich-Buchecker, C. O.; Sauvage, J.-P. *Bioorg. Chem. Front.* **1991**, *2*, 195-248; f) Chambron, J. C.; Dietrich-Buchecker, C. O.; Sauvage, J.-P. *Top. Curr. Chem.* **1993**, *165*, 131-162; g) Gibson, H. W.; Marand, H. *Adv. Mater.* **1993**, *5*, 11-21; h) Gibson, H. W.; Bheda, M. C.; Engen, P. T. *Prog. Polym. Sci.* **1994**, *19*, 843-945; i) Amabilino, D. B.; Parsons, I. W.; Stoddart, J. F. *Trends Polym. Sci.* **1994**, *2*, 146-52; j) Amabilino, D. B.; Stoddart, J. F. *Chem. Rev.* **1995**, *95*, 2725-2828; k) H. W. Gibson in *Large Ring Molecules* (Ed.: Semlyen, J. A.), Wiley, New York, **1996**, 191-202; l) Belohradsky, M.; Raymo, F. M.; Stoddart, J. F. *Collect. Czech. Chem. Commun.* **1996**, *61*, 1-43; m) Raymo, F. M.; Stoddart, J. F. *Trends Polym. Sci.* **1996**, *4*, 208-211; n) Belohradsky, M.; Raymo, F. M.; Stoddart, J. F. *Collect. Czech. Chem. Commun.* **1997**, *62*, 527-557; o) Jäger, R.; Vögtle, F. *Angew. Chem. Int. Ed. Engl.* **1997**, *36*, 930-944; p) Raymo, F. M.; Stoddart, J. F. *CHEMTRACTS: Org. Chem.* **1998**, *11*, 491-511; q) Raymo, F. M.; Stoddart, J. F. *Chem. Rev.* **1999**, *99*, 1643-1664; r) Breault, G. A.; Hunter, C. A.; Mayers, P. C. *Tetrahedron* **1999**, *55*, 5265-5293; s) Seel, C.; Vögtle, F. *Chem. Eur. J.* **2000**, *6*, 21-24; t) Nielsen, M. B.; Lombolt, C.; Becher, J. *Chem. Soc. Rev.* **2000**, *29*, 153-164.
- ¹³Amabilino, D. B.; Ashton, P. R.; Pérez-García, L.; Stoddart, J. F. *Angew. Chem. Int. Ed. Engl.* **1995**, *34*, 2378-2380; b) Gillard, R. E.; Raymo, F. M.; Stoddart, J. F. *Chem. Eur. J.* **1997**, *3*, 1933-1940; c) Amabilino, D. B.; Ashton, P. R.; Stoddart, J. F.; White, A. J. P.; Williams, D. J. *Chem. Eur. J.* **1998**, *4*, 460-468; d) Cantrill, S. J.; Rowan, S. J.; Stoddart, J. F. *Org. Lett.* **1999**, *1*, 1363-1366; e) Rowan, S. J.; Stoddart, J. F. *Org. Lett.* **1999**, *1*, 1913-1916; f) Fujita, M.; Ibukuro, F.; Hagihara, H.; Ogura, K. *Nature* **1994**, *367*, 720-723; g) Mohr, B.; Weck, M.; Sauvage, J.-P.; Grubbs, R. H. *Angew. Chem. Int. Ed. Engl.* **1997**, *36*, 1301-1308; h) Weck, M.; Mohr, B.; Sauvage, J.-P.; Grubbs, R. H. *J. Org. Chem.* **1999**, *64*, 5463-5471; i) Fujita, M. F. *Acc. Chem. Res.* **1999**, *32*, 53-61; j) Ibukuro, F.; Fujita, M.;

- Yamaguchi, K.; Sauvage, J.-P. *J. Am. Chem. Soc.* **1999**, *121*, 11014-11015; k) Try, A. C.; Harding, M. M.; Hamilton, D. G.; Sanders, J. K. M. *Chem. Commun.* **1998**, 723-724; l) Kidd, T. J.; Leigh, D. A.; Wilson, A. J. *J. Am. Chem. Soc.* **1999**, *121*, 1599-1600; m) Baer, A. J.; Macartney, D. H. *Inorg. Chem.* **2000**, *39*, 1410-1517; n) Chichak, K.; Walsh, M. C.; Branda, N. R. *Chem. Commun.* **2000**, 847-848; o) Jeong, K.-S.; Choi, J. S.; Chang, S. Y.; Chang, H. Y. *Angew. Chem. Int. Ed.* **2000**, *39*, 1692-1695.
- ¹⁴Fyfe, M. C. T.; Stoddard, J. F. *Acc. Chem. Res.* **1997**, *30*, 393-401.
- ¹⁵a) Lindsey, J. S. *New J. Chem.* **1991**, *15*, 153-180; b) Whitesides, G. M.; Mathias, J. P.; Seto, C. T. *Science* **1991**, *254*, 1312-1319; c) Philp, D.; Stoddard, J. F. *Synlett* **1991**, 445-458; d) Whitesides, G. M.; Simanck, E. E.; Mathias, J. P.; Seto, C.T.; Chin, D. N.; Mammen, M.; Gordon, D. M. *Acc. Chem. Rev.* **1995**, *28*, 37-44; e) Philp, D.; Stoddard, J. F. *Angew. Chem. Int. Ed.* **1996**, *35*, 1155-1196; f) Rebek, Jr. *J. Chem. Soc. Rev.* **1996**, *25*, 255-264; g) Conn, M. M.; Rebek, Jr. *J. Chem. Rev.* **1997**, *97*, 1647-1668; h) Rebek, Jr. *Acc. Chem. Res.* **1999**, *32*, 278-286; i) Fyfe, M. C. T.; Stoddard, J. F. *Adv. Supramol. Chem.* **1999**, *5*, 1-53; j) Fyfe, M. C. T.; Stoddard, J. F. *Coord. Chem. Rev.* **1999**, *183*, 139-155; k) Gracias, D. H.; Tien, J.; Breen, T. L.; Hsy, C.; Whitesides, G. M. *Science* **2000**, *289*, 1170-1172.
- ¹⁶a) Berná, J.; Leigh, D. A.; Lubomska, M.; Mendoza, S. M.; Pérez, E. M.; Rudolf, P.; Teobaldi, G.; Zerbetto, F. *Nat. Mater.* **2005**, *4*, 704; (b) Green, J. E.; Choi, J. W.; Boukai, A.; Bunimovich, Y.; Johnston-Halperin, E.; Delonno, E.; Luo, Y.; Sheriff, B. A.; Xu, K.; Shin, Y. S.; Tseng, H.-R.; Stoddard, J. F. Heath, J. R. *Nature* **2007**, *445*, 414; (c) Panman, M. R.; Bodis, R.; Shaw, D. J.; Bakker, B. H.; Newton, A. C.; Kay, E. R.; Brouwer, A. M.; Buma, W. J.; Leigh, D. A.; Woutersen, S. *Science* **2010**, *328*, 1255; (d) Zhang, Z.-J.; Zhang, H.-J.; Wang, H.; Liu, Y. *Angew. Chem. Int. Ed.* **2011**, *50*, 10834.
- ¹⁷Vlivoreil, A.; Dietrich-Buchecker, C. O.; Sauvage, J.-P. *J. Am. Chem. Soc.* **1994**, *116*, 9399-9400.
- ¹⁸a) Anelli, P. L.; Spencer, N.; Stoddard, J.-F. *J. Am. Chem. Soc.* **1991**, *113*, 5131-5133; b) Anelli, P. L.; Asakawa, M.; Ashton, P. R.; Bissell, R. A.; Clavier, G.; Gorski, R.; Kaifer, A. E.; Langford, S. J.; Mattersteig, G.; Menzer, S.; Philp, D.; Slawin, A. M. Z.; Spencer, N.; Stoddard, J. F.; Tolley, M. S.; Williams, D. J. *Chem.*

Eur. J. **1997**, *3*, 1113-1135. For an interesting quantum-mechanical description of the shuttling process associated with a [2]rotaxane, see Leigh, D. A.; Troisi, A.; Zerbetto, F.; *Angew. Chem. Int. Ed.* **2000**, *39*, 350-353.

¹⁹Badjic, J. D.; Ronconi, C. M.; Stoddard, J. F.; Balzani, V.; Silvi, S.; Credi, A. J. *Am. Chem. Soc.*, **2006**, 1489-1499.

²⁰Astumian, R. D. *Proc. Natl. Acad. Sci. U.S.A.* **2005**, *102*, 1843-1847.

²¹a) Collier, C. P.; Wong, E. W.; Belohradsky', M.; Raymo, F. M.; Stoddard, J. F.; Kuekes, P. J.; Williams, R. S.; Heath, J. R. *Science* **1999**, *285*, 391-394; b) Avellini, T.; Li, H.; Coskun, A.; Barin, G.; Trabolsi, A.; Basuray, A. N.; Dey, S. K.; Credi, A.; Silvi, S.; Stoddard, J. F.; Venturi, M. *Angew. Chem. Int. Ed.* **2012**, *51*, 1611-1615.

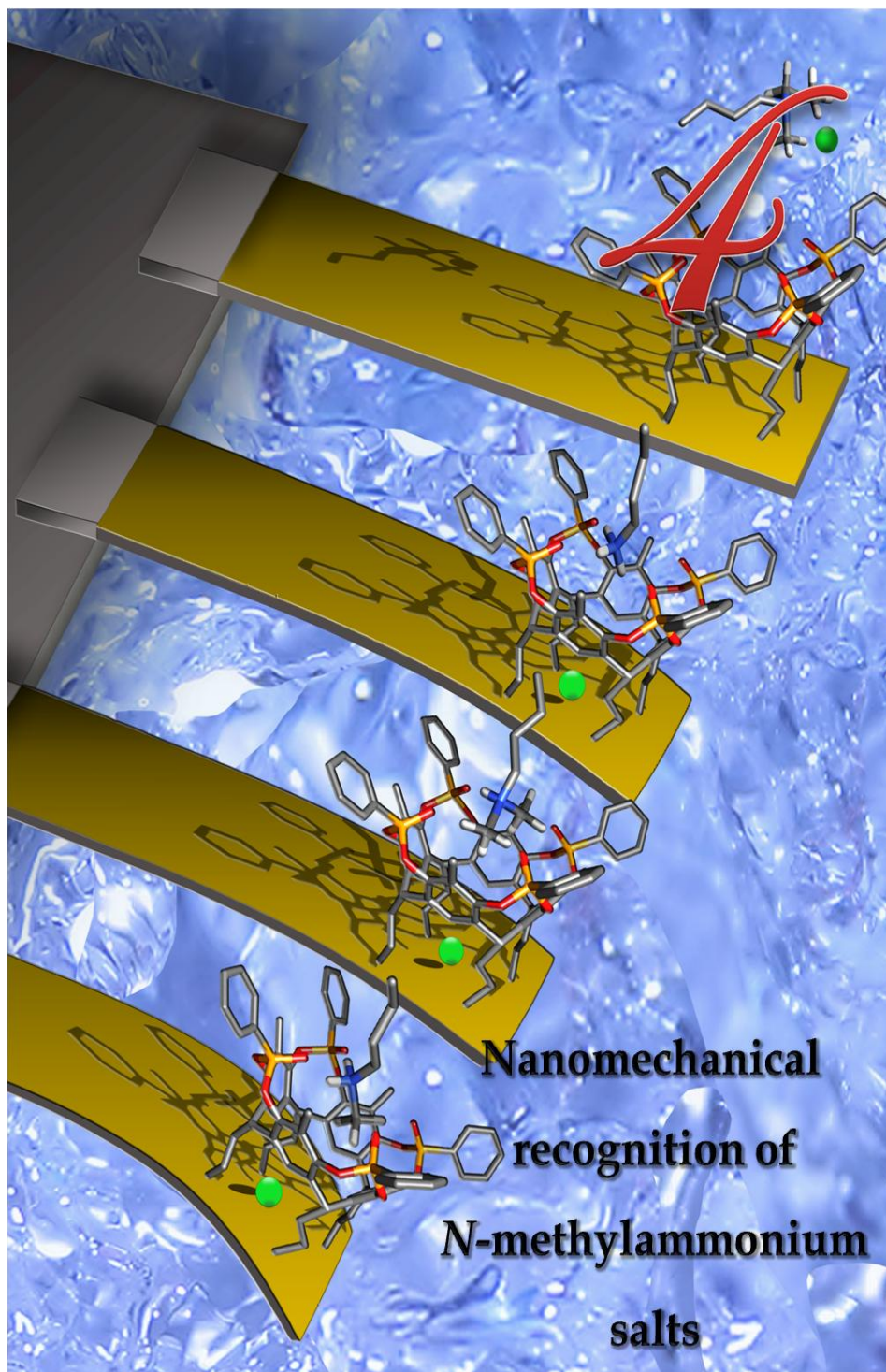
²²a) Berná, J.; Leigh, D. A.; Lubomska, M.; Mendoza, S. M.; Pérez, E. M.; Rudolf, P.; Teobaldi, G.; Zerbetto, F. *Nat. Mater.* **2005**, *4*, 704-710; b) Juluri, B. K.; Kumar, A. S.; Liu, Y.; Ye, T.; Yang, Y.-W.; Flood, A. H.; Fang, L.; Stoddard, J. F.; Weiss, P. S.; Huang, T. J. *ACS Nano* **2009**, *3*, 291-300; c) Lussis, P.; Svaldo-Lanero, T.; Bertocco, A.; Fustin, C.-A.; Leigh, D. L.; Duwez, A.-S. *Nat. Nanotechnol.* **2011**, *6*, 553-557.

²³a) Ge, Z.; Hu, J.; Huang, F.; Liu, S. *Angew. Chem. Int. Ed.* **2009**, *48*, 1798-1802; b) Hsueh, S.-Y.; Kuo, C.-T.; Lu, T.-W.; Lai, C.-C.; Liu, Y.-H.; Hsu, H.-F.; Peng, S.-M.; Chen, C.-H.; Chiu, S.-H. *Angew. Chem. Int. Ed.* **2010**, *49*, 9170-9173.

²⁴a) Pérez, E. M.; Dryden, D. T. F.; Leigh, D. A.; Teobaldi, G.; Zerbetto, F. *J. Am. Chem. Soc.* **2004**, *126*, 12210-12211; b) Wang, Q.-C.; Qu, D.-H.; Ren, J.; Chen, K.; Tian, H. *Angew. Chem. Int. Ed.* **2004**, *43*, 2661-2665; c) Leigh, D. A.; Morales, M. Á. F.; Pérez, E. M.; Wong, J. K. Y.; Saiz, C. G.; Slawin, A. M. Z.; Carmichael, A. J.; Haddleton, D. M.; Brouwer, A. M.; Buma, W. J.; Wurfel, G. W. H.; León, S.; Zerbetto, F. *Angew. Chem. Int. Ed.* **2005**, *44*, 3062-3067; d) Li, Y. J.; Li, H.; Li, Y. L.; Liu, H. B.; Wang, S.; He, X. R.; Wang, N.; Zhu, D. B. *Org. Lett.* **2005**, *7*, 4835-4838; e) Zhou, W.; Li, J.; He, X.; Li, C.; Lv, J.; Li, Y.; Wang, S.; Liu, H.; Zhu, D. *Chem. Eur. J.* **2008**, *14*, 754-763; f) Gassensmith, J. J.; Matthys, S.; Lee, J.-J.; Wojcik, A.; Kamat, P.; Smith, B. D. *Chem. Eur. J.* **2010**, *16*, 2916-2921.

- ²⁵Bottari, G.; Leigh, D. A.; Pérez, E. M. *J. Am. Chem. Soc.* **2003**, *125*, 13360-13361.
- ²⁶a) Marlin, D. S.; González Cabrera, D.; Leigh, D. A.; Slawin, A. M. Z. *Angew. Chem. Int. Ed.* **2006**, *45*, 77 – 83; b) Marlin, D. S.; González Cabrera, D.; Leigh, D. A.; Slawin, A. M. Z. *Angew. Chem. Int. Ed.* **2006**, *45*, 1385-1390; c) Lin, C. F.; Lai, C.-C.; Liu, Y.-H.; Peng, S.-M.; Chiu, S.-H. *Chem. Eur. J.* **2007**, *13*, 4350-4355; d) Huang, Y.-L.; Hung, W.-C.; Lai, C.-C.; Liu, Y.-H.; Peng, S.-M.; Chiu, S.-H. *Angew. Chem. Int. Ed.* **2007**, *46*, 6629 – 6633; e) Mullen, K. M.; Davis, J. J.; Beer, P. D. *New J. Chem.* **2009**, *33*, 769-776; f) Serpell, C. J.; Chall, R.; Thompson, A. L.; Beer, P. D. *Dalton Trans.* **2011**, *40*, 12052-12055.
- ²⁷a) Nguyen, T. D.; Tseng, H.-R.; Celestre, P. C.; Flood, A. H.; Liu, Y.; Stoddart, J. F.; Zink, J. I. *Proc. Natl. Acad. Sci. USA* **2005**, *102*, 10029-10034; b) Fernandes, A.; Viterisi, A.; Coutrot, F.; Potok, S.; Leigh, D. A.; Aucagne, V.; Papot, S. *Angew. Chem. Int. Ed.* **2009**, *48*, 6443-6447; c) Ferris, D. P.; Zhao, Y.-L.; Khashab, N. M.; Khatib, H. A.; Stoddart, J. F.; Zink, J. I. *J. Am. Chem. Soc.* **2009**, *131*, 1686-1688; d) Fernandes, A.; Viterisi, A.; Aucagne, V.; Leigh, D. A.; Papot, S. *Chem. Commun.* **2012**, *48*, 2083-2085.
- ²⁸Blanco, V.; Carlone, A.; Hänni, K. D.; Leigh, D. A.; Lewandowski, B. *Angew. Chem. Int. Ed.* **2012**, *51*, 5166-5169.
- ²⁹Ashton, P. R.; Philp, D.; Spencer, N.; Stoddart, J. F. *J. Chem. Soc. Chem. Comm.* **1991**, 1677-1679.
- ³⁰Ashton, P. R.; Ballardini, R.; Balzani, V.; Constable, E. C.; Credi, A.; Kocian, O.; Langford, S. J.; Preece, J. A.; Prodi, L.; Schofield, E. R.; Spencer, N.; Stoddart, J. F.; Wenger, S. *Chem. Eur. J.* **1998**, *4*, 2413-2422.
- ³¹Arduini, A.; Ferdani, R.; Pochini, A.; Secchi, A.; Ugozzoli, F. *Angew. Chem. Int. Ed.* **2000**, *39*, 3453-3455.
- ³²McConnell, A. J.; Serpell, C. J.; Thompson, A. L.; Allan, D. R.; Beer, P. D. *Chem. Eur. J.* **2010**, *16*, 1256-1264
- ³³Liu, Y.; Song, S.-H.; Chen, Y.; Zhao, Y. L.; Yang, Y.-W. *Chem. Commun.* **2005**, 1702-1704.

- ³⁴a) Tokunaga, Y.; Akasaka, K.; Hisada, K.; Shimomura, Y.; Kakuchi, S.; *Chem. Commun.* **2003**, 2250–2251; b) Tokunaga, Y.; Akasaka, K.; Hashimoto, N.; Yamanaka, S.; Hisada, K.; Shimomura, Y.; Kakuchi, S.; *J. Org. Chem.* **2009**, *74*, 2374–2379.
- ³⁵Baroncini, M.; Silvi, S.; Venturi, M.; Credi, A. *Chem. Eur. J.* **2010**, *16*, 11580–11587.
- ³⁶Biavardi, E.; Battistini, G.; Montalti, M.; Yebeutchou, R. M.; Prodi, L.; Dalcanale, E. *Chem. Commun.* **2008**, *14*, 1638–1640.
- ³⁷Pierro, T.; Gaeta, C.; Talotta, C.; Casapullo, A; Neri P. *Organic Lett.* **2011**, *13*, 2650–2653.
- ³⁸Yoshizawa, H.; Kubota, T.; Itani, H.; Minami, K.; Miwa, H.; Nishitani, Y. *Bioorganic & Medicinal Chemistry* **2004**, *12*, 4221–4231.
- ³⁹Thibeault, D.; Morin, J.-F. *Molecules* **2010**, *15*, 3709–3730.
- ⁴⁰Yan, X.; Wei, P.; Xia, B.; Huang, F.; Zhou, Q. *Chem. Commun.* **2012**, *48*, 4968–4970.



4.1 INTRODUCTION[§]

General scenario. Probing small molecules bearing amino-functionalities is a key issue from both the fundamental and the applied sides. N-methylated moieties, in particular, are present in a broad range of biologically active compounds, from drugs¹ to cancer biomarkers² and neurotransmitters.³ These molecules are traditionally probed by liquid-and-gas-chromatography-based mass or light spectrometry⁴ or, limited to amphetamines and analogues, by label-based immunoassays and immunosensors.⁵

Label-free, direct, real-time and in-fluid sensing remains highly desirable, but to date is severely hindered by the very low weight of the molecules, typically below 200 Da, that renders mass-based sensors, such as SPR (Surface Plasmon Resonance) and QCM (Quartz Crystal Microbalance) ineffective.⁶

We recently showed that the free energy released by a bimolecular ligand-receptor (*viz.* host-guest) interaction confined at a solid-solution interface splits into chemical and mechanical surface work, the latter determined by the work the host performs to “accommodate” the guest at the solid-solution interface. This work appears as a variation of the surface stress (surface pressure) and probes the recognition event in a label-free and energy-based fashion. Since it ranges from few to several tens of mJ/m² surface work can be transduced/measured by the so-called mechanical biosensors,⁷ that include microcantilever (MC) beams⁸ and COn tact Angle MOlecular REcognition (CONAMORE) assays.⁹

Cantilever-based chemical sensors are limited, however, by the availability of coatings that interact exclusively and selectively with the analyte of interest. So far, for selective chemical and biological sensing, the choice of MC coating has been restricted to DNA or antibodies^[9, 10, 11] neglecting the large pool of available synthetic receptors.

[§] This chapter is based on: Dionisio, M.; Oliviero, G.; Menozzi, D.; Federici, S.; Yebeutchou, R. M.; Schmidtchen, F.-P.; Dalcanale, E.; Bergese, P. *J. Am. Chem. Soc.* **2012**, *134*, 2392-2398.

Phosphonate cavitands have established themselves as an outstanding, versatile class of synthetic receptors (hosts),¹² whose molecular recognition properties have been exploited in gas sensing,¹³ supramolecular polymers,¹⁴ surface self-assembly¹⁵ and product protection.¹⁶ Their ability to bind *N*-methylated ammonium salts via a synergistic mix of weak interactions such as H-bonding, dipole-dipole and CH- π interactions has been already documented in the gas phase,¹⁷ in solution¹⁸ and on surfaces.¹⁹

The guest-induced modulation of these interactions across the alkylammonium salt series and their impact on the overall binding has not been studied so far.

In this paper we present a fundamental study toward understanding the viability of nanomechanical sensors for probing small molecules bearing amino-functionalities. In particular, as sketched in figure 1, we achieved label-free selective detection of *N*-methylammonium salts in methanol by MCs functionalized with tetraphosphonate cavitands. These molecules are low molecular weight (LMW) species of a mass equal or lower than 150 Da and that differ between each other only by a methyl group, which is 15 Da. Such unprecedented selectivity was attained thanks to the use of tetraphosphonate cavitands as receptors (figure 1).

The observed complexation trend was independently confirmed and rationalized by Isothermal Titration Calorimetry (ITC) measurements,²⁰ performed both as direct titration and displacement titration experiments.²¹ Finally, the cavitand functionalized MCs were benchmarked by detecting sarcosine in aqueous environment.

This case of study is of topical interest in biomedical diagnostics, because sarcosine has been recently singled out as a possible early marker of the aggressive forms of prostate cancer.²

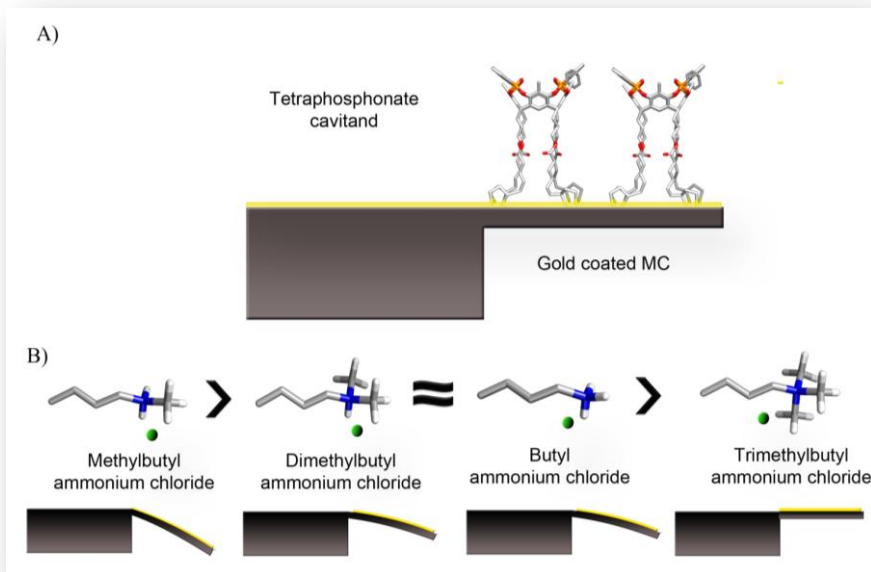
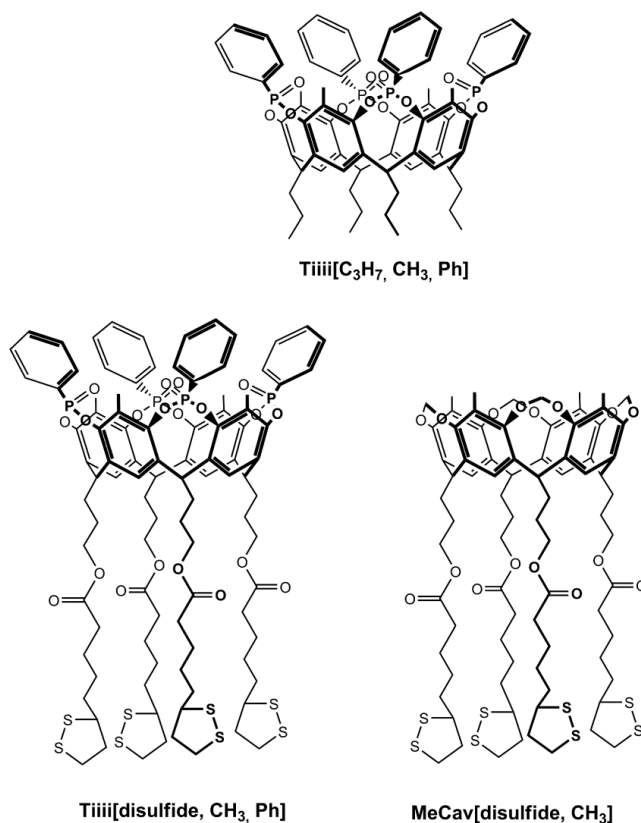


Figure 1. Working principle of the selective detection of N-methylammonium salts by cavitand functionalized MCs. **A)** Si MCs ($500 \times 100 \times 1 \mu\text{m}^3$) with the top faces coated by a 20 nm Au are functionalized with a disulfide functionalized cavitand; **B)** The different binding energies of complexation of the active cavitand with the different N-methylammonium salts are mirrored by different variations of the surface stress that in turn are balanced by different MC deflections.

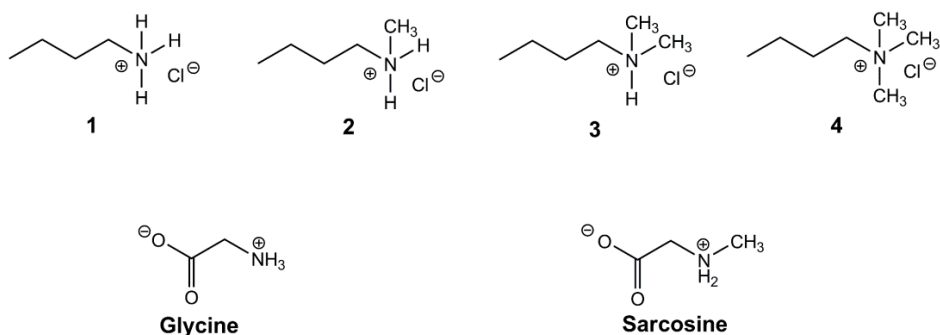
4.2 RESULTS AND DISCUSSION

Cavitands and guests. The compounds used in the present work are shown in figure 2. The preparations of active cavitands **Tiiii**[C₃H₇, CH₃, Ph]¹⁸ and **Tiiii**[disulfide, CH₃, Ph]²² has already been described, while the synthesis of the reference cavitand **MeCav**[disulfide, CH₃] is reported in the experimental section. In order to be easily immobilized on MCs, **Tiiii**[disulfide, CH₃, Ph] and **MeCav**[disulfide, CH₃] cavitands were functionalized at the lower rim with four lipoic acid units (see scheme 1). This allowed the cavitand deposition on the top face of the MC with a stability comparable to thiols.²³



Scheme 1. Scheme of the molecular structure of the cavitands. **Tiiii**[C₃H₇, CH₃, Ph] is the cavitand used for the ITC experiments, **Tiiii**[disulfide, CH₃, Ph] and **MeCav**[disulfide, CH₃] are the active and the reference cavitands functionalized at the lower rim with lipoic groups, used for the MC experiments.

Guests **1-3** (see scheme 2) were prepared by protonation with HCl of the corresponding commercial amines, followed by crystallization from diethyl ether. Guest **4** was prepared via methylation of *N,N*-dimethylbutylamine with methyl iodide, followed by anion exchange with Dowex© 22 chloride form (see experimental section for more details).



Scheme 2. Scheme of the molecular structure of the six guests: butylammonium chloride (**1**), *N*-methylbutylammonium chloride (**2**), *N,N*-dimethylbutylammonium chloride (**3**), *N,N,N*-trimethylbutylammonium chloride (**4**), glycine and sarcosine zwitterions.

MC experiments: protocol. Arrays of eight rectangular silicon MCs ($500 \times 100 \times 1 \mu\text{m}^3$) with the top faces coated by a 20 nm Au thin film were employed (Concentris GmbH, Basel, CH). The arrays were cleaned with acetone and ozone-UV before functionalization with the cavitand. Each MC was then incubated for three hours in a 1×10^{-5} M dichloroethane solution of the cavitand by means of micro-capillaries managed with the Cantisens Functionalization Unit (Concentris GmbH, Basel, CH). Following this procedure MC arrays functionalized with the active **Tiiii[disulfide, CH₃, Ph]** and the control **MeCav[disulfide, CH₃]** cavitands were prepared.

Molecular recognition experiments were conducted by the Cantisens Research MC platform (Concentris GmbH, Basel, CH), which, in particular, is equipped with a microfluidic system to handle liquid delivery to the MCs and multiple lasers for simultaneous measurement of the deflection of the individual MCs. All experiments were conducted at $0.83 \mu\text{L/s}$ liquid flux. MC arrays were allowed to stabilize under pure methanol for about 20 minutes before the injection of the methylammonium salt (guest). After injection the

guest was allowed to flow in the measurement chamber for about one and a half minutes (injection time frame) and then the pure methanol flux restored again. MC deflections were tracked against time during all these steps. Following this procedure, all guests at identical concentrations (1×10^{-5} M) were scanned against active as well as control MC arrays. The same experimental procedure for the MC molecular recognition tests was employed for the detection of sarcosine against glycine. In particular, milliQ water was employed as flowing liquid and sarcosine and glycine were diluted in water in order to reach a molar concentration of 1×10^{-4} M. Both the molecules were then tested on arrays functionalized with the active cavitands.

ITC experiments: protocol. ITC experiments were performed with an ITC-MCS calorimeter by MicroCal (GE Healthcare) at the temperature of 303 K and room pressure. The solutions were prepared in dry methanol (carefully degassed prior to use).

Direct titration experiments were performed by injecting 2-10 μ L aliquots of the guest into a 10 fold lower concentrated cavitand **Tiiii**[C_3H_7 , CH_3 , Ph] solution hosted in the reaction cell (cell volume = 1.35 mL) and the heat released upon binding tracked against time. In order to account for unspecific heats of dilution each guest was also titrated into pure methanol (blank titration). In all cases the signal from blank titrations were negligible with respect to the binding signal. Each experiment was replicated 3 times.

Displacement titration experiments consisted in the titration of the weaker guest into the host solution and the consecutive titration of the stronger guest in the obtained solution (displacement titration). Both the titrations were conducted following the protocols given above for the direct binding experiments. The displacement experiments were counterchecked by directly titrating the weakest guest into the solution of the corresponding strongest complex.

MC experiments: results. Arrays of eight gold coated MCs, functionalized with **Tiiii**[**disulfide**, CH_3 , Ph], were exposed to a methanol solutions of the four chosen guests at a molar concentration of 1×10^{-5} M. The mean signal of the eight MCs was monitored during the flow of each guest through the microfluidic chamber.

To rule out nonspecific responses due to physisorption, the MC bending should be referred to a reference MC. In view of this, we synthesized the control cavitand **MeCav**[**disulfide**, CH_3], which is structurally similar to the active one.

The active and control cavitands **Tiiii[disulfide, CH₃, Ph]** and **MeCav[disulfide, CH₃]** (scheme 1) differ only for the upper rim bridging group. The active one is a tetraphosphonate cavitand able to recognize the *N*-methylammonium salts after establishing H-bonding, dipole-dipole and CH- π interactions, while in the control one the P=O units are substituted by methylene groups as the bridging groups. In the absence of the P=O bridges no recognition towards the *N*-methylammonium salt series was observed.²⁴

Figure 2A shows the four deflection signals for guests **1-4** obtained by monitoring the mean deflection of the eight MCs of an array functionalized with **Tiiii[disulfide, CH₃, Ph]** while flowing the guests solutions into the chamber. In the selected reference system, a positive deflection ($\Delta z > 0$) corresponds to the upward bending of the cantilever due to tensile surface stress (with respect to the cantilever top face), and a negative deflection ($\Delta z < 0$) to a downward bending of the cantilever due to compressive surface stress. As it has been explained in the previous section, the guests were let to flow in the measurement chamber for about 90 seconds (injection time frame) after the injection and then the pure methanol flux restored again. The deflection curves perfectly match this timing, in fact the binding kinetic reaches a maximum deflection 90 seconds after the guest entrance into the chamber and then the release kinetics takes place. The curves show a deflection of -80 nm when guest **2** is introduced in the chamber, while a deflection of -50 nm occurs when guests **1** and **3** are injected. Guest **4** induces the lowest deflection with respect to the other three guests. As it is shown by the curves, the deflection signal reaches a peak, but not an equilibrium value and the release kinetics seems to happen in two steps. The two steps release is clear in the guest **2** trace, while in the other three it is barely visible. This deflection trend was measured for all the performed static experiments and is possibly generated by interactions between the injected guests and the cavitands also during the release period.

Figure 2B displays the signal obtained by monitoring the mean deflection of the eight MCs of an array functionalized with the reference cavitand **MeCav[disulfide, CH₃]**. The deflection remains unchanged after the injection of each of the four guests (injections were conducted under the same conditions of the experiments with the active cavitand **Tiiii[disulfide, CH₃, Ph]**).

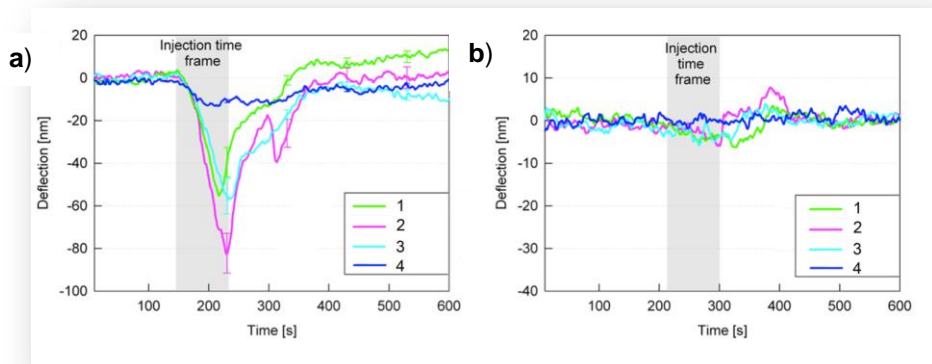


Figure 2. MC absolute deflections during the injection of a 1×10^{-5} M methanol solution of methylammonium guests (grey area). Each line represents the mean deflection of the eight MCs and the error bars the SD of the mean at selected points. **a)** MCs functionalized with the active cavitant **Tiiii[disulfide, CH₃, Ph]**. **b)** MCs functionalized with the control cavitant **MeCav[disulfide, CH₃]**.

The absence of responses supports the choice of the reference cavitant and implies that the deflection responses of the active cavitant MCs reported in figure. 2A are due only to the specific interactions between the host and the guests and rules out any unspecific event.

The obtained results were statistically validated by replicating the same series of experiments on four different arrays of eight MCs functionalized with the active cavitant **Tiiii[disulfide, CH₃, Ph]**. The mean value of the deflection peaks of the four arrays and the error, intended as the overall standard deviation of the mean, are shown in the bar chart reported in figure 3A. The trend of the interaction intensities indicated in figure 2A is confirmed: the highest response is obtained when *N*-methylbutylammonium chloride **2** is injected ($\overline{\Delta Z} = (-80 \pm 10)$ nm), a comparable deflection is measured when salts **1** and **3** are in the chamber ($\overline{\Delta Z} = (-55 \pm 6)$ nm) and the weakest response comes from salt **4** ($\overline{\Delta Z} = (-10 \pm 2)$ nm).

These data, at the best of our knowledge, are the first that report statistically validated label-free recognition of LMW molecules. Namely, the cavitant functionalized MCs allow for detection and discrimination of guest molecules that weigh from 109 to 152 Da and differ between each other for one or more methyl groups (15 Da each) only.

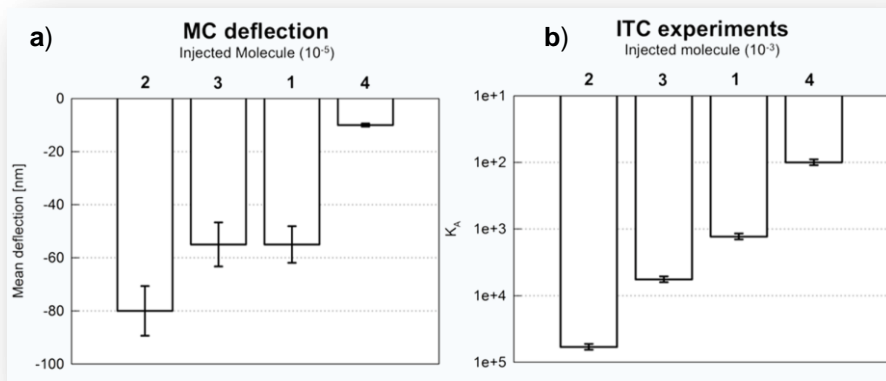


Figure 3. *a)* Bar chart of MC deflections, the mean value and the SD of the mean refer to four replicates. *b)* Bar chart of the K evaluated by ITC, the mean value and the SD of the mean refer to three replicates.

Deflection results can be addressed in terms of the applied surface stress (σ) triggered by the host-guest complexation. The relation between the variation of the surface stress ($\Delta\sigma$) applied along the MC top face and its resulting deflection is given by Stoney's equation:

$$\Delta\sigma = \frac{1}{4} s \frac{\Delta z E t^2}{L^2 (1 - \nu)} \quad (1)$$

where Δz is the MC deflection, E is the MC Young's modulus, t is the MC thickness, L is the MC length, ν is the MC Poisson's ratio and s is the Sader correction factor.²⁵ $\Delta\sigma$ is related to the properties of the stress inducer, whose role in our case is played by the host-guest complexation confined at the interface between the MC surface and the solution. For the gold coated silicon MCs used in this work $E = 168.5$ GPa, $t = 1$ μm , $L = 500$ μm , $\nu = 0.25$ and $s = 0.96$.

The surface stress generated by the interaction between guest **2** and the tetraphosphonate cavitand was determined to be equal to (17 ± 2) mJ/m^2 , while it was found to be (12 ± 1) mJ/m^2 for the interaction with guests **1** and **3**. The

stress was much lower for the interaction between the cavitand and guest **4**, namely (2 ± 0.4) mJ/m².

From the above arguments we conclude that MC deflection is directly related to $\Delta\sigma$, that in turn translates the surface work driven by the host-guest complexation. At the molecular level this work is very likely triggered by the interplay between host-guest complexation, cavitand desolvation and interface adsorption, as also suggested by the order of magnitude of $\Delta\sigma$, that falls in the range of intermolecular forces.²⁶ Therefore, the ability of the cavitand functionalized MCs to discriminate mass differences as minute as a methyl group is due to the fact that the deflection response of the MCs to the cavitand-guest recognition event is related to the energy of the event rather than to the mass of the guest.

We recently framed analogous scenarios featuring biomolecular ligand-receptor interactions by implementing *ad hoc* thermodynamic models,^[7, 27] but unfortunately none of them can be straightforwardly extended to the present system, mainly because of the differences between the biomolecule and the cavitand solid-solution interfacial phases and experimental conditions. Therefore, in order to support the interpretation of the relation between MC deflection and cavitand-guest recognition free energy we investigated the thermodynamics of host-guest recognition in solution by ITC.

ITC experiments: results. The complexation preferences of tetraphosphonate cavitands toward ammonium chloride guests **1-4** were independently assessed by ITC. In particular, direct as well as displacement binding experiments were performed in order to gain a quantitative thermodynamic picture of the host-guest interaction series.

Representative titration data of the direct binding experiments between butylammonium (guest **1**), *N*-methylbutylammonium (guest **2**) and *N,N*-dimethylbutylammonium (guest **3**) with cavitand **Tiii[C₃H₇, CH₃, Ph]** are shown in figure 4. Data for *N,N,N*-trimethylbutylammonium (guest **4**) are not reported in figure 4 as the interaction was too low to give significant titration signal. In the top panels of the figure the downward peaks (heat pulses) represent the change in the feedback current associated with the consecutive injections of a small volume of guest solution into the ITC reaction cell containing a solution of **Tiii[C₃H₇, CH₃, Ph]**. The peak area is directly proportional to the enthalpy of guest binding. The differences in the magnitude of the peak intensities in the different panels are due the different choice in the host-guest concentration that was chosen case by case in order to obtain an

optimal titration signal. The molarities were fixed at 4.5 mM, 0.7 mM and 3.0 mM for the guests **1**, **2** and **3**, respectively.

After integration with respect to time and normalization per moles of added guest, the data were converted into the sigmoidal binding curves shown in the bottom panels of figure 4, representing the normalized heat released from each injection against the molar ratio of the host and guest partners in the ITC cell.

Thermodynamic parameters of the host-guest interactions (namely, the equilibrium constant K , and the change in enthalpy, entropy and free energy ΔH , ΔS and ΔG) were extrapolated from the binding curves. The single-site (monovalent) model to fit the binding curve was adopted, supported by the crystal structure of a related $\text{Tiii}[\text{H}, \text{CH}_3, \text{Ph}] \cdot 2$ complex²⁰ and on the Job's plot titration of $\text{Tiii}[\text{C}_3\text{H}_7, \text{CH}_3, \text{Ph}]$ with the related sarcosine methyl ester hydrochloride guest (see figure 5). As evidenced in figure. 4, this choice was nicely confirmed by the excellent agreement between the fit curve (continuous line) and the experimental points (filled circles).

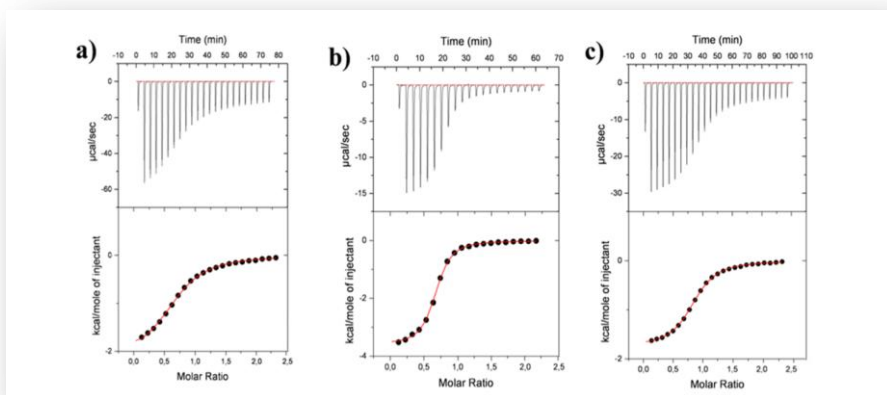


Figure 4. ITC data output of titrations in methanol at 303 K representing: **a)** the titration curve of guest **1**, **b)** of guest **2** and **c)** of guest **3** into the host solution of cavitand $\text{Tiii}[\text{C}_3\text{H}_7, \text{CH}_3, \text{Ph}]$.

The determined K values are displayed in figure 3B and summarized with the other thermodynamic parameters in table 1. The strongest interaction is observed for complex $\text{Tiii}[\text{C}_3\text{H}_7, \text{CH}_3, \text{Ph}] \cdot 2$, with $K = (3.9 \pm 0.8) \cdot 10^5 \text{ M}^{-1}$. This preference is due to the synergistic activation of all three interaction modes

available between **2** and the **Tiiii** cavitant: (i) CH₃-π interactions between the *N*-CH₃ moiety and the cavity of **1**, (ii) cation-dipole interactions between the positively charged nitrogen and the P=O dipoles and (iii) the two concurrent hydrogen bonds between two adjacent P=O on the upper rim of **Tiiii**[C₃H₇, CH₃, Ph] and the NH₂⁺ unit.

The observed *K* decrease about two orders of magnitude with guests **1** and **3**. In the case of **3** the drop in binding strength is associated to the removal of one H-bond with the host, while for **1** it is imputable to the lack of CH₃-π interactions. The two different interactions provide a comparable enthalpic contribution to the overall binding, with a slightly entropic gain in favor of CH₃-π interactions.

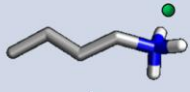
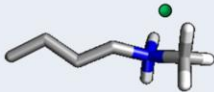
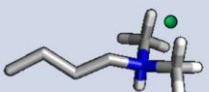

Guest	$K \pm \delta K$ (M ⁻¹)	$\Delta H \pm \delta H$ (KJ•mol ⁻¹)	$\Delta G \pm \delta G$ (KJ•mol ⁻¹)	$T\Delta S \pm T\delta S$ (KJ•mol ⁻¹)
 1	$1.5 \pm 0.8 \cdot 10^3$	-8.7 ± 0.2	-18.5 ± 1.0	9.8 ± 1.7
 2	$3.9 \pm 0.8 \cdot 10^5$	-16.1 ± 0.6	-31.9 ± 0.5	15.8 ± 1.0
 3	$6.1 \pm 0.7 \cdot 10^3$	-8.7 ± 0.1	-22.0 ± 0.3	13.3 ± 0.5
 4	INTERACTION TOO LOW TO BE MEASURED			

Table 1. Summary of ITC measurements of the titrations of the guests **1-4** into the solution of **Tiiii**[C₃H₇, CH₃, Ph] in methanol at 303 K.

The ΔH and $T\Delta S$ results indicate that, in all the three cases, the complexation is both enthalpy and entropy driven. The unusual entropic gain can be coarsely interpreted in terms of an increase in solvent entropy associated with the desolvation (*viz.* solvent displacement) of both host and guest upon complexation.

Displacement binding experiments were performed in order to determine the affinity scale of the different guests toward cavitand **Tiiii**[**C₃H₇**, **CH₃**, **Ph**] under competitive conditions. This is of particular interest for future applications with low weight molecules with amino functionalities belonging to the biological and biomedical realms. To this aim, the effectiveness for specific binding to cavitand **Tiiii**[**C₃H₇**, **CH₃**, **Ph**] of the guest with higher K , **2**, in direct competition with the guests with lower K , **1** and **3**, was evaluated by displacement titration, following the procedures described in the materials and methods section.

The results are summarized in table 2 (see figure 7 in the experimental section for ITC titration curves). Passing from entry I to entry II a decrease of half an order of magnitude of the displacement constant can be noticed. In both cases we can observe a replacement of the pre-bounded guests **1** and **3** with the strongest guest **2**, but in the second case the value is lower. This trend nicely agrees with that obtained from standard titrations: the guest **1** has a weaker interaction with the host with respect to guest **3**. As a control experiment, the two reversed order titrations were also performed (see entries Ia and IIa of table 2). In both cases negligible power pulses were observed, meaning that no exchange occurred when the guests **1** and **3** were titrated in the preformed complex **Tiiii**[**C₃H₇**, **CH₃**, **Ph**]**•2**. Finally we directly checked guests **1** and **3** versus each other. As expected, the titration signal was too low to be significant. Results from these experiments resulted in agreement with the direct binding experiments when analyzed by the monovalent competitive model (table 3, see experimental section for calculation details).²⁸

MC experiments versus ITC experiments. The comparison of figures 3A and 3B evidences that MC deflections due to the complexation of the different guests with the immobilized cavitand follow a trend that fairly matches the trend of the complexation equilibrium constants in solution. Beyond the limits posed by comparing non-equilibrium and equilibrium data, this suggests that the MC deflection fairly mirrors the host-guest complexation free energy and in turn therefore qualitatively sorts the complexation properties of the host-guest partners. Work is in progress to implement MC experiments and develop a theoretical framework to relate solution and surface thermodynamics together with MC nanomechanical transduction.

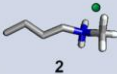
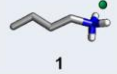

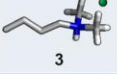
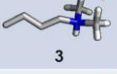
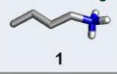
Entry	Guest	Host-guest complex	$K \pm \delta K$ (M^{-1})	$\Delta H \pm \delta H$ ($KJ \cdot mol^{-1}$)	ΔG ($KJ \cdot mol^{-1}$)	$T\Delta S$ ($KJ \cdot mol^{-1}$)
I	 2	Tiiii[C ₃ H ₇ , CH ₃ , Ph]•1	$1.7 \pm 0.1 \cdot 10^4$	-13.1 ± 0.1	-24.6	11.5
Ia	 1	Tiiii[C ₃ H ₇ , CH ₃ , Ph]•2	NO exchange			
II	 2	Tiiii[C ₃ H ₇ , CH ₃ , Ph]•3	$5.3 \pm 0.2 \cdot 10^3$	-9.6 ± 0.1	-21.6	12.0
IIa	 3	Tiiii[C ₃ H ₇ , CH ₃ , Ph]•2	NO exchange			
III	 3	Tiiii[C ₃ H ₇ , CH ₃ , Ph]•1	Exchange, but not evaluable			
IIIa	 1	Tiiii[C ₃ H ₇ , CH ₃ , Ph]•3	NO exchange			

Table 2. ITC data obtained from the displacement titrations, using Tiiii[C₃H₇, CH₃, Ph] as host. All the experiments were performed in methanol.

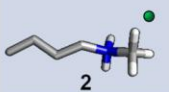
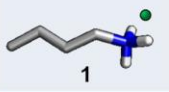
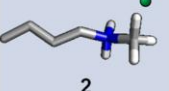
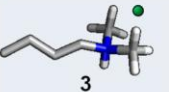
Guest	Host-guest complex	$K \pm \delta K (M^{-1})$ THEORETICAL	$K \pm \delta K (M^{-1})$ EXPERIMENTAL
	Tiiii[C ₃ H ₇ , CH ₃ , Ph]•1	$4.5 \pm 1.2 \cdot 10^4$	$1.7 \pm 0.1 \cdot 10^4$
	Tiiii[C ₃ H ₇ , CH ₃ , Ph]•2	$5.8 \pm 1.6 \cdot 10^{-1}$	No exchange
	Tiiii[C ₃ H ₇ , CH ₃ , Ph]•3	$1.2 \pm 0.6 \cdot 10^4$	$5.3 \pm 0.2 \cdot 10^3$
	Tiiii[C ₃ H ₇ , CH ₃ , Ph]•2	2.7 ± 1.4	No exchange

Table 3. Comparison of calculated and experimental K values for the displacement titrations.

Glycine versus Sarcosine detection in water. By shifting perspective, the discussion laid out above implies that the cavitated functionalized MCs can be deployed for screening LMW molecules bearing N-methylated moieties.

To benchmark this, the MCs were employed to assay sarcosine versus glycine, two amino acids that differ only for a N-methyl group. In addition, detection of sarcosine has an immediate biomedical impact, as it has been recently put under the spot by a dispute arose after the publication of two papers on Nature² and on the European Urology journals,²⁹ regarding the possibility to employ this molecule as a reliable marker for the early detection of prostate cancer.² The experiments were run in water to match biological solvent conditions. Moreover, the direct comparison between glycine and sarcosine in methanol was not possible since glycine is insoluble in methanol. In water at neutral pH both amino acids are in their zwitterionic forms. Arrays of eight gold coated MCs, functionalized with the active cavitated, were exposed to water solutions of sarcosine and glycine at a molar concentration of 1×10^{-4} M. The mean signal of the eight MCs was monitored during the flow of each guest through the microfluidic chamber. In figure 5, each curve represents the mean deflection of the eight MCs and the error bars the SD of the mean at selected points when glycine and sarcosine are injected into the chamber. The same

procedure was used as for guests **1-4** except that pure water was used instead of methanol as solvent. The curves show a deflection of -55 nm when sarcosine is introduced in the chamber, while the MCs don't deflect when glycine flows, univocally indicating sarcosine detection and discrimination over glycine.

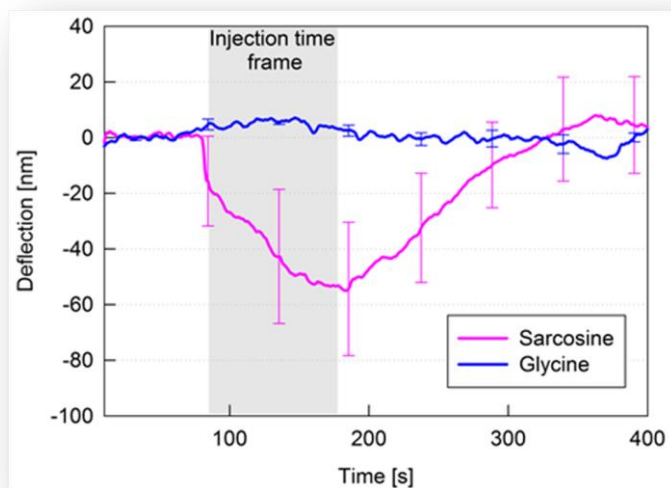


Figure 5. MC absolute deflection during the injection of 1×10^{-4} M sarcosine and glycine solutions in water (grey area). Each line represents the mean deflection of the eight MCs and the error bars the SD of the mean at selected points.

4.3 CONCLUSIONS

We showed that tetrakisphosphate cavitand functionalized MCs allow for real-time label-free selective screening across the N-methylammonium salt series. An unprecedented performance, if one considers that these LMW molecules weight from 109 to 152 Da and differ between each other only by a few methyl-groups (15 Da each).

The physicochemical origin of this outstanding selectivity was investigated by complementing MC experiments with ITC analysis of the thermodynamics of the host-guest interaction. It turned out that the MC deflection signal directly mirrors the host-guest complexation affinity. Therefore, the unique ability to sort LMW with mass differences as minute as a methyl group arises from the synergistic integration of the nanomechanical transduction mechanism of the MC with the complexation properties of the tetrakisphosphate cavitand. Work is in progress to perfect this picture by a tailored thermodynamic model.

This cavitand-MC platform was successfully benchmarked as a sensor by assaying sarcosine against glycine in aqueous solution. This result opens the route to applications in the “real” world and might immediately impact fundamental and applied research that need screening of LMW compounds bearing N-methylated moieties, that range from drugs to cancer biomarkers and neurotransmitters.

Acknowledgements

This work was funded by the grant Nanomechanical Sensors for Anfetamins (SNAF) (Regione Lombardia-INSTM), by Fondazione CARIPARMA through the project SpA and by the German-Italian exchange Program (Vigoni Program).

4.4 EXPERIMENTAL SECTION

General Methods. All commercial reagents were ACS reagent grade and used as received. Solvents were dried and distilled using standard procedures. ^1H NMR spectra were recorded on Bruker Avance 400 (400 MHz) and Bruker Avance 300 (300 MHz) NMR spectrometers. All chemical shifts (δ) were reported in parts per million (ppm) relative to proton resonances resulting from incomplete deuteration of NMR solvents. Electrospray ionization ESI-MS experiments were performed on a Waters ZMD spectrometer equipped with an electrospray interface. Exact mass was determined using a LTQ ORBITRAP XL Thermo spectrometer equipped with an electrospray interface. Cavitand **Tiiii[disulfide, CH₃, Ph]** and resorcinarene **Res[C₃H₆OH, CH₃]** were prepared following a published procedure.²²

Synthesis.

Mecav[C₃H₆OH, CH₃]

Res [C₃H₆OH, CH₃] (3.2 g, 4.11 mmol) was dissolved in dry DMF (20 mL) in a Schlenk tube. To the solution were added CH₂ClBr (5.33 mL, 82 mmol) and K₂CO₃ (3.39 g; 25 mmol). The mixture was stirred at 85°C for 3h. After neutralization with HCl 2%, the resultant precipitate was collected by filtration, and the white solid was the pure product **Mecav[C₃H₆OH, CH₃]** (Yield 88%).

^1H NMR (DMSO-*d*₆, 400 MHz): δ (ppm) 7.45 (s, 4H, ArH); 5.88 (d, 4H, OCH_{in}H_{out}O, $^2J = 7.5$ Hz); 4.61 (t, 4H, ArCH, $^3J = 8.00$ Hz); 4.45 (t, 4H, CH₂OH, $^3J = 4.96$ Hz); 4.20 (d, 4H, OCH_{in}H_{out}O, $^2J = 7.5$ Hz); 3.51 (m, 8H, CH₂CH₂CH₂OH); 2.36 (m, 8H, CH₂CH₂CH₂OH); 1.90 (s, 12H, ArCH₃); 1.44 (m, 8H, CH₂CH₂CH₂OH). ESI-MS: *m/z* calculated for C₄₈H₅₆O₁₂: 824.95. Found: 847.78. [M+Na]⁺.

MeCav[disulfide, CH₃]

To a solution of **Mecav[C₃H₆OH, CH₃]** (242 mg, 0.29 mmol) in CH₂Cl₂ (12 mL), DCC (363 mg, 1.76 mmol), DMAP (108 mg, 0.88 mmol), and lipoic acid (363 mg, 1.76 mmol) were added. The resulting suspension was stirred overnight at room temperature. After aqueous workup the organics were collected and concentrated, then ethyl ether was added until a white precipitate was observed. The solution was filtered off from the white residue and concentrated under reduced pressure. Crude product was purified by column chromatography eluting with hexane/ethyl acetate (3/2 v/v) to afford

Mecav[disulfide, CH₃] as a slightly yellow solid (228 mg, 0.12 mmol, 40% yield).

¹H NMR (CDCl₃, 300 MHz): δ (ppm) 6.96 (s, 4H, ArH); 5.91 (d, 4H, OCH_{IN}H_{OUT}O, ²J = 6.9 Hz); 4.85 (t, 4H, ArCH, ³J = 8.1 Hz); 4.26 (d, 4H, OCH_{IN}H_{OUT}O, ²J = 6.9 Hz); 4.19 (t, 8H, CH₂CH₂CH₂O, ³J = 6.5 Hz); 3.56 (m, 4H, CH(S)(S)), 3.16 (m, 8H, CH(S)(S)CH₂), 2.43 (m, 4H, CH(S)(S)CH₂CHH); 2.33 (m, 16H, CH₂CH₂CH₂OC(O) + OC(O)CH₂CH₂); 1.99 (s, 12H, ArCH₃); 1.93 (m, 4H, CH(S)(S)CH₂CHH); 1.69 (m, 24H, OC(O)CH₂CH₂CH₂+O(CO)CH₂CH₂CH₂CH₂+O(CO)CH₂CH₂CH₂CH₂CH), 1.47 (m, 8, CH₂CH₂CH₂OC(O)); **HR ESI-MS**: m/z calculated. for C₈₀H₁₀₄O₁₆S₈ [M]⁺:1576.5090. Found: 1594.5471 [M+NH₄]⁺.

Butylammonium chloride (1)

Butylamine (2 g, 27 mmol) was dissolved in 15 mL of CH₂Cl₂ and HCl was added until the complete neutralization of the base was reached. The solution was stirred for 3 hours at room temperature. The solvent was evaporated under reduced pressure and the white precipitate was recrystallized from diethyl ether affording the pure product in 90% yield.

¹H NMR (CD₃CN, 400 MHz): δ (ppm) 7.89 (bs, 3H, NH₃⁺), 2.93 (t, 2H, CH₂NH₃⁺, J=7.9 MHz), 1.69 (m, 2H, CH₂CH₂NH₃⁺), 1.44 (m, 2H, CH₃CH₂), 0.96 (t, 3H, CH₃CH₂, J=6.3 MHz). **ESI-MS**: m/z 73.7 [M⁺].

N-methylbutylammonium chloride (2)

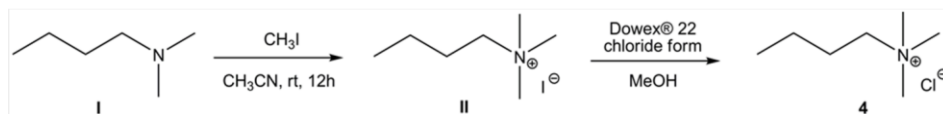
N-methylbutylamine (2 g, 23 mmol) was dissolved in 15 mL of CH₂Cl₂ and HCl was added until the complete neutralization of the base was reached. The solution was stirred for 3 hours at room temperature. The solvent was evaporated under reduced pressure and the white precipitate was recrystallized from diethyl ether affording the pure product in 90% yield.

¹H NMR (CD₃CN, 300 MHz): δ (ppm) 9.21 (bs, 2H, NH₂⁺), 2.91 (m, 2H, CH₂NH₂⁺), 2.57 (t, 3H, NH₂⁺CH₃, J=4.2 Hz), 1.75 (m, 2H, CH₂CH₂NH₂⁺), 1.42 (m, 2H, CH₃CH₂), 0.95 (t, 3H, CH₃CH₂, J=7.1 Hz). **ESI-MS**: m/z 88.5 [M⁺].

N,N-dimethylbutylammonium chloride (3)

N,N-dimethylbutylamine (2 g, 19.80 mmol) was dissolved in 15 mL of CH₂Cl₂ and HCl was added until the complete neutralization of the base was reached. The solution was stirred for 3 hours at room temperature. The solvent was evaporated under reduced pressure and the white precipitate was recrystallized from diethyl ether affording the pure product in 90% yield.

^1H NMR (CD_3CN , 300 MHz): δ (ppm) 12.08 (bs, 1H, NH^+), 2.95 (m, 2H, CH_2NH^+), 2.68 (bs, 6H, $\text{NH}^+(\text{CH}_3)_2$), 1.76 (m, 2H, $\text{CH}_2\text{CH}_2\text{NH}^+$), 1.41 (m, 2H, CH_3CH_2), 0.96 (t, 3H, CH_3CH_2 , $J=8.0$ Hz). ESI-MS: m/z 101.7 [M^+].



Scheme 3. Synthesis of N, N, N-trimethylbutylammonium chloride (4).

N,N,N-trimethylbutylammonium iodide (II)

To a solution of **I** (2 g, 19.80 mmol) in 20 mL of acetonitrile, methyl iodide (5.6g, 39.5 mmol) was added. The reaction was stirred at room temperature for 12 hours. The solvent was then removed under reduced pressure affording product **II** after recrystallization in diethyl ether in 85% yield.

^1H NMR (CD_3CN , 300 MHz): δ (ppm) 3.35 (m, 2H, CH_2N^+), 3.11 (bs, 9H, $\text{N}^+(\text{CH}_3)_3$), 1.73 (m, 2H, $\text{CH}_2\text{CH}_2\text{N}^+$), 1.37 (m, 2H, CH_3CH_2), 0.99 (t, 3H, CH_3CH_2 , $J=6.8$ Hz). ESI-MS: m/z 115.8 [M^+].

N,N,N-trimethylbutylammonium chloride (4)

Before use, the Dowex® 22 resin chloride form was first washed with bidistilled water in a flask, to remove any fine particle that could be generated in the packaging and delivering step. It was let to settle for about ten minutes and then the supernatant was eliminated. The resin was loaded into the column and activated with HCl 1N. After further washes, first with water and then with methanol, compound **II** was dissolved in methanol and then loaded in the column, using pure methanol as eluent. The pure product **4** was collected with a 60% yield. The exchange was actually confirmed by ESI MS negative ions and silver assays.

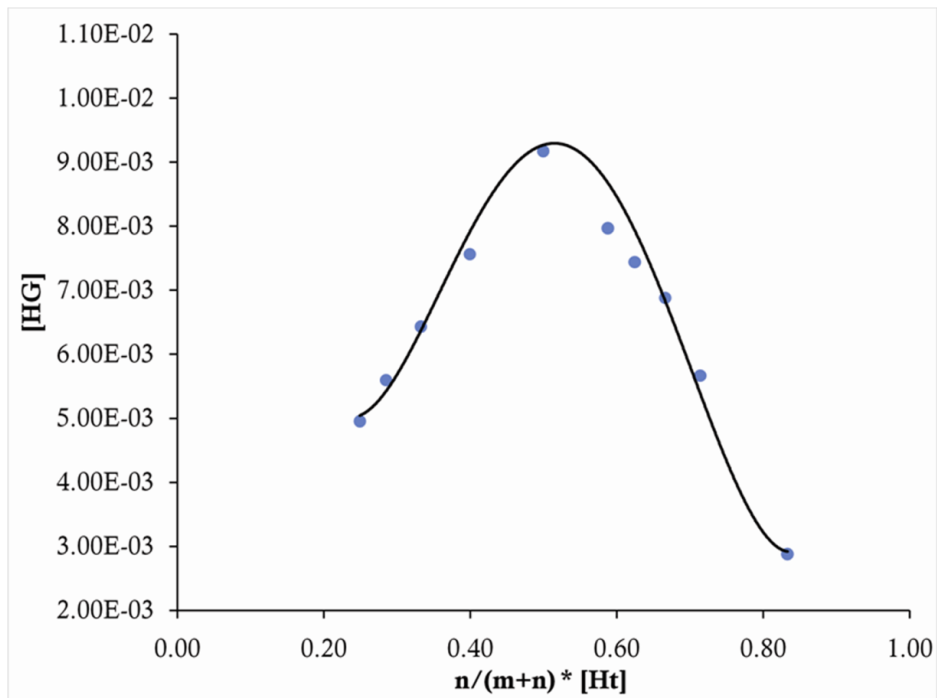
^{31}P NMR Job Plot of complex $\text{Tiii} \cdot \text{sarcosine methyl ester}$.

Figure 6. Job Plot for complexation of receptor $\text{Tiii}[\text{C}_3\text{H}_7, \text{CH}_3, \text{Ph}]$ with sarcosine methyl ester hydrochloride determined in MeOD with ^{31}P NMR by varying the mole fractions of the host and the guest, $[\text{x}]+[\text{y}] = 1.59 \cdot 10^{-2}$ M. Integration ratios between complexed and uncomplexed phosphorous peak of $\text{Tiii}[\text{C}_3\text{H}_7, \text{CH}_3, \text{Ph}]$ were utilized.

Displacement titrations. In figure 7 are showed the output of the displacement titrations. In both cases the strongest (competitor) guest **2** was titrated into the solution of the complexes from the weaker (binding) guest and the host, respectively **1**•Tiiii[C₃H₇, CH₃, Ph] and **3**•Tiiii[C₃H₇, CH₃, Ph]. The control experiments performed by titrating the weaker guest into the solution of the strongest complex are not shown since the heat pulses were almost negligible.

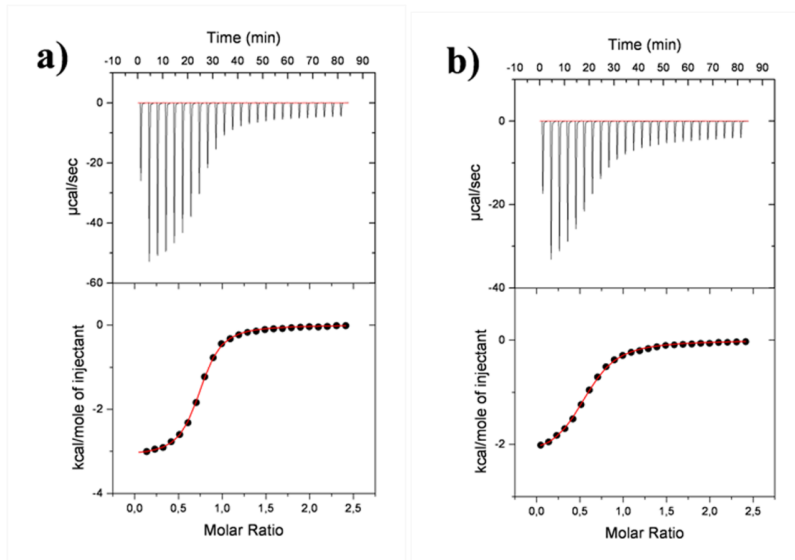


Figure 7. ITC data output: **a)** represents the titration curve of guest **2** in the solution of the preformed complex **1**•Tiiii[C₃H₇, CH₃, Ph] and **b)** represents the titration curve of guest **2** in the solution of the pre-bound complex **3**•Tiiii[C₃H₇, CH₃, Ph].

Apparent binding affinities calculations. The binding affinity of the host-guest interaction from the above displacement titration experiments, K^* (often referred as apparent binding affinity), can be related to the affinities of the binding guest, K_L , and of the competitor guest, K_I evaluated from direct titration.

The experiments are classic monovalent competitive titration, where a candidate guest *I* competes directly with a previously bound guest *L* for the binding site on the host *R*. For this system, it can be shown that that law of mass action reads (see for example Haynie, D.T. *Biological Thermodynamics*; Cambridge University Press, Cambridge 2008):

$$[R \cdot L]_I = \frac{[R]_T [L]}{K_{d,L} \left(1 + \frac{[I]}{K_{d,I}} \right) + [L]} \quad (2)$$

where for formal convenience the binding affinities have been substituted with the related dissociation constants ($K_d = K^{-1}$), $[R \cdot L]_I$ is the equilibrium concentration of the host-guest complex $R \cdot L$ in the presence of the competitor I , $[L]$ is the equilibrium concentration of L , and $[I]$ is the equilibrium concentration of I . If we compare Eq. 2 to the law of mass action for R and L in the absence of the competitor I (e.g. before the competitive titration begins)

$$[R \cdot L]_0 = \frac{[R]_T [L]}{K_{d,L} + [L]} \quad (3)$$

we straightforwardly obtain the relation between the $R \cdot L$ apparent dissociation constant, K_d^* and the L and I direct dissociation constants, $K_{d,L}$ and $K_{d,I}$:

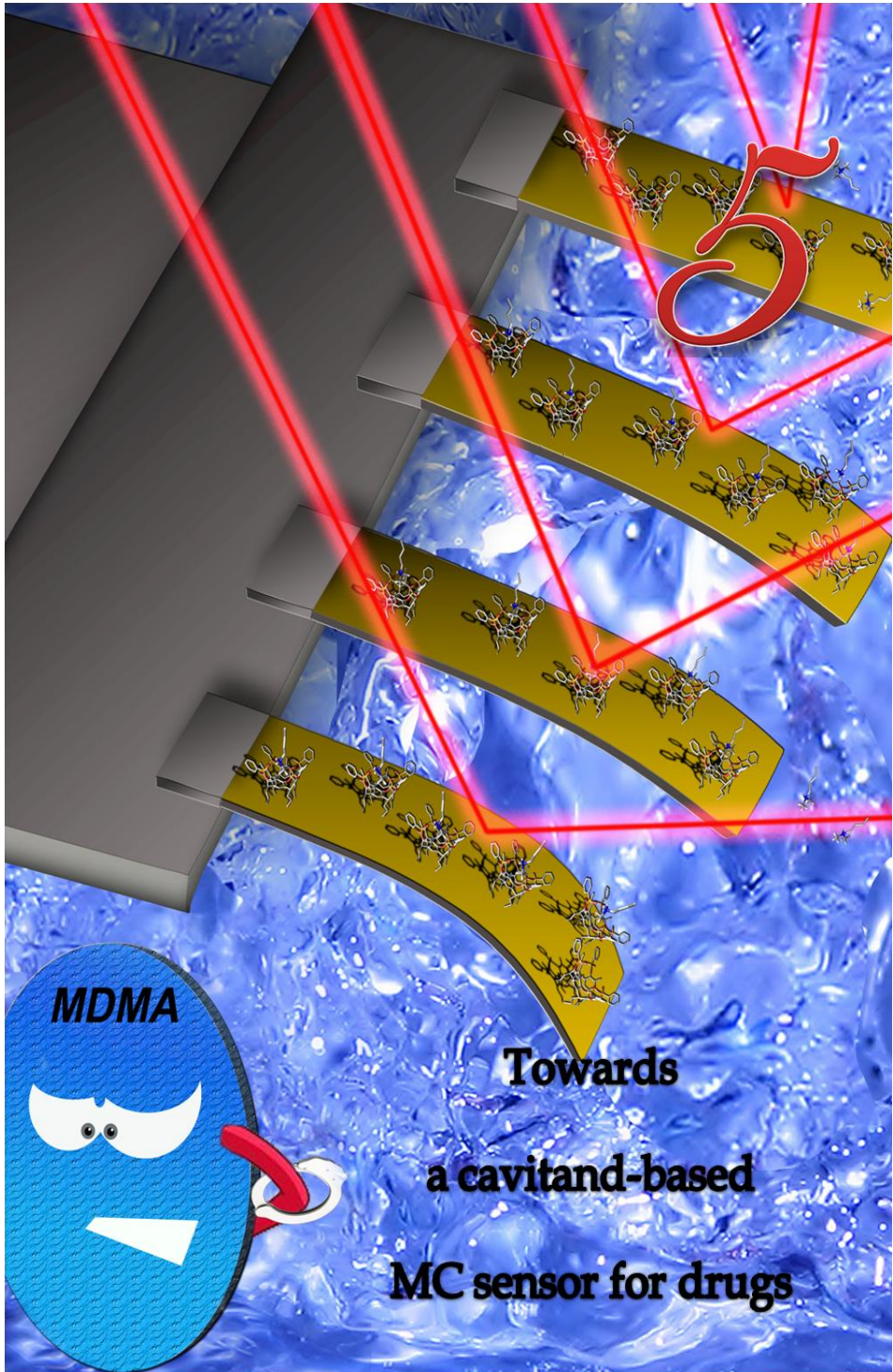
$$K_d^* = K_{d,L} + \frac{K_{d,L} [I]}{K_{d,I}} \quad (4)$$

4.5 REFERENCES

- ¹ ATLAS on Substance Use (2010), *Resources for the prevention and treatment of substance use disorders*, World Health Organisation, 2011.
- ² Sreekumar, A.; Poisson, L. M.; Rajendiran, T. M.; Khan, A. P.; Cao, Q.; Yu, J.; Laxman, B.; Mehra, R.; Lonigro, R. J.; Li, Y.; Nyati, M. K.; Ahsan, A.; Kalyana-Sundaram, S.; Han, B.; Cao, X.; Byun, J.; Omenn, G. S.; Ghosh, D.; Pennathur, S.; Alexander, D. C.; Berger, A.; Shuster, J. R.; Wei, J. T.; Varambally, S.; Beecher, C.; Chinnaiyan, A. M. *Nature* **2009**, 457, 910-914.
- ³ Von Bohlen und Halbach, O.; Dermietzel, R. *Neurotransmitters and Neuromodulators: Handbook of receptors and Biological Effects*; Wiley-VCH, Weinheim **2006**.
- ⁴ Bosker, W. M.; Huestis, M. A. *Clin. Chem. (Washington, DC, U. S.)* **2009**, 55, 1910-1931.
- ⁵ (a) Soares, M. E.; Carvalho, F.; Bastos, M. L. *Biomed. Chromatogr.* **2001**, 15, 452-456; (b) Fang, C.; Chung, Y.-L.; Liu, J.-T.; Lin, C.-H. *Forensic Sci. Int.* **2002**, 125, 142-148; (c) Butler, D.; Pravda, M.; Guilbault, G. *Anal. Chim. Acta* **2006**, 556, 333-339.
- ⁶ Bergese, P.; Cretich, M.; Oldani, C.; Oliviero, G.; Di Carlo, G.; Depero, L. E.; Chiari, M. *Curr. Med. Chem.* **2008**, 15, 1706-1719.
- ⁷ Arlett, J. L.; Myers, E. B.; Roukes, M. L. *Nat. Nanotechnol.* **2011**, 6, 203-215.
- ⁸ Fritz, J. *Analyst* **2008**, 133, 855-863.
- ⁹ (a) Bergese, P.; Oliviero, G.; Colombo, I.; Depero, L. E. *Langmuir* **2009**, 2, 9-11; (b) Oliviero, G.; Maiolo, D.; Leali, D.; Federici, S.; Depero, L. E.; Presta, M.; Mitola, S.; Bergese, P. *Biosens. Bioelectron.* **2010**, 26, 1571-1575.
- ¹⁰ Kang, K.; Sachan, A.; Nilsen-Hamilton, M.; Shrotriya, P. *Langmuir* 2011, DOI: 10.1021/la202067y.
- ¹¹ Sepaniak, M.; Datskos, P.; Lavrik, N.; Tipple, C. *Anal. Chem.* **2002**, 74, 568-575A.

- ¹²(a) Dutasta, J.-P. *Top. Curr. Chem.* **2004**, 232, 55–91; (b) Pinalli, R.; Suman, M.; Dalcanale, E. *Eur. J. Org. Chem.* **2004**, 451–462; (c) Nifantyevev, E. E.; Maslennikova, V. I.; Merkulov, R. V. *Acc. Chem. Res.* **2005**, 38, 108–116.
- ¹³Melegari, M.; Suman, M.; Pirondini, L.; Moiani, D.; Massera, C.; Ugozzoli, F.; Kalenius, E.; Vainiotalo, P.; Mulatier, J.-C.; Dutasta, J.-P.; Dalcanale, E. *Chem. Eur. J.* **2008**, 14, 5772–5779.
- ¹⁴(a) Yebeutchou, R.M.; Tancini, F.; Demitri, N.; Geremia, S.; Mendichi, R.; Dalcanale, E. *Angew. Chem. Int. Ed.* **2008**, 47, 4504–4508; (b) Tancini, F.; Yebeutchou, R. M.; Pirondini, L.; De Zorzi, R.; Geremia, S.; Scherman, O. A.; Dalcanale, E. *Chem. Eur. J.* **2010**, 16, 14313–14321.
- ¹⁵Tancini, F.; Genovese, D.; Montalti, M.; Cristofolini, L.; Nasi, L.; Prodi, L.; Dalcanale, E. *J. Am. Chem. Soc.* **2010**, 132, 4781–4789.
- ¹⁶Yebeutchou, R. M.; Dalcanale, E. *J. Am. Chem. Soc.* **2009**, 131, 2452–2453.
- ¹⁷Kalenius, E.; Moiani, D.; Dalcanale, E.; Vainiotalo, P. *Chem. Commun.* **2007**, 3865–3867.
- ¹⁸Biavardi, E.; Battistini, G.; Montalti, M.; Yebeutchou, R. M.; Prodi, L.; Dalcanale, E. *Chem. Commun.* **2008**, 1638–1640.
- ¹⁹Biavardi, E.; Favazza, M.; Motta, A.; Fragala, I. L.; Massera, C.; Prodi, L.; Montalti, M.; Melegari, M.; Condorelli, G. G.; Dalcanale, E. *J. Am. Chem. Soc.* **2009**, 131, 7447–7455.
- ²⁰Schmidtchen, F.-P., *Isothermal Titration Calorimetry in Supramolecular Chemistry*, in: *Analytical Methods in Supramolecular Chemistry* (Schalley, C.A. ed.), Wiley-VCH, Weinheim, **2007**, p.55-78.
- ²¹Velazquez-Campoy, A.; Freire, E. *Nat. Protocols* **2006**, 1, 186–191
- ²²Dionisio, M.; Maffei, F.; Rampazzo, E.; Prodi, L.; Pucci, A.; Ruggeri, G.; Dalcanale, E. *Chem. Commun.* **2011**, 47, 6596–6598.
- ²³Wei, A. *Chem. Commun.* **2006**, 1581–1591.

- ²⁴For the sensing properties of SAMs of MeCav see: Schierbaum, K. D.; Weiss, T.; van Velzen, E. U.; Engbersen, J. F.; Reinhoudt, D. N.; Gopel, W. *Science* **1994**, *265*, 1413-1415.
- ²⁵Evans, D. R.; Craig, V. S. J. *J. Phys. Chem. B* **2006**, *110*, 19507-19514.
- ²⁶Israelachvili, J.N. *Intermolecular and Surface Forces, with Applications to Colloidal and Biological Systems*, Academic Press; London 1985.
- ²⁷De Puig, H.; Federici, S.; Baxamusa, S.H.; Bergese, P.; Hamad-Schifferli, K. *Small* **2011**, *7*, 2477-2484.
- ²⁸ Haynie, D.T. *Biological Thermodynamics*; Cambridge University Press, Cambridge 2008.
- ²⁹ Jentzmik, F.; Stephan, C.; Miller, K.; Schrader, M.; Erbersdobler, A.; Kristiansen, G.; Lein, M.; Jung, K. *European Urology* **2010**, *58*, 12-8; discussion 20-1.



5.1 INTRODUCTION

General scenario. About 230 million people, that corresponds to 5% of the world's adult population, are estimated to have used an illicit drug at least once in 2010. Drugs abusers are appraised to be about 27 million, which is 0.6 per cent of the world adult population. Illicit drugs consumption appears to be generally stable in the last few years, though it continues to be rising in several developing countries. Unfortunately, the new trends in illicit drugs use are characterized by a concentration among youth, especially young males living in urban environments, and by an expanding range of psychoactive substances.¹

In the last decades the production and the consumption of Amphetamine-Type Stimulants (from now on referred to as ATS) has become a worldwide social problem. In figure 1 the 2012 World Drugs Report¹ shows the drugs abuse trend over 2008-2010. After cannabinoids, the ATS (including ecstasy) is the second group of drugs most widely used globally, followed by opioids, opiates and cocaine.

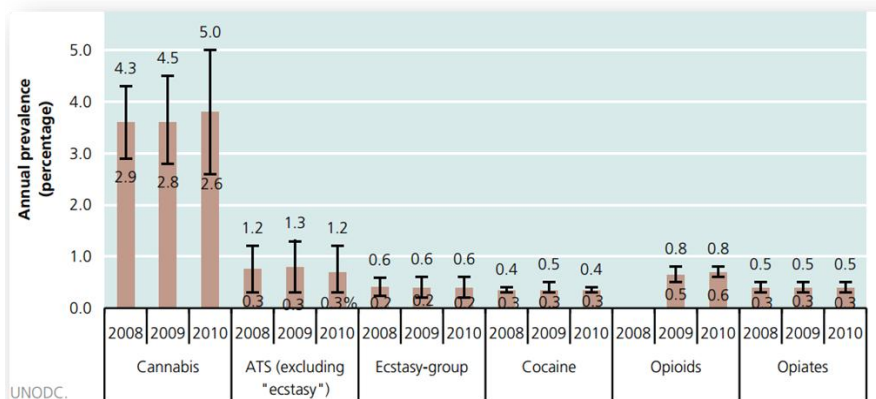


Figure 1. Annual prevalence of illicit drugs use among the population aged 15-64, 2008-2010. Source UNODC World Drug Report 2012.

For what concerns the European situation, after cannabis, ATS substances including ecstasy and cocaine are the main illicit drugs abused. In figure 2, 3 and 4 the worldwide and European prevalence of, respectively, ATS substances, ecstasy and cocaine in 2010 (or latest year) is shown.

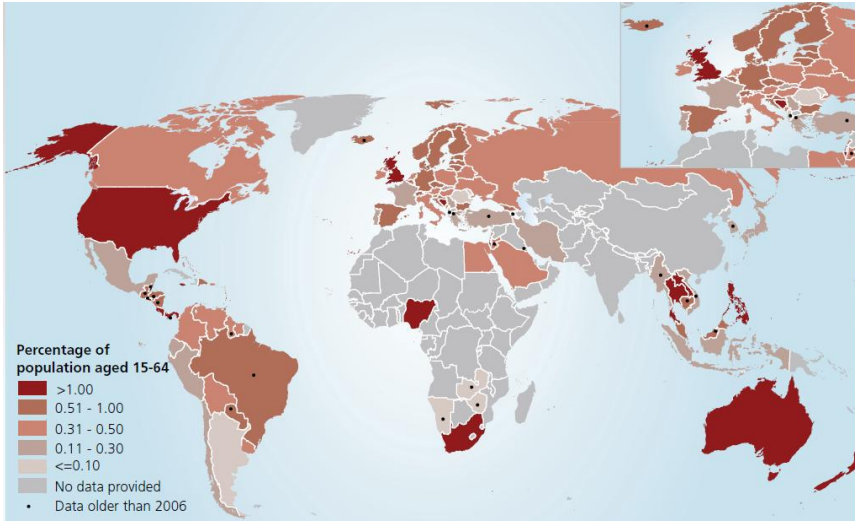


Figure 2. Prevalence of amphetamine-type stimulants excluding ecstasy in 2010, or latest year. Source: UNODC estimates based on annual report questionnaire data and other official sources.

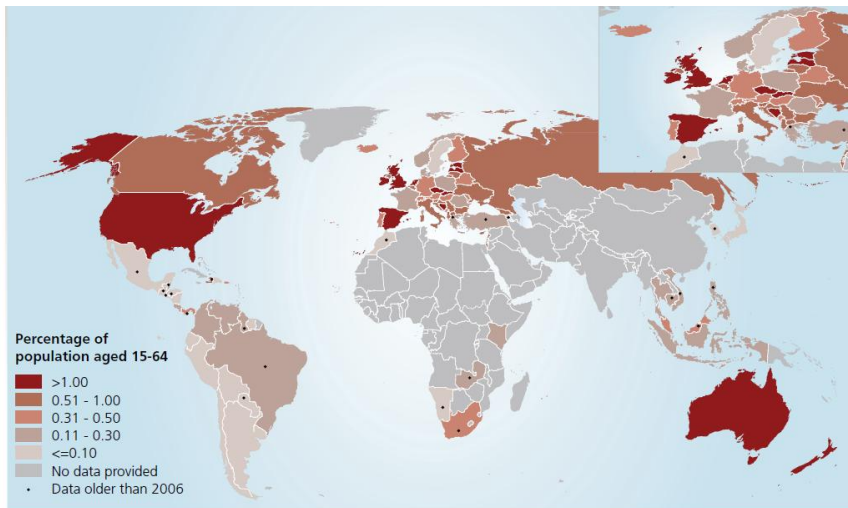


Figure 3. Prevalence of ecstasy in 2010, or latest year. Source: UNODC estimates based on annual report questionnaire data and other official sources.

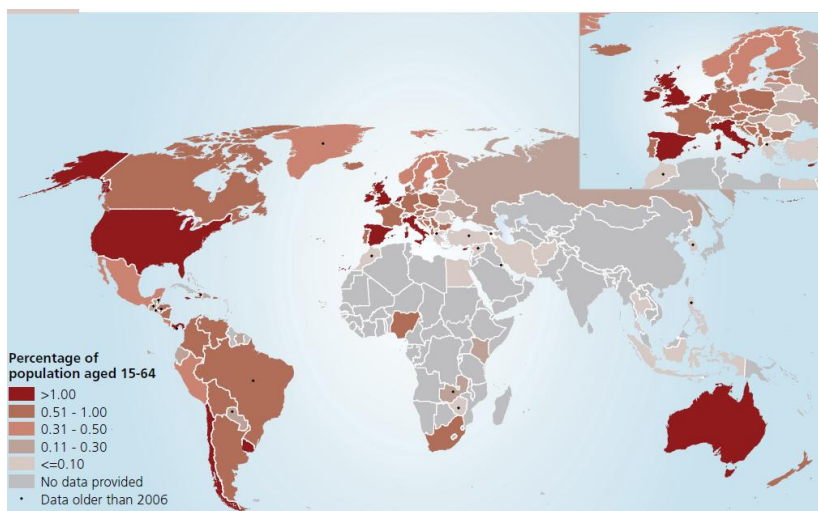


Figure 4. Prevalence of cocaine in 2010, or latest year. Source: UNODC estimates based on annual report questionnaire data and other official sources.

This chapter describes the preliminary studies toward a MC sensor for the detection of the whole amphetamine class plus cocaine as hydrochloride salts.

Cocaine. Cocaine (figure 5) is an alkaloid derived from the coca plant. It was already used in the 3000 B.C. by chewing the coca leaves because of the sense of fatigue suppression and the energy increase. This method to assimilate the drug was the only one used until 1860, when cocaine was isolated for the first time by Albert Niemann. In 1970 this drug was declared illicit except for pharmaceutical purposes in the Controlled Substances Act.²

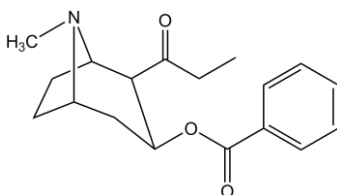


Figure 5. Structure of cocaine.

The operation mechanism of cocaine relies in the block of the reuptake of the neurotransmitters like norepinephrine, dopamine, and serotonin causing an

increase of their concentrations. The main side-effects are vasoconstriction, tachycardia and hyperthermia.³ Stimulation of the central nervous system stimulation can also cause an increase in alertness, energy, talkativeness, repetitive behavior, a diminish in appetite, an alteration in sexual behavior and it provides a local anesthetic action (which results from its ability to block the sodium channel in neuronal cells).⁴

Synthesis. Illicit natural cocaine is produced following three steps:⁵

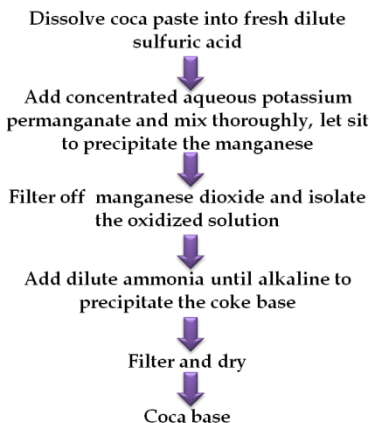
1. extraction of the crude coca paste from the coca leaf;
2. purification of coca paste to coca base;
3. conversion of coke base to cocaine hydrochloride.

1. Extraction can be performed following two different techniques that are solvent extraction technique and acid extraction technique, both shown in scheme 1. The solvent technique is the traditional method and the most common one still used. The acid technique is a more recently developed methodology and requires minor quantities of organic solvents.



Scheme 1. Schematic representation of the solvent extraction technique (on the left) and the acid extraction technique (on the right).

2. The conversion of coke paste to coke base is essentially a purification procedure and is shown in scheme 2. The purity of the paste could vary from 30% to 80% depending on the extraction technique, the variety of coca leaves and the operators skills.



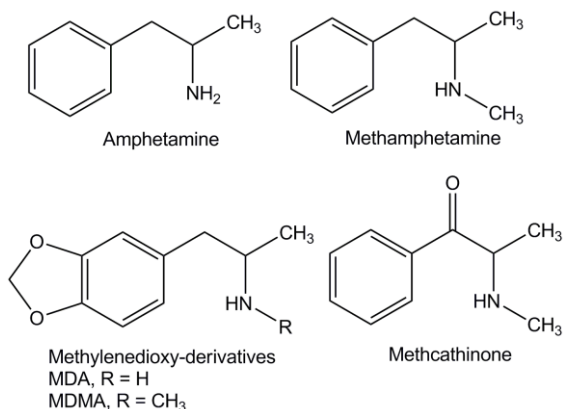
Scheme 2. Schematic representation of the purification steps from coca paste to coca base.

3. The final step of the process consists in the salification of the coca base into the cocaine hydrochloride. Coca base is dissolved in diethyl ether and a solution of concentrated hydrochloric acid into acetone is slowly added. After mixing, the cocaine hydrochloride precipitates in the form of crystals that are ready to be filtered off and easily recovered from the solution. Purity of the final product can vary from 80 to 97%.

The necessity to produce cocaine in more hidden ways avoiding the growing and harvesting of coca leaves has started to develop synthetic procedures that can be carried out from the beginning to the end in laboratory. These methods still remains the less used since they need a high level of synthetic expertise and well-equipped laboratory facilities.

ATS substances. Amphetamines, methamphetamines, their methylenedioxy-derivatives and methcathinones (scheme 3) are synthetic drugs that belongs to the ATS group. They have a stimulant effect on the central nervous system, being able to increase the levels of adrenaline, noradrenaline, dopamine, acetylcholine and serotonin. The alteration of these

neurotransmitters causes hypertension and tachycardia, gives a feeling of increased confidence, sociability and energy. It also causes appetite and fatigue suppression, leading to insomnia. After the end of the effects (that can last several hours), the main consequences on the users are irritability, restless feelings, anxiety, depression and lethargy.



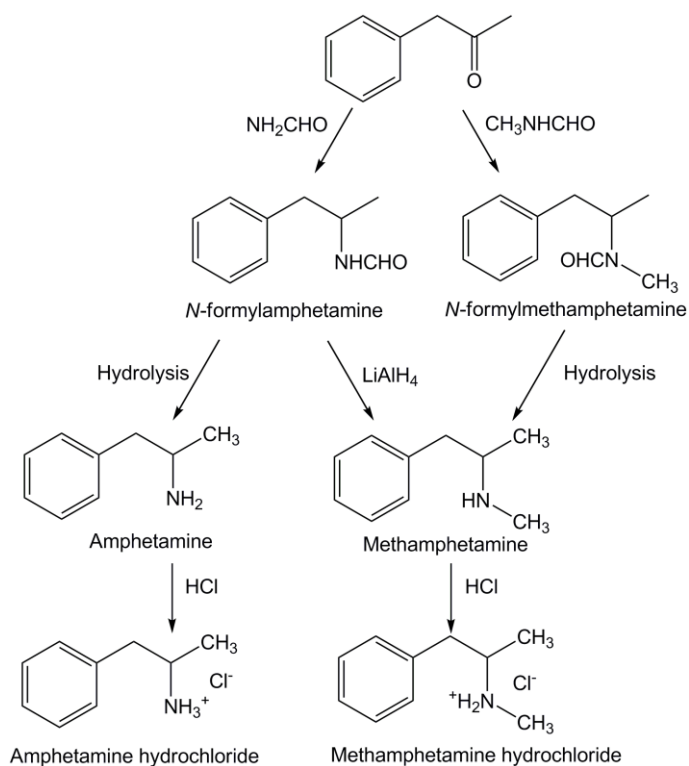
Scheme 3. *ATS structures.*

Some of the substances in the ATS group were initially tested in psychotherapy for their ability to enhance emotions and empathy (i.e. MDA),⁶ others were used in the treatment of eating disorders (i.e. MDMA).⁷ Then in the seventies this type of drugs were declared illicit and classified as Psychotropic Substances, because of their alteration of the behavior, their toxicity not only for the brain nerve endings but also for the kidneys, liver and heart cells. These substances also cause long term attrition of the organs, mainly of the hearth since it is always subjected to a huge stress. Addiction and habit-forming are also standard effects that have been encountered in the ATS abusers.⁸

Even if Amphetamine-Type Stimulants demonstrated to have very similar central and peripheral effects in humans they can differ a lot in terms of potency, time of onset and duration of action. Despite belonging to the ATS category, MDMA and its derivatives show a number of clinical pharmacological differences with respect to both amphetamines and methamphetamines-type structures.⁹ In fact MDMA and other phenethylamine drugs (MDA...) occupy an intermediate position between stimulants and hallucinogens, originating the new class of *entactogen*, proposed for the first time by Nicholson in 1986.¹⁰

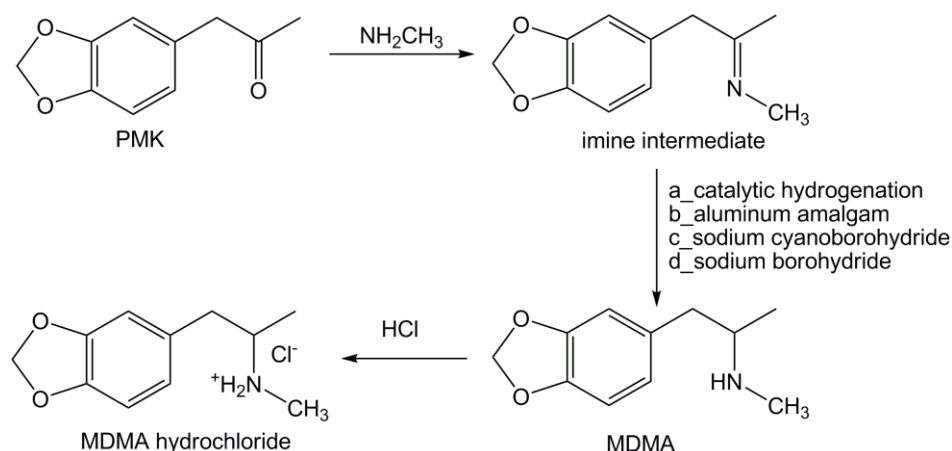
Entactogen means "touching form within" and refers to the class of compounds that has a combination of hallucinogenic and stimulants effects.

Synthesis. Despite the birth of new methods for the amphetamine synthesis, one of the oldest and still frequently used is the Leuckart reaction. This procedure was described for the first time in 1885, but it is one of the most common methods used still nowadays for the formation of amphetamines and methamphetamines. It starts with the condensation between 1-phenylpropan-2-one (BMK) and formamide in the presence of formic acid for the amphetamine synthesis, while for the formation of methamphetamine *N*-methylformamide and formic acid are used. The subsequent step is equal for both amphetamines and methamphetamines, namely the hydrolysis of the intermediates *N*-formylamphetamine and *N*-formylmethamphetamine. To obtain the drug in the hydrochloridric salt form one last step with HCl is needed (scheme 4).



Scheme 4. The Leuckart method in the synthesis of primary and secondary amines. The last step is the salification to obtain the hydrochloride form.

For the synthesis of MDMA and sometimes for the formation of other *N*-alkylated MDA derivatives another synthesis is preferred: the reductive amination route (scheme 5). This method starts from the reductive amination of 3,4(methylenedioxy)phenyl)-2-propanone PMK (or BMK for the synthesis of methamphetamines) with a primary amine. The first step is the formation of an imine that is then reduced to the corresponding desired product via different methodologies like catalytic hydrogenation, aluminum amalgam, sodium cyanoborohydride and sodium borohydride.



Scheme 5. The reductive amination route for the synthesis of MDMA. The last step is the salification to obtain the hydrochloride form.

Drug sensors devices: state of the art. Clandestine manufacturers are driven mainly by two different but equally important goals: the first one is to synthesize drugs that the users want and seek because of their recreational effects, the other but not less important is to design new substances that fall out of the law borders and legislation to avoid prosecution. A new type of psychotropic substance cannot be considered illicit from the beginning, but just when the procedure to evaluate the riskiness of the substance under examination has finished its bureaucratic iter. In this way the "kitchens" have a lot of room and time to design, manufacture and sell new psychotropic substances, with the risk to produce even more dangerous and powerful substances. These new substances are called "synthetic highs" or "designer drugs" and they are synthetic drugs that use not yet illegal compounds to mimic the highs of outlawed substances from amphetamines to cocaine. In fact,

for ATS in particular, various structural modifications can be made during the synthesis (figure 6), however, the active group that cannot be modified in any type of these psychotropic substances is the aminic moiety, because of the loss of the stimulant mechanism.

More and more often these compounds are synthesized and sold not in the free base form but in the salt form, that generally is either a hydrochloride or a sulphate salt, to decrease the vapor pressure in order to avoid the detection of their presence by traditional methods like the use of dogs.

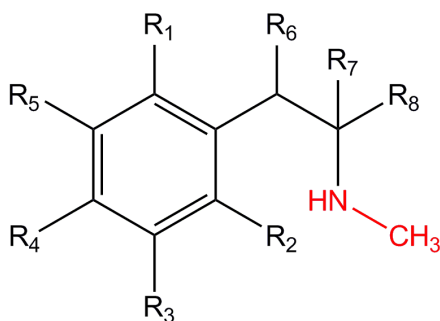


Figure 6. Scheme of an ATS structure with all the possible structural modifications.

In the depicted scenario, the importance to identify not only the already illegal drugs, but also all the new derivatives comes out as a big challenge for the forensic laboratories.

The state of the art for the portable drug detection devices that can perform field tests to have preliminary results comprises:

- ∅ color tests; they show a lot of false positive because of the occurrence of cross color reactions with a lot of products, such as shampoos.
- ∅ SABRE 2000 (Smiths Detection); it is a portable Ion Mass Spectrometry (IMS) device that doesn't meet all the operational needs for the users and sometimes it is considered even ineffective.
- ∅ Transport Kit Portable FT-IR (Thermo Electron Corporation) and Mobile-IR Portable FT-IR spectrometer (Bruker Optics) are both two FT-IR portable devices; the first one is neither watertight nor solvent resistant and both of them have the issue that they can be handled just by trained laboratory personnel.

- ∅ GC-Ionscan® (Smiths Detection) is an IMS based detector and is the most promising one; the issues related with this type of technique concern the potential dangerousness of the radioactive source and the onerous cost of the source lamp.

Even if the portable detector can give a preliminary indication of the type of substance under examination, the final investigation relies mostly on laboratory analysis and techniques, such as gas¹¹ and liquid¹² chromatography combined with mass spectroscopy,^[11a, 11b] UV absorbance,¹³ fluorescence and chemiluminescence that can reach a detection limit of 2.5 ng/mL.^[14, 15] Capillary electrophoresis¹⁶ has also been used in combination with fluorescence reaching a detection limit of 0.05 µM, while a threshold of few ng/mL can be reached when immunologic method are used together with an amperometric detector.¹⁷

For what concerns cocaine detection, nowadays, the main and most reliable methods to reveal the presence of cocaine are:

- ∅ enzyme-based immunoassays like enzyme multiplied immunoassay technique (EMIT)¹⁸ and enzyme-linked immunosorbent assay (ELISA);¹⁹
- ∅ gas chromatography coupled with mass spectrometry (GC-MS);²⁰
- ∅ high performance liquid chromatography (HPLC);²¹
- ∅ innovative methods like aptamers functionalized cantilevers (still not used in the laboratories as routine techniques).²²

The excipients concern. The real issue when trying to design a new drug detector device is that the "street samples", so the real substances that are sold on the streets, never concur with the pure drug. The active principle content can vary from a minimum of 5% to a maximum of 60%, the remaining percentage is covered by excipients.

"The excipients, which can also be called auxiliary substances, are raw materials designed to enter into the composition of pharmaceutical preparations on a different basis than the active substances. They are conceived to give preparations a particular form or to be incorporated. Excipients correspond either to a chemical entity, or to a more or less complex mixture of synthetic or natural origin. Products of natural origin are used either directly, or after having been processed chemically." (Le Hir, 1997)

The functions of the excipients are:

- ∅ to facilitate the administration of the substance;
- ∅ to improve efficiency of the active compound;

∅ to ensure stability and conservation of the substance.

They are classified in different categories depending on the type of role:

- ∅ *diluents* are inert powders that fill up the volume when the quantity of the active compound is not enough to obtain a tablet of adequate size (lactose, fructose, mannitol, sucrose, glucose, maltose, vitamin c, cellulose...);
- ∅ *binders* are usually used in the solid or liquid form and they have the role to bind together all the components and to give cohesion to the tablet that otherwise would be fluffy and loose (agar, cellulose, glucose, flour...);
- ∅ *lubricants* are powders that have threefold activity, i.e. improving the fluidity, decrease the sticking of the grains and reduce frictions between particles (stearic acid, boric acid);
- ∅ *disintegrators* allow the penetration of the water inside the tablet, hence they accelerate the disintegration of the tablet and the dispersion of the active compound in the human body (unlike the other categories only one good disintegrator is used, i.e. starch);
- ∅ *others* like wetting agent, buffer, dyes, flavorings, absorbing and desorbing agent.²³

The case records of the street samples is quite wide since a large number of excipients can be chosen and the quantities can differ a lot depending also from the type of active principle. Despite this large option, one of the most common and used composition in the case of ecstasy hydrochloride is the one with lactose and caffeine. The analysis of a good drug sensor device should not be affected by those interferents but it should just be sensitive to the presence of the active compound.

What is still missing from the state of the art of drug sensors is a device able to give a response on a portable device time scale but with higher degree of reliability, safety for the users and, above all, potentially able to detect not only ATS and cocaine but also synthetic highs without alteration in the output due to the presence of the excipients.

The Dalcanale's group has embarked to design and construct a new type of drug sensor device that could be able to meet the specifics pointed out.

Ammonium salts can be considered as the simplest mimic of the ATS, since both substances present an ammonium moiety that can be recognized by the three synergistic interactions with the upper rim of the cavity, interactions that can be switched on and off depending on the type of ammonium moiety. The complexing properties of tetraphosphonate cavitands towards ammonium salts

were studied both in solution via ITC and at the interface via MC (see chapter 4 for more details).

For this work the first step was to translate the complexation properties of tetraphosphonate cavitands from the simple alkylammonium salts to the more complex drug structures, exploiting the same MC concept already successfully used for the recognition of the series of *N*-alkylammonium salts and for molecules with biological interest like sarcosine (see chapter 4 for details).

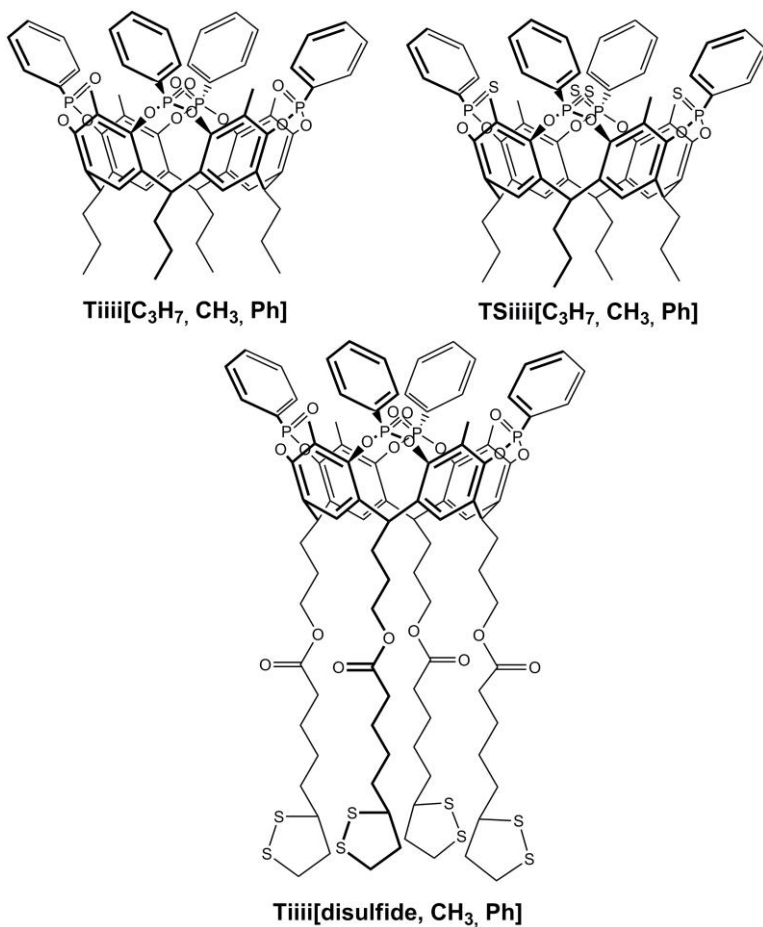
In this chapter we present the preliminary results, first in solution via ^{31}P NMR and then at the solid-liquid interface via microcantilevers, of the selective recognition ability of tetraphosphonate cavitands towards illicit drugs.

The strength and the peculiarity of this new detector concept, that is different from any other currently present on the market, is the ability of cavitand receptors to recognize selectively the methylammonium hydrochloride part, that is the active centre of the psychotropic substances. This property makes the cavitand able not only to detect some selected ATS drugs, their precursors and cocaine, but potentially any new synthetic high because of the need to let the ammonium part unmodified.

5.2 RESULTS AND DISCUSSIONS

Cavitands and guests. For what concerns the choice of the cavitands, we decided to use the **Tiiii**[C₃H₇, CH₃, Ph] for the preliminary studies in solution, **TSiiii**[C₃H₇, CH₃, Ph] as reference in solution and **Tiiii**[disulfide, CH₃, Ph] (scheme 6) for the MC experiments.

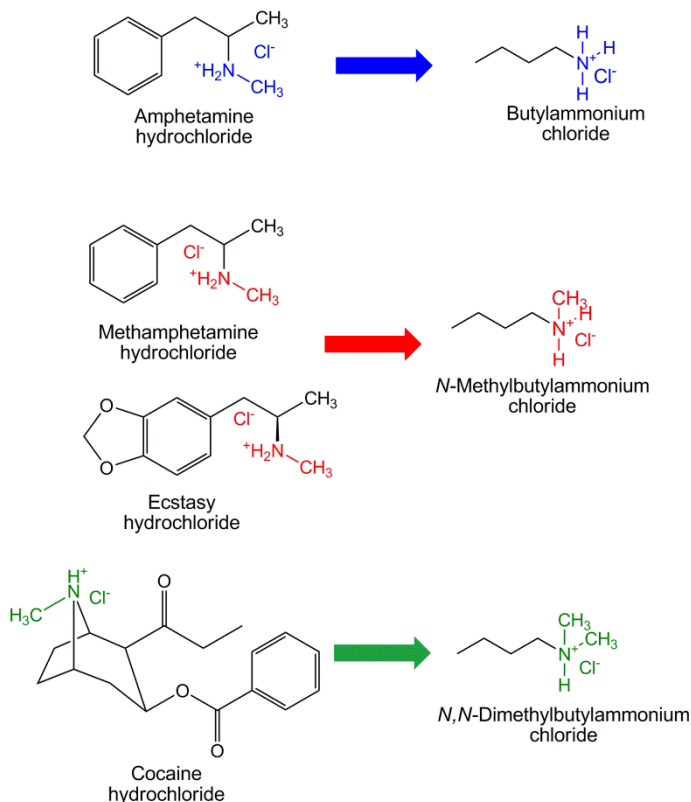
Tiiii[C₃H₇, CH₃, Ph],²⁴ **Tiiii**[disulfide, CH₃, Ph],²⁵ and **TSiiii**[C₃H₇, CH₃, Ph] (see chapter 2) have already been described elsewhere.



Scheme 6. Structures of the host cavitands used in the present work.

The use of drugs in scientific experiments is regulated by *Ministero della Salute* through the presentation of an approved research project. In our case the

project is FP7 European Project DIRAC. Meanwhile we were waiting for the authorization, a set of experiments was conducted using ammonium salts as proxy for drugs (see scheme 7).



Scheme 7. Scheme of the selected drugs and their proxy tested in the present work. The common moieties belonging to the drugs and the ammonium salts are highlighted in different colors.

NMR qualitative tests. Before testing the illicit substances on the microcantilevers, qualitative tests in solution were performed with ammonium salts to test if any correlation between the two classes was present.

NMR titration can provide quantitative data when the association constant of the complexation under examination is included in the $10 < K_{\text{ass}} < 10^4$ range. This is due to the fact that the NMR works in a $1/K_{\text{ass}}$ concentration regime and the 10^{-4} M is the lowest threshold under which the NMR cannot be used as a suitable technique for quantitative information. Since ammonium salts

demonstrated to be complexed by tetrakisphosphate cavitands in methanol with association constants included in the range $10^3 < K_{\text{ass}} < 10^5$ (see the ITC measurements in chapter 4) we decided to use NMR as a qualitative indication of the complexation mode for ammonium salts as proxy of illicit substances.

The experiments were conducted in $\text{CD}_3\text{OD}-d_4$ at 25°C monitoring the ^{31}P signal of the upper rim of the host (see figure 7). This signal is diagnostic of an host-guest complexation: if a positive charged guest is present inside the cavity, the phosphorus signal undergoes to a down-field shift due to the deshielding effect of the charged guest. The first spectra recorded (**a**) is the one belonging to the free host in solution, the second (**b**) after the addition of 0.5 equivalents of the guest and the last one (**c**) after the addition of 1.0 equivalent of the substrate.

Figure 7 shows that the chemical shift variation is present in all three cases with a different intensity.

The higher downfield shift is experienced in the presence of methylbutylammonium chloride ($\Delta\delta=2.5$ ppm). This complexation preference was expected since all the three synergistic interactions are turned on:

- ∅ CH- π interactions between the acidic methyl of the guest and the π -basic cavity of the receptor;
- ∅ cation-dipole interactions between the positive charge of the ammonium moiety and the highly polarized P=O bond on the upper rim of the cavitand;
- ∅ two adjacent hydrogen bonding between the $^+\text{NH}_2$ hydrogens on the mimic and the oxygen of the host.

Dimethylbutylammonium chloride can interact with the cavitand via cation-dipole interactions, CH- π interactions and one hydrogen bond. The loss of one hydrogen bond decreases the association constant of the complexation with respect to a secondary ammonium salt as testified by the smaller ^{31}P shift observed ($\Delta\delta=1.4$ ppm).

Butylammonium salt interacts with the host via hydrogen bonding and cation-dipole interactions. The phosphorus shift drop experienced ($\Delta\delta=0.70$) by the butylammonium chloride is related to the loss of the CH- π interactions (see also chapter 4).

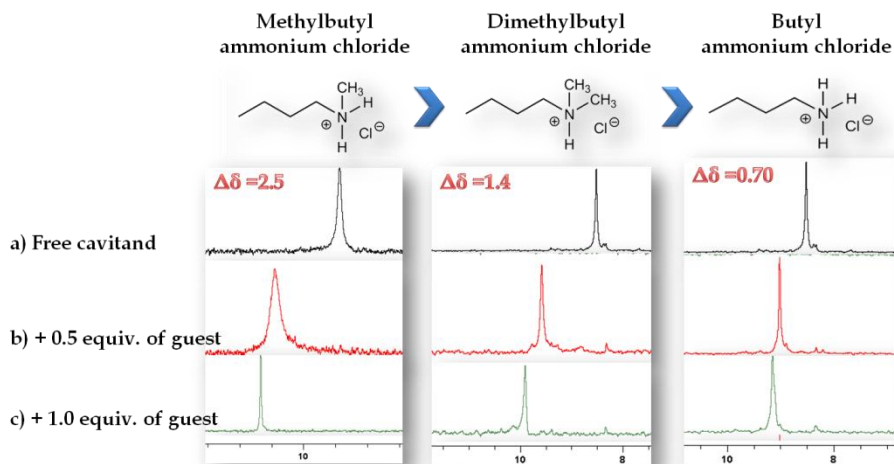


Figure 7. ^{31}P NMR of $\text{Tiiii}[\text{C}_3\text{H}_7, \text{CH}_3, \text{Ph}]\cdot\text{methyldimethylbutyl/butyl ammonium chloride}$ qualitative complexation test: a) spectra of the free cavitand; b) spectra recorded after the addition of 0.5 equivalents of the guest c) spectra recorded after the addition of 1.0 equivalent of the guest. All spectra were recorded in MeOD.

Assessment of non specific interactions. To exclude the nonspecific interactions from the overall binding complexation, thiophosphonate cavitand $\text{TSiiii}[\text{C}_3\text{H}_7, \text{CH}_3, \text{Ph}]$ was chosen. The $\text{P}=\text{S}$ group, being by far less polarizable than the $\text{P}=\text{O}$ group, is a very poor H-bond acceptor and also is less prone to cation-dipole interactions. $\text{CH}-\pi$ interactions are still present since they do not involve the nature of the bridging units. ^{31}P NMR titrations were then repeated following the host-guest interaction between tetrathiophosphonate cavitand and the three selected proxy guests.

The output was univocal: no chemical shift variations were observed. Since the main driving forces of the complexation are the hydrogen bonding and the cation-dipole interactions that, with this type of host, are totally or partially quenched, $\text{CH}-\pi$ interactions alone are not sufficient to guide the insertion of the guest into the receptor cavity.

Therefore, the presence of the $\text{P}=\text{O}$ group on the upper rim is a necessary condition in drug recognition.

Biphasic system. The microcantilever detection requires molecular recognition at the solid-liquid interface. We decided to mimic the solid-liquid interface by monitoring the complexation at the liquid-liquid interface via ^{31}P

NMR, using two immiscible solvents. We opted for the chloroform/water system, where the **Tiiii** is soluble in chloroform only and the guests are water soluble. Moreover, water is the solvent of choice for microcantilever sensing.

The output is reported in figure 8. Again, the larger downfield shift is observed in the case of methylbutylammonium chloride ($\Delta\delta=2.3$). The presence of two peaks associated to the complexed and non complexed cavita nd , indicates a slow exchange process on the NMR time scale. Moving to chloroform/water interface increases the complexation strength of methylbutylammonium guest by strengthening the solvophobic CH- π interactions.

These CH- π interactions are pivotal for maintaining hydrogen bonding and cation-dipole interactions with the P=O group, which otherwise will be wiped out by the presence of water. This is confirmed by the absence of ^{31}P shift variation in the case of dimethylbutylammonium and butylammonium guests. (figure 8). The presence of water amplifies the difference in complexation in favor of the methylbutylammonium guest.

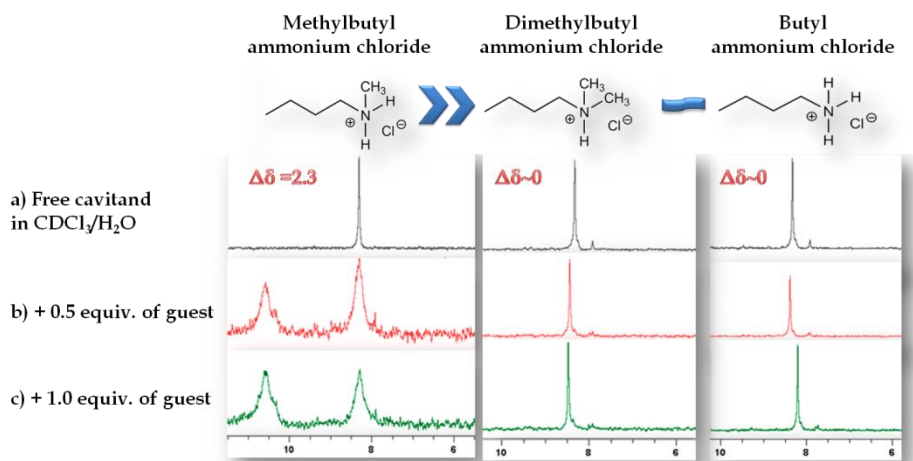


Figure 8. ^{31}P NMR of **Tiiii**[C_3H_7 , CH_3 , Ph]•methylbutyl/dimethylbutyl/butyl ammonium chloride qualitative complexation test: a) spectra of the free cavita nd in $\text{CDCl}_3/\text{H}_2\text{O}$; b) spectra recorded after the addition of 0.5 equivalents of the guest c) spectra recorded after the addition of 1.0 equivalent of the guest.

By extrapolating the results obtained from the proxy both in methanol solution and at the chloroform/water interface, the expected complexation

strength scale between tetraphosphonate cavitands and drugs is reported in figure 9.

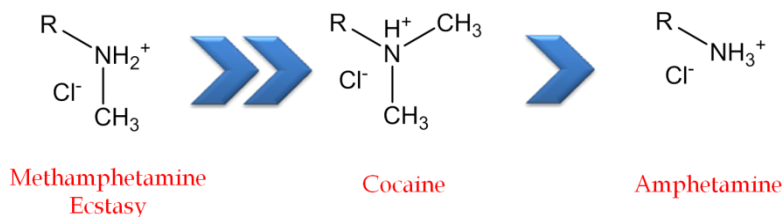
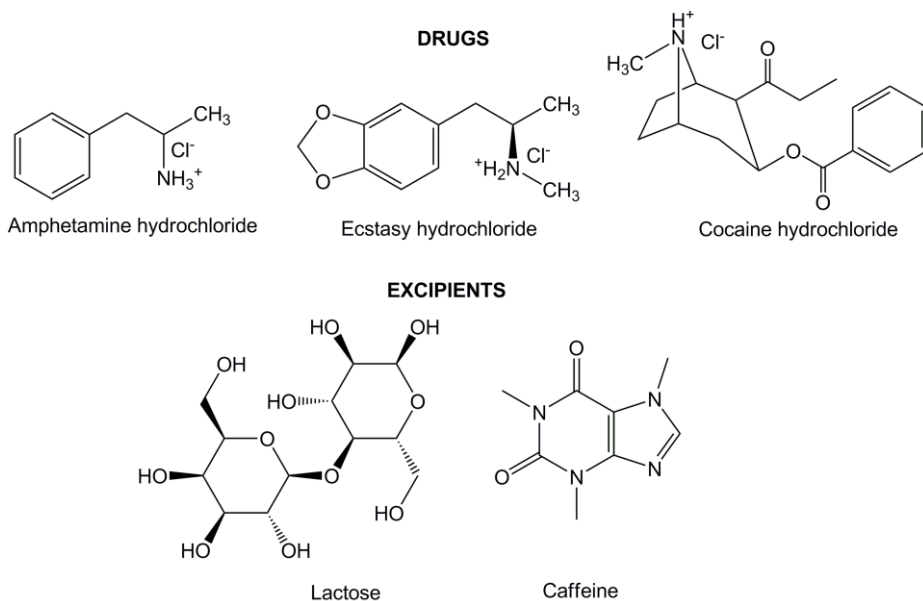


Figure 9. Expected complexation strength scale between tetraphosphonate cavitands and drugs based on the results obtained both in solution and at the interface with the ammonium salts series. Drugs are reported in red.

MC experiments. The MC measurements were conducted with the selected guests and interferents shown in scheme 8. By that time, the authorization to buy and use drugs was delivered by *Ministero della Salute*.

Lactose was tested first alone and then in a mixture 1:1 with caffeine. The street sample tested was a 1:1:1 mixture of ecstasy : lactose : caffeine.



Scheme 8. Structure of the compounds tested on the microcantilevers.

The same protocol already described for ammonium salts detection in chapter 4 was chosen. The solvent used for this new set of measurements was water instead of methanol. The choice was guided by the intention to use a solvent that will not impair the cavitand layer on gold after few measurements and to maximize solvophobic CH- π interactions.

Arrays of eight gold coated MCs, functionalized with **Tiiii[disulfide, CH₃, Ph]**, were exposed to a water solutions of the four chosen guests at a molar concentration of 1×10^{-3} M. The mean signal of the eight MCs was monitored during the flow of each guest through the microfluidic chamber.

The preliminary output is shown in figure 10.

Excipients were tested first: 1×10^{-3} M solutions in water of lactose and lactose and caffeine in a 1:1 ratio were prepared. The array of eight cantilevers was exposed to the water stream of lactose alone and after of the excipients mixture.

The deflections of figure 10 (labeled with yellow and blue colors) show a very similar behavior and a maximum deflection of -20 nm. This response is due to the presence of non specific physisorption on the monolayer surface that causes the deflection of the system.

In the microcantilevers experiments, when testing the difference in the responses due to a proper host-guest complexation or to a non specific force, a reliable result resides in the monitoring of a differential between the two output, not necessarily in an absolute difference.

Hence we expected that the outcome for the drugs should be different enough from the one obtained in the case of the excipients to have a clear distinction between the two.

The array of gold coated cantilever was then exposed to a 1×10^{-3} M solution of cocaine hydrochloride. As shown in figure 10 the curve achieved the same deflection as the interferents. In this case the host-guest complexation strength of the **Tiiii[disulfide, CH₃, Ph]•cocaine** complex equals the physisorption forces monitored in the case of the interferents. So, based on those preliminary results, no distinction can be made between interferents and cocaine hydrochloride, in line with the liquid-liquid titrations.

The positive results arrived with ecstasy. In fact the deflection in this case drifted away from the previous outputs showing a clear recognition in the case of MDMA hydrochloride, achieving a deflection value of -30 nm.

The presence of a bulkier group on the $^+NH_2-CH_3$ unit in ecstasy with respect to the proxy doesn't interfere with the recognition process, opening the

way for a general recognition mode of all methamphetamines, regardless of the substituents.

What was not so obvious was the deflection observed in the case of the amphetamine guest, that reached almost -50 nm. The reason relies most probably in the CH- π interactions that are originated from the methyl in β position to the ammonium group. In fact even if the methyl is not directly attached to the positive charged nitrogen and therefore its acidity is decreased, it can enter into the cavity driven by hydrophobic interactions.

Interesting is the result obtained with the ecstasy street sample: in this case in fact the deepest deflection was observed. The differences between the street sample and the pure ecstasy is probably related to the additive contributions to deflection of excipients.

From these preliminary results, the gold coated cantilevers functionalized with the tetraphosphonate cavitands are able to detect not only the pure drugs but also the street samples.

In order to obtain reliable and reproducible results the non specific interactions towards the interferents should be minimized to avoid the overlap with the cocaine output.

To do so and to obtain a chemically stable monolayer, the cantilever will be changed from gold to silicon. In this way the **Tiii** will be covalently linked to the surface and not chemisorbed like in the case of the gold surface.²⁶

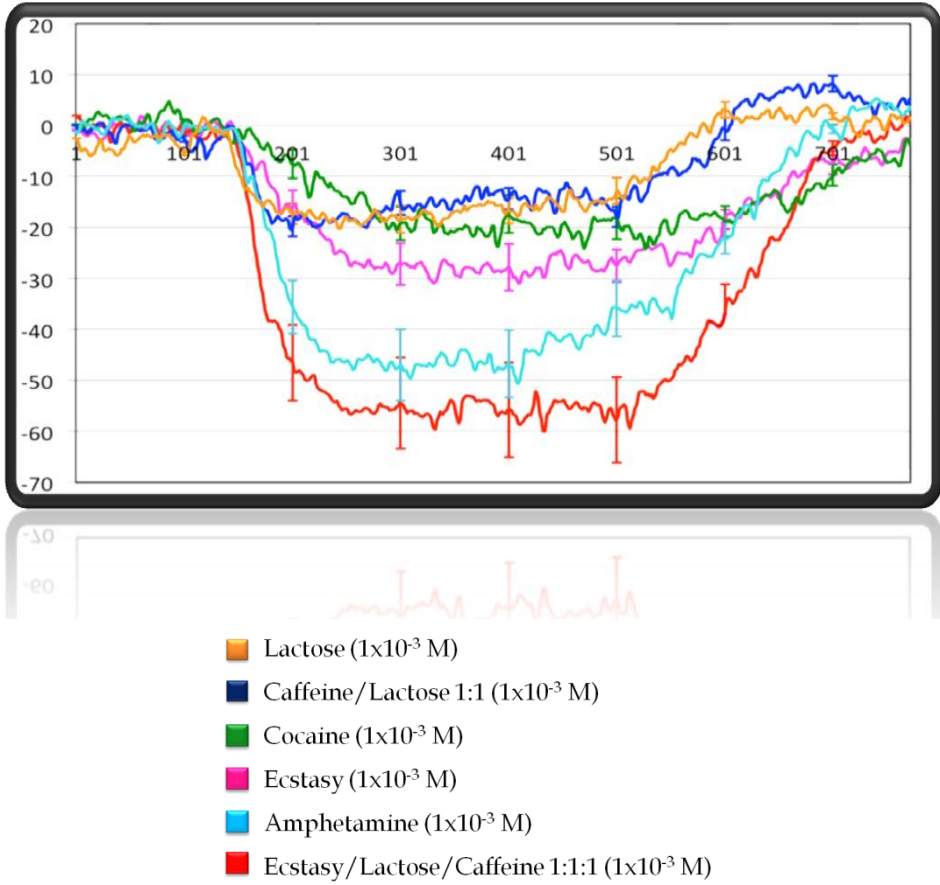


Figure 10. MC deflections of selected drugs and their excipients.

5.3 CONCLUSIONS

In this work preliminary results of a new conception of drug sensor device based on the recognition properties of tetraphosphonate cavitands are presented.

The tests started in solution to evaluate and compare qualitatively the complexation ability of **Tiiii** towards the simplest mimic of ATS group, i.e. the ammonium salts series via ^{31}P NMR. The results were in agreement to what expected from the previous results obtained in chapter 4.

Selected drugs and interferents were then tested at the solid-liquid interface via microcantilevers. Preliminary tests showed that the gold coated cantilevers functionalized with the tetraphosphonate cavitands are able to detect not only the pure drugs but also the street samples. However, non specific interactions like physisorption on the gold surface play an important role in the cantilever deflection, reducing and in some cases resetting the relative difference between interferents and drugs.

Acknowledgements

This work was funded by the grant Nanomechanical Sensors for Amphetamines (SNAF) (Regione Lombardia-INSTM) and by Fondazione CARIPARMA. Thanks to dott. P. Bergese, dott. G. Oliviero and dott. S. Federici for the microcantilevers measurements.

5.4 EXPERIMENTAL SECTION

General Methods. ^{31}P NMR spectra were recorded on Bruker Avance 400 (400 MHz) NMR spectrometer.

Cavitand **Tiiii[disulfide, CH₃, Ph]**,²² **Tiiii[C₃H₇, CH₃, Ph]**,²³ **TSiiii[C₃H₇, CH₃, Ph]** (chapter 2) and ammonium salts (chapter 4)²⁷ were prepared following a published procedure.

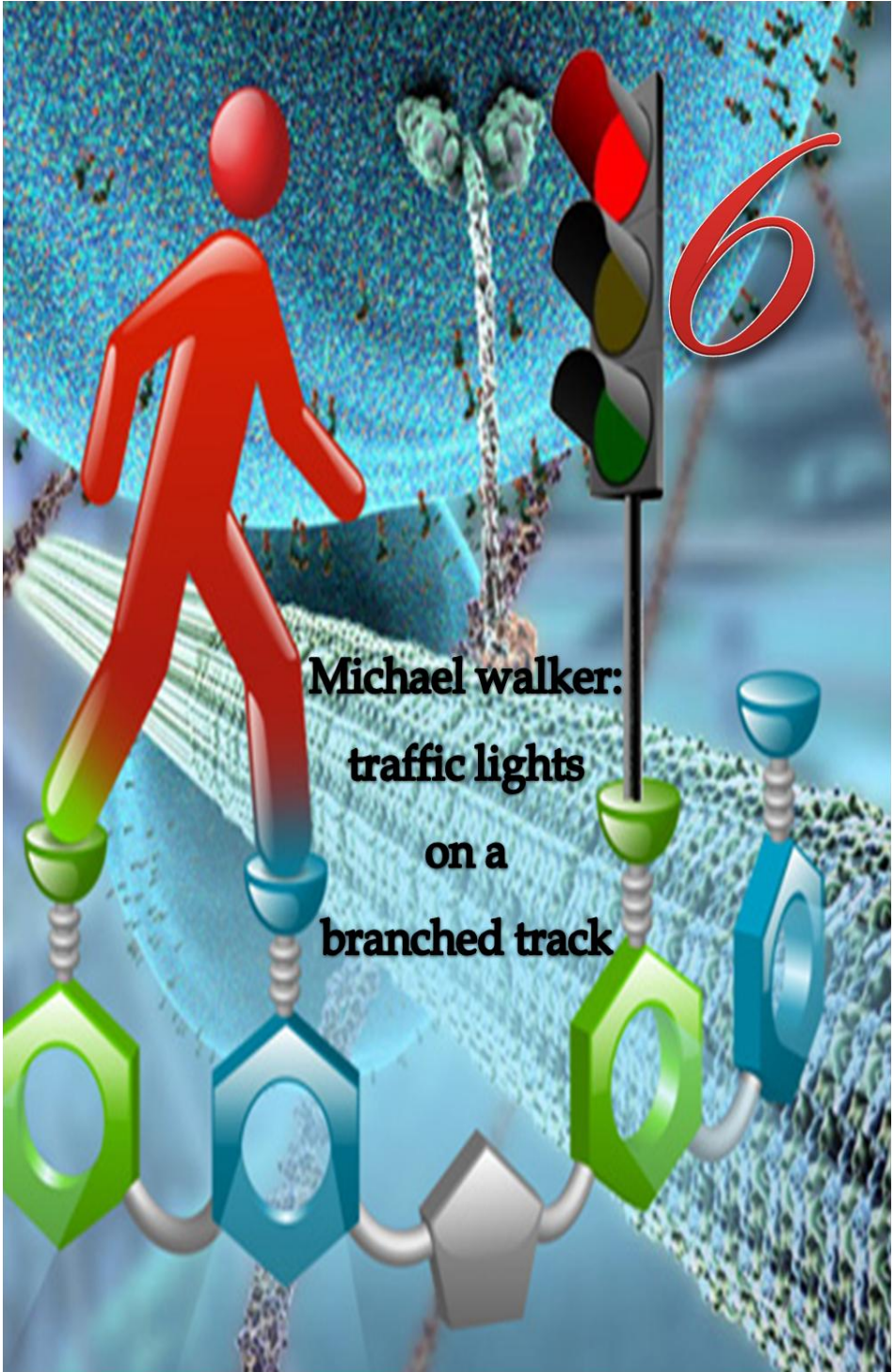
Drugs were obtained from SALARS with the authorization of *Ministero della Salute* and used as received.

5.5 REFERENCES

- ¹ UNODC: **2012** World Drug Report. June **2012**. Vienna, Austria: United Nations Office on Drugs and Crime, **2012**. Available at: http://www.unodc.org/documents/data-and-analysis/WDR2012/WDR_2012_web_small.pdf
- ² Warner, E. A. *Annals of Internal Medicine* **1993**, *119*, 233-235.
- ³ Lathers, C. M.; Tyau, L. S.; Spino, M. M.; Agarwal, I. J. *Clin. Pharmacol.* **1988**, *28*, 584-593.
- ⁴ Gawin, F. H.; Ellingwood, E. H. Jr. *N Engl J Med.* **1988**, *318*, 1173-1182.
- ⁵ Casale, J. F.; Klein, R. F. X. *Forensic Science Review* **1993**, *5*, 95-107.
- ⁶ Naranjo, C.; Shulgin, A. T.; Sargent, T. *Med. Pharmacol. Exp.* **1967**, *17*, 359-364.
- ⁷ Merck, E. German Patent Office, **1914**.
- ⁸ a) Karch, S. B. The pathology of drug abuse, CRC Press, Boca Raton, FL; 156; b) Carvalho, F.; Felix Carvalho, Remia, F.; Amado, F.; Domingues, P.; Correia, A. J. F.; Bastos, M. L. *Chemical research in toxicology* **1996**, *9*, 1031; c) O'Connor, B. *Br. J. Hosp. Med.* **1994**, *52*, 507-514; d) Forrest, A. R. W. *Forensic Sci. Int.* **1995**, *64*, 57-59.
- ⁹ Schifano, F.; Corkery, J.; Naidoo, V.; Oyefeso, A.; Ghodse, H. *Neuropsychobiology* **2010**, *61*, 122-130.
- ¹⁰ Nichols, D. E. J. *Psychoactive drugs* **1986**, *18*, 305-313.
- ¹¹ a) Pellegrini, M.; Rosati, F.; Pacifici, R.; Zucaro, P.; Rosmolo, F. S.; Lopez, A. J. *Chromatogr. B* **2002**, *769*, 243-251; b) Marquet, P.; Lacasiie, E.; Battu, C.; Faubert, H.; Lachatre, G. *J. Chromatogr. B* **1997**, *700*, 77-82; c) Ortuno, J.; Pizarro, N.; Farre, M.; Mas, M.; Segura, J.; Cami, J.; Brenneisen, R.; de la Torre, R. *J. Chromatogr. B* **1999**, *723*, 221-232; d) Ensslin, H. K.; Kovar, K.-A.; Maurer, H. H. *J. Chromatogr. B* **1996**, *683*, 189-197.k

- ¹²a) Herraéz-Hernandez, R.; Campins-Falco, P.; Andres, J. V. *Analyst* **2001**, 126, 581-586; b) Sadeghipour, F.; Veuthey, J.-L. *J. Chromatogr. A* **1997**, 787, 137-143.
- ¹³Sadeghipour, F.; Giroud C.; Rivier, L.; Veuthey, J.-L. *J. Chromatogr. A* **1997**, 761, 71-78.
- ¹⁴Huestis, M. A.; Cone, E. J. *Ann. N. Y. Acad. Sci* **2007**, 104-121.
- ¹⁵Kraemer, T. *Anal. Bioanal. Chem.* **2007**, 388, 1415-1435.
- ¹⁶ a) Fang, C.; Chyng, Y. L., Ju-Tsung, L.; Lin, C. H. *Forensic Sci. Int.* **2002**, 125, 142-148; b) Lanz, M.; Brenneisen, R.; Thormann, W. *Electrophoresis* **1997**, 18, 1035-1043.
- ¹⁷Butler, D.; Pravda, M.; Guilbault, G. G. *Anal. Chim. Acta* **2006**, 556, 333-339.
- ¹⁸a) Baker, J. E.; Jenkins, A. *Am. J. Forensic Med. Pathol.* **2008**, 29, 141-144; b) Contreras, M. T.; Hernandez, A. E.; Gonzalez, M.; Gonzalez, S.; Ventura, R.; Pla, A.; Valverde, J. L.; Segura, J.; de la Torre, R. *Forensic Science International* **2006**, 164, 168-171; c) Mead, J. A.; Niekro, J.; Staples, M. *Clin. Chem.* **2003**, 49, A122-A122.
- ¹⁹a) Lopez, P.; Martello, S.; Bermejo, A. M.; De Vincenzi, E.; Tabernero, M. J.; Chiarotti, M. *Anal. Bioanal. Chem.* **2010**, 397, 1539-1548; b) Spiehler, V.; Isenschmid, D. S.; Matthews, P.; Kemp, P.; Kupiec, T. J. *Anal. Toxicol.* **2003**, 27, 587-591; c) Kerrigan, S.; Phillips, W. H. *Clin. Chem.* **2001**, 47, 540-547.
- ²⁰a) Barroso, M.; Dias, M.; Vieira, D. N.; Queiroz, J. A.; LopezRivadulla, M. *Rapid Commun. Mass Spectrom.* **2008**, 22, 3320-3326; b) Cristoni, S.; Basso, E.; Gerthoux, P.; Mocarelli, P.; Gonella, E. *Rapid Commun. Mass Spectrom.* **2007**, 21, 2515-2523; c) Valente-Campos, S.; Yonamine, M.; Moreau, R.; Silva, O. A. *Forensic Science International* **2006**, 159, 218-222.
- ²¹a) Jagerdeo, E.; Montgornery, M. A.; Sibum, M.; Sasaki, T. A.; LeBeau, M. A. J. *Anal. Toxicol.* **2008**, 32, 570-576; b) Johansen, S. S.; Bhatia, H. M. *J. Chromatogr. B* **2007**, 852, 338-344; c) Nesmerak, K.; Sticha, M.; Cvancarova, M. *Anal. Lett.* **2010**, 43, 2572-2581.

- ²²Kang, K.; Sachan, A.; Hamilton, M.-N.; Shrotriya, P. *Langmuir* **2011**, *27*, 14696-14702.
- ²³Baer, I. PhD thesis, *The analysis of excipients in ecstasy tablets and their contribution in a drug profiling context*, Université de Lausanne, **2007**.
- ²⁴Biavardi, E.; Battistini, G.; Montalti, M.; Yebeutchou, R. M.; Prodi, L.; Dalcanale, E. *Chem. Commun.* **2008**, 1638-1640.
- ²⁵Dionisio, M.; Maffei, F.; Rampazzo, E.; Prodi, L.; Pucci, A.; Ruggeri, G.; Dalcanale, E. *Chem. Commun.* **2011**, *47*, 6596-6598.7
- ²⁶Biavardi, E.; Favazza, M.; Motta, A.; Fragalà, I. L.; Massera, C.; Prodi, L.; Montalti, M.; Melegari, M.; Condorelli, G. G.; Dalcanale, E. *J. Am. Chem. Soc.* **2009**, *131*, 7447-7455.
- ²⁷Dionisio, M.; Oliviero, G.; Menozzi, D.; Federici, S.; Yebeutchou, R. M.; Schmidtchen, F.-P.; Dalcanale, E.; Bergese, P. *J. Am. Chem. Soc.* **2012**, *134*, 2392-2398.



**Michael walker:
traffic lights
on a
branched track**

6.1 INTRODUCTION

General Scenario. Nature has always been a great source of inspiration for scientists. In the last decades, one of the most challenging topics in chemistry has been the creation of artificial molecular transport systems,^[1, 2] taking inspiration from kinesin,³ dynein⁴ and myosin⁵ motor proteins that can "walk" along polymeric filaments transporting cargoes (figure 1).

Although their molecular architectures and cellular roles can differ significantly, all naturally occurring motor proteins share several important characteristics.⁶ First, they convert an energy input (supplied by either nucleotide hydrolysis or ionic gradients) into mechanical and/or chemical work. Second, their molecular design restricts the degrees of freedom of the motor and/or the substrate. For example, DNA and RNA polymerases "pull" the blueprint nucleic acid strand in only one direction through a narrow clamp and molecular walkers migrate along rigid, essentially one-dimensional, tracks. Third, all molecular motor proteins operate under conditions of low Reynold's number where inertia and momentum are irrelevant and viscous forces and random thermal motion dominate dynamics. In other words they must "swim in molasses and walk in a hurricane".⁷

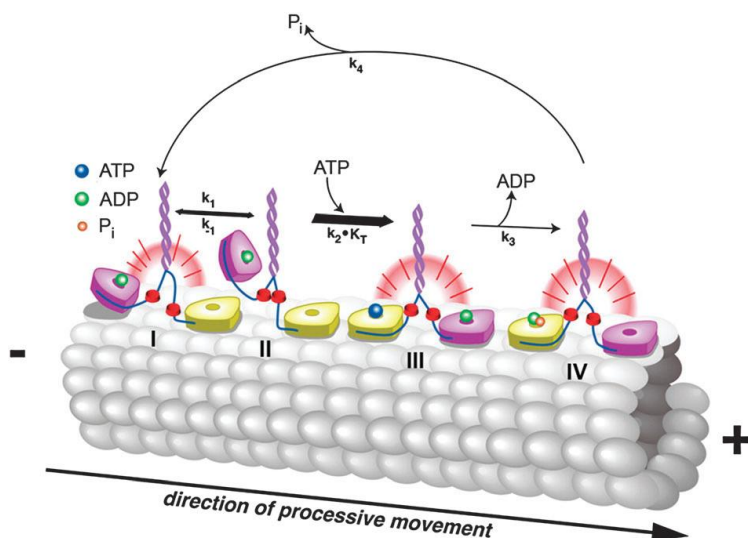
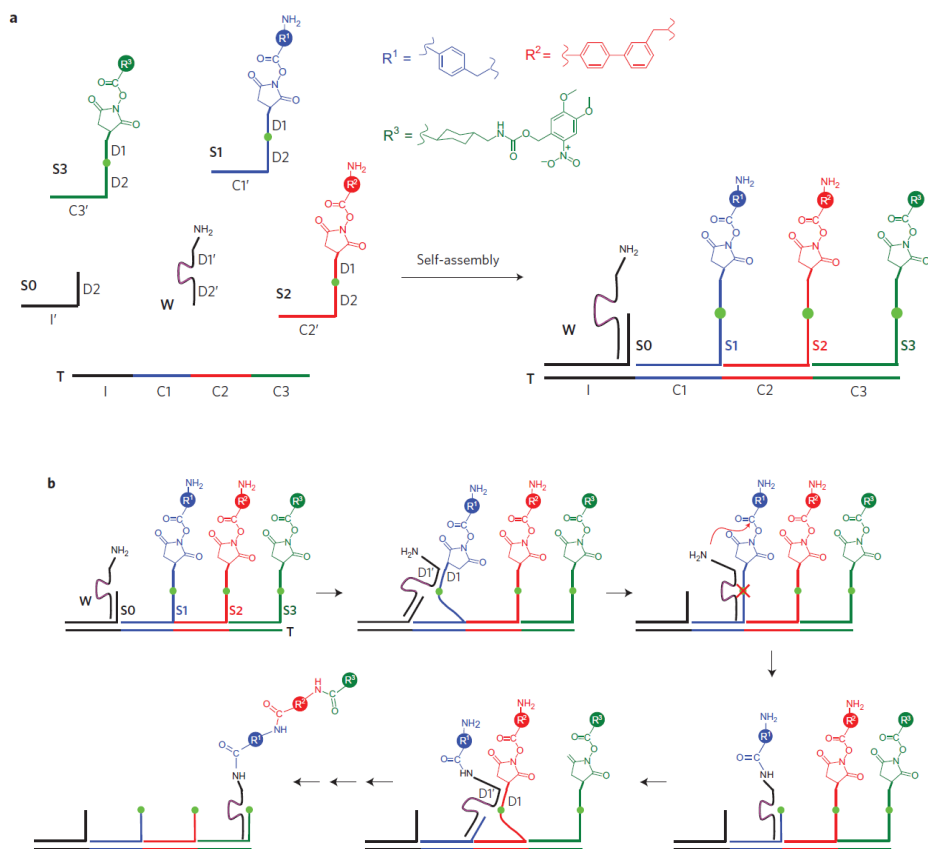


Figure 1. Schematic representation of the walking mechanism of kinesin-I. The fuel for the walking process comes from the ATP hydrolysis.⁶

"Walking" describes a specific and autonomous mechanism in which the protein carries out progressive, processive, repetitive, mostly-directional changes of its point of contact with the molecular track without completely detaching from it.⁸ In detail:

- ⊘ *progressivity* is the capability of the molecular motor to be reset at the end of each mechanical cycle without invalidating the task that was performed.
- ⊘ *Processivity* is the capability of the walking molecule to remain attached to the scaffold during the walking process.
- ⊘ *Repetitivity* is the ability to perform the same cycle more and more over.
- ⊘ *Directionality* is the feature to walk preferentially in one direction.
- ⊘ *Autonomy* is the characteristic to continue the task performed until the fuel is present.⁶

In literature are reported several DNA based molecular motors² (see scheme 1 for an example) but up to date very few examples of synthetic motors exhibit the proper walking characteristics.



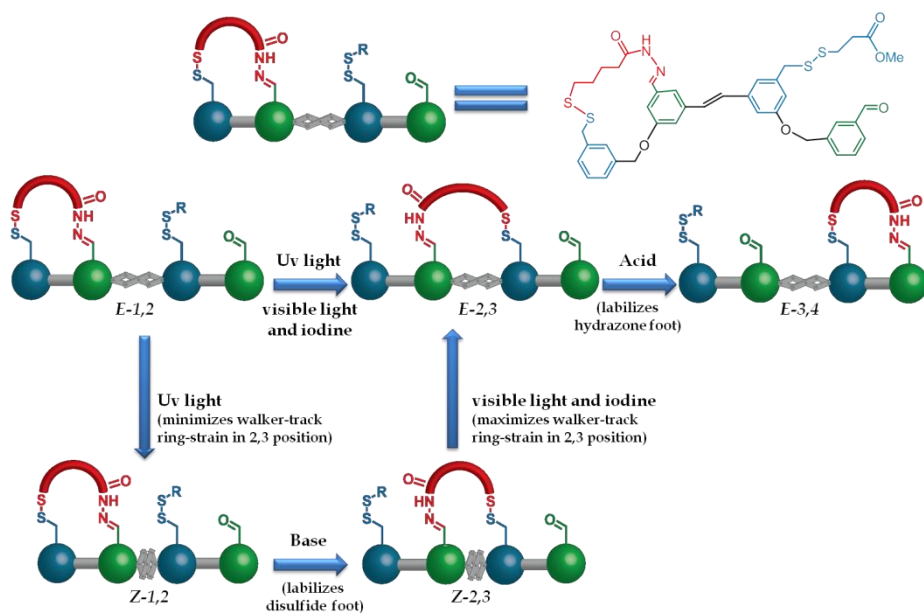
Scheme 1. DNA walker moving along a DNA track that can be used to perform a series of amine acylation reactions in a single solution without any external intervention. Overview: **a**) the system described in figure comprises six DNA or DNA-linked molecules. Three substrates (S1–S3) and an initiator (S0) can hybridize on a single-stranded DNA track (T). Each substrate has an amino acid NHS ester at its 5' end and two ribonucleotides (green dot) in the middle of its DNA sequence. The DNA walker (W) contains a 3' amine group and an RNA-cleaving DNAzyme (purple line) that can cleave the ribonucleotides in the substrates. **b**) DNAsome-mediated multistep synthesis of a triamide product. All steps take place in a single solution under one set of reaction conditions without external intervention.²ⁱ

Professor Leigh's group started to focus on the design and the construction of small molecules that are able to walk on a track without completely detaching from it.

One of the first published examples^{1c} is represented in scheme 2, in which a walker constituted of a disulfide foot (labile in base, locked in acid) and a hydrazone foot (labile in acid, locked in base) can migrate in both directions on a stilbene based track, depending on the type of external stimuli applied:

- ⊖ acid/base for the selective dissociation of one of the feet;
- ⊖ UV/visible light to influence the ring strain between walker and track by isomerization of the stilbene unit contained in the track.

However, external intervention is needed for the walking process in all the non-DNA motors.



Scheme 2. Schematic representation of the working principle of a light-driven walker-track system based on selective labile feet and adjustable ring strain between walker and track.

To take this studies one step further, it was necessary to construct a motor that possesses the ability to walk in a completely autonomous way, without any external stimuli.

Already in 1970, Lawton proposed the "equilibrium transfer alkylating agents" (ETAC), reagents that are able to form reversible covalent bonds between pairs of accessible nucleophilic sites on proteins through a series of inter- and intramolecular Michael and retro-Michael reactions until the most thermodynamically stable crosslink is reached.⁹ In figure 2 the process mechanism is illustrated. Consider the interaction between a walker unit that carries one or more electron withdrawing groups and a protein with several nucleophilic sites available (SH, NH...). Michael addition of the walker on one of the exposed nucleophilic residues (1) would be followed by retro-Michael of the leaving group (overall equivalent to an S_N2' process) with the unmasking of the latent double bond (2-3). The covalently attached species 3 can now undergo an intramolecular Michael reaction yielding a cross-linked derivative 4. This process could continue until the lowest energy cross linked product has been formed.

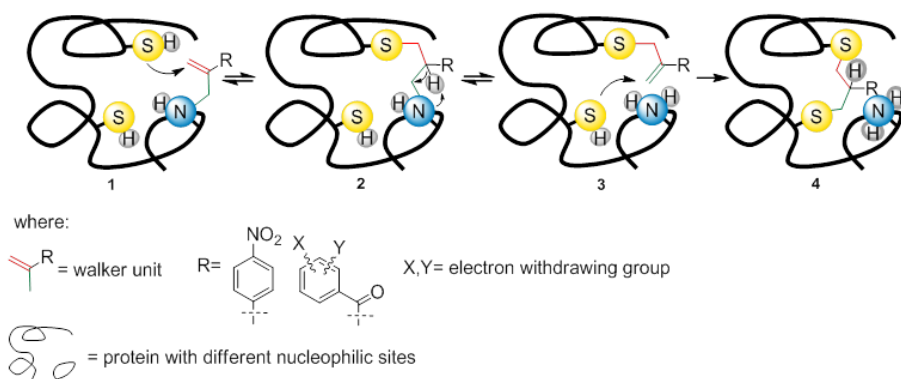
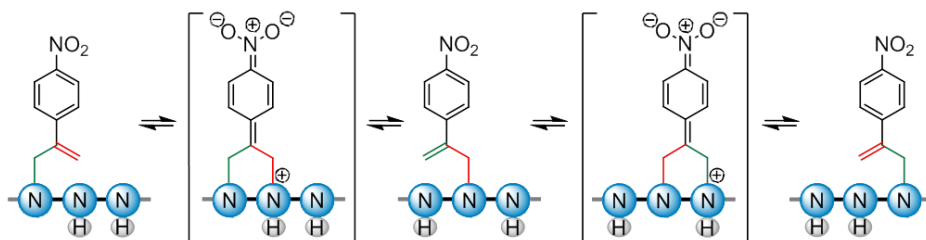


Figure 2. Schematic representation of an ETAC migration from one nucleophilic site of a protein to another via subsequent Michael reactions. The process continues until the most thermodynamically stable cross-linked product has been established.

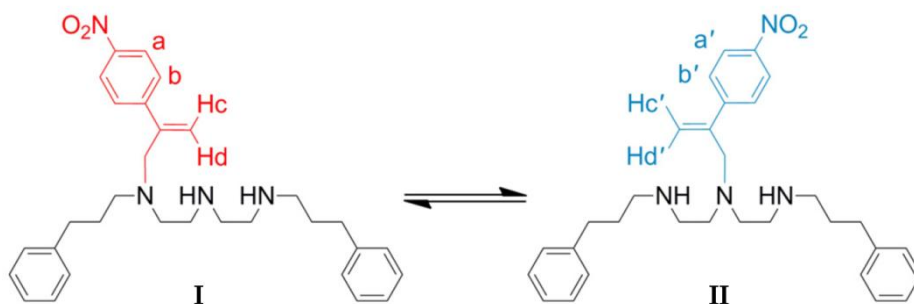
Small molecules that walk along a track. Taking inspiration from Lawton's studies, David Leigh's group has recently described a new type of walking system: the first synthetic small molecule that walks down a linear track with a high degree of processivity *without any external stimuli* (scheme 3).¹⁰ The walking mechanism starts with the attack of the amino group nucleophilic site on the double bond of the walker, with the consequent formation of a bridged intermediate (shown in brackets) in which the α -methylene-4-nitrostyrene has both legs attached to the polyamine track. Afterwards the

walker can undergo a retro-Michael reaction unmasking the double bond of the walker and forcing it to migrate from the first amine to the second one. Then the Michael and retro-Michael reaction can continue until the most thermodynamically stable distribution of the walker is reached. Unlike ETAC reagents in which cross-linked products are the favored one, in this case the products in which the walker is attached by only one leg is the thermodynamically stable one.



Scheme 3. Operating mechanism of *a*-methylene-4-nitrostyrene on a polyamine track exploiting Michael and retro-Michael reactions without external intervention.

The walking mechanism was followed by ^1H NMR, monitoring the changes of the vinyl protons of the double bond (scheme 4, Hc/Hc', Hd/Hd') in DMSO- d_6 . The 1,4-*N,N*-migration process reached almost the 1:1 ratio between the 2 isomers after 15 hours (entry c).



Scheme 4. 1,4-*N,N*-migration of *a*-methylene-4-nitrostyrene between two secondary amines.

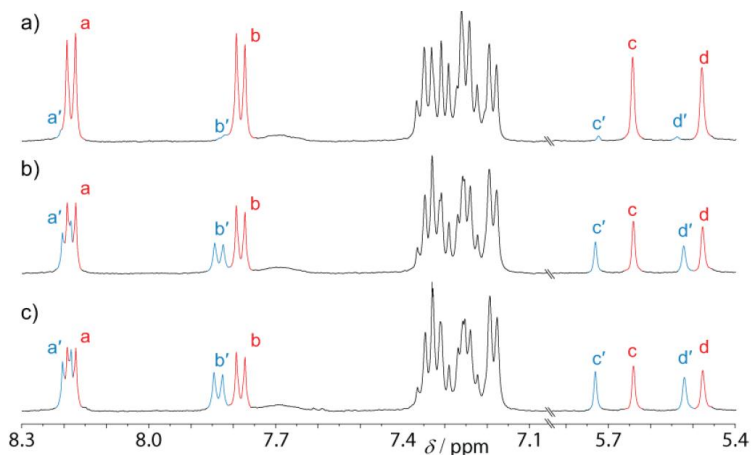


Figure 3. Relevant portions of ^1H NMR spectra of exchange between isomers **I** and **II**. a) $t=5$ minutes, **I:II** ratio 1:0.06; b) $t=2$ hours, **I:II** ratio 1:0.6; c) $t=15$ hours, **I:II** ratio 1:0.9. The letters correspond to the proton labeled in scheme 4. All spectra were recorded in $\text{DMSO-}d_6$.

The walking mechanism is highly solvent dependent, in fact in chlorinated solvent no formation of **II** was observed, while in CD_3OD the conversion calculated was less than the 10% after 15 hours and in CD_3CN the conversion reached the 25% after 15 hours. $\text{DMF-}d_7$ and $\text{DMSO-}d_6$, instead, showed a ratio between **I** and **II** very close to 1:1, respectively after 15 and 4.5 hours (all experiments were performed at room temperature).

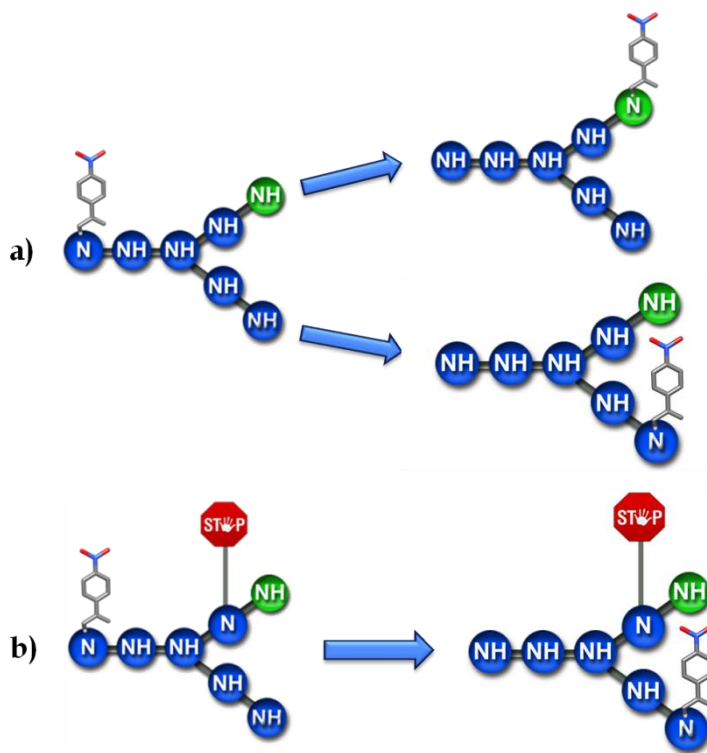
The demonstration of a major intramolecular walking mechanism was achieved by increasing tenfold the concentration of the starting walker-track conjugate and monitoring no substantial changes neither in the rate constant of the reaction nor in the ratio between **I** and **II**.

After demonstrating that this type of walker can migrate on a track independently, the next step was to control this type of walking by forcing the Michael walker in one preferred direction. A way to solve this issue is to find a so-called "traffic lights" that with his presence (and absence) influences the walking direction. In ETAC reagents no external control was possible during the Michael and retro-Michael reactions, while the insertion of a traffic lights on the track should be the first step towards an autonomous and at the same time controlled walking process.

Herein we present the work done in order to find a suitable candidate as a Michael walker traffic lights and the preliminary walking tests made.

6.2 RESULTS AND DISCUSSION

Choice of the traffic lights. A traffic lights is an amine protecting group, its function is shown in scheme 5: the presence of a traffic light on a branched track should give to the Michael walker a preferential walking direction, while, once the protecting group is cleaved, the walker should be able to migrate in every direction.

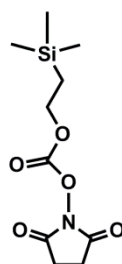


Scheme 5. Operating mechanism of a traffic lights. a) Without the presence of a traffic lights the walker is potentially able to reach both ends of the track (green and blue NH); b) after the traffic light attachment the Michael walker is able to pursue just one forced direction (blue NH); once that the stopper has been removed, the walker regains the possibility to move freely in both directions (a).

The choice of the protecting group must fulfill a series of requirements, listed below:

- ∅ it must be cleaved after the Michael walker attachment on the track, in conditions that don't affect the stability of the walker-track bond, with a non basic and non reductive treatment, because of the probability that those conditions help the detachment of the walker from the track.
- ∅ it must be stable to reductive amination and to deprotection of the TFA group, since these are the last steps of the target branched track synthesis;
- ∅ it must be stable to Boc deprotection, because two different amine protecting groups are required on the track to have a selective position attachment of the walker, cleaving one group at the time in different conditions.

The first choice was 1-[2-(Trimethylsilyl)ethoxycarbonyloxy]pyrrolidin-2,5-dione (Teoc, figure 4), one of the (few) protecting group that satisfies all the requirements listed, being stable to certain acid and basic conditions and to reductive amination.

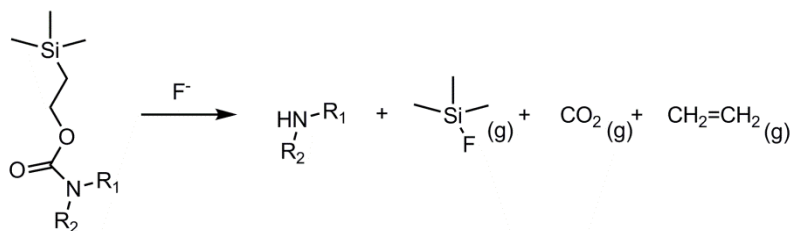


1-[2-(Trimethylsilyl)ethoxycarbonyloxy]pyrrolidin-2,5-dione
(Teoc)

Figure 4. Structure of Teoc

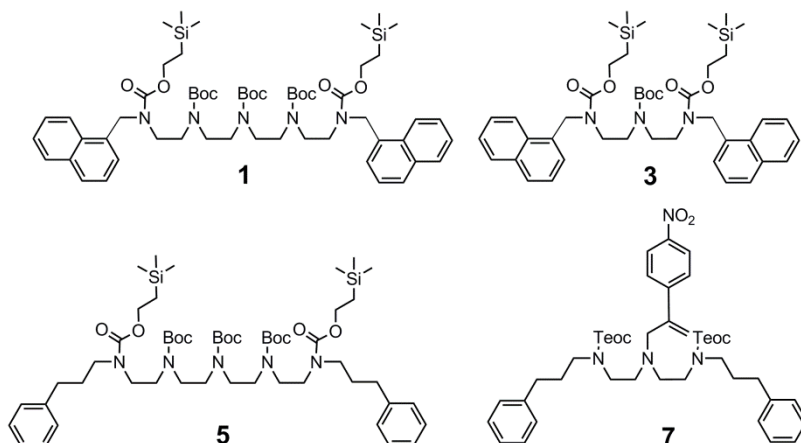
The Teoc group undergoes fragmentation when treated with fluoride ions giving gaseous byproducts (scheme 6).

The most used agents are TBAF^[11a, 10b, 10c] and KF, the last one used usually in combination with acids or crown ethers.^{10a}



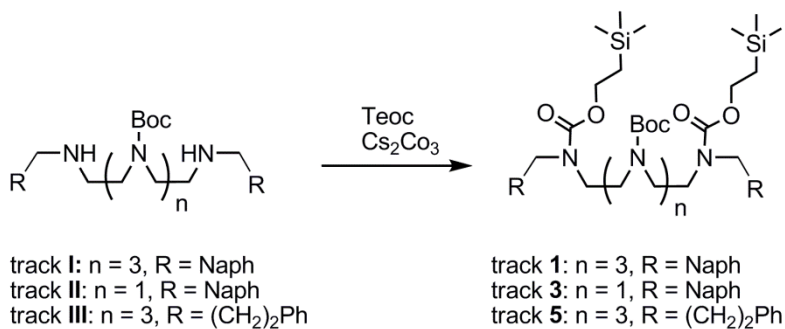
Scheme 6. Teoc fragmentation reaction.

Tracks and walker. In scheme 7 the tracks used for the Boc deprotection studies (**1**, **3** and **5**) and for the walking tests in the presence of the traffic lights (**7**) are shown.



Scheme 7. Compounds used in the present work.

Compounds **1**, **3**, and **5** were formed by reacting already available track **I**, **II** and **III**⁹ with Teoc and Cs₂CO₃ as a base (scheme 8, see experimental part for details). Synthesis of track **7** is reported in scheme 12 (see experimental part for details).



Scheme 8. Formation of Teoc protected tracks, general procedure.

Work was structured as reported below:

- ∅ find the suitable conditions to achieve selective deprotection of Boc in the presence of Teoc to free the amine on which the walker will be attached;
- ∅ since branched tracks are difficult to prepare, first the design and the synthesis of a linear model track was obtained;
- ∅ attachment of the Michael walker on the track;
- ∅ explore the optimal conditions to remove Teoc protecting group and monitor the walking process.

Herein the results obtained are explained and discussed.

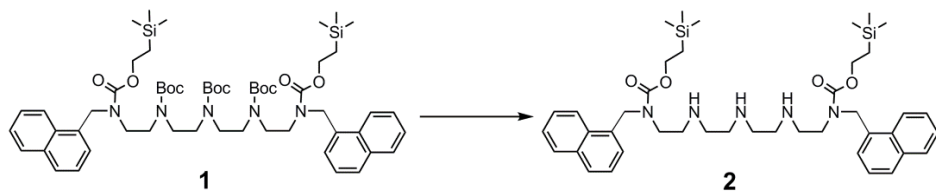
Selective Boc deprotection studies. Initially, the selective deprotection of Boc in the presence of Teoc (scheme 9) was tested exploring the traditional Boc cleavage conditions with acids.

The results obtained are summarized in table 1.

Treating track **1** with trifluoroacetic acid leads to the complete deprotection of both Teoc and Boc groups without any selectivity (entries **a** and **b**).

Milder conditions were then chosen (entries **c** and **d**), using HCl 1.25 M solution in MeOH as the cleavage agent.

The deprotection was again totally unselective: after 24 hours the track **1** was completely deprotected.



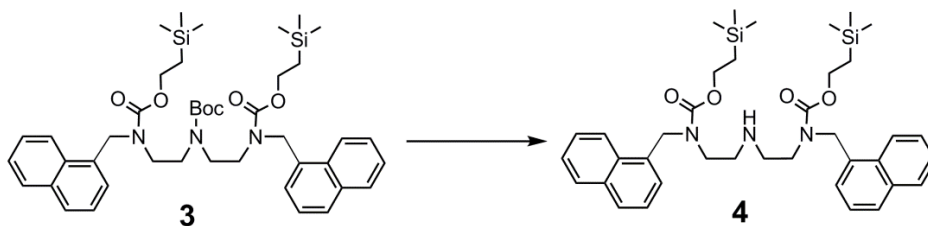
Scheme 9. *Selective Boc deprotection reaction.*

	Deprotection conditions	Result
a	20% TFA in CH ₂ Cl ₂ , 2 h	Complete deprotection of both Boc and Teoc
b	10% TFA in CH ₂ Cl ₂ , 1 h	Complete deprotection of both Boc and Teoc
c	HCl 1.25 M in MeOH, 1 h	Partial deprotection of one and two Boc
d	HCl 1.25 M in MeOH, 1 d	Complete deprotection of both Boc and Teoc

Table 1. *Deprotection conditions tested and results obtained.*

Since no control of the selectivity was possible under acidic conditions, another route was tried: ceric ammonium nitrate ((NH₄)₂Ce(NO₃)₆) (from now on referred to as CAN) is an efficient catalyst for Boc removal that acts under neutral conditions. The mechanism involves the oxidation of the carbonyl group, subsequent fragmentation to give the carboxylate radical and the final decarboxylation step.¹²

In table 2 the conditions tested and the outcomes are summed up. The mildest conditions were tried first, using CAN in catalytic amount at room temperature (entry **a**), but just a partial deprotection of the Boc was reached. Tuning the temperature (entry **b** and **d**) and the equivalents (entry **c** and **e**) didn't increase the conversion while putting a large excess (entry **f**) of CAN led to both Boc and Teoc cleavage.



Scheme 10. Selective Boc deprotection reaction.

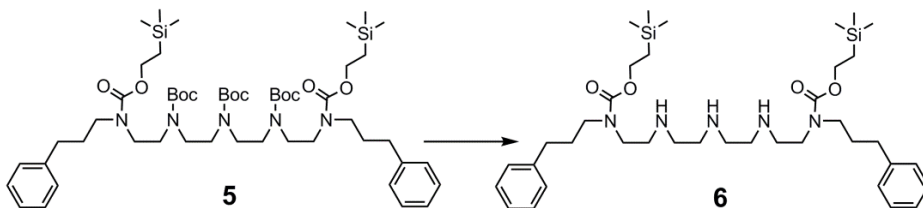
	Deprotection conditions	Result
a	CAN in catalytic amount at r.t., days	Partial deprotection of the Boc
b	CAN in catalytic amount at reflux, days	Partial deprotection of the Boc
c	CAN in stoichiometric amount at r.t., days	Partial deprotection of the Boc
d	CAN in stoichiometric amount at reflux, days	Just partial deprotection of the Boc
e	CAN in excess (5 equivalents) at r.t. then reflux, days	Partial deprotection of the Boc
f	CAN in large excess (10 equivalents) at reflux, 1 day	Complete deprotection of both Boc and Teoc

Table 2. Deprotection conditions tested and results obtained.

Naphthilic amines on the track demonstrated to be very prone to the Teoc detachment under both acidic and neutral conditions. The reactivity of non benzylic amines was then tested, to evaluate if the nitrogen position with respect to the benzyl group could play a role in the deprotection studies.

In scheme 11 the new track **5** is shown. The amino ending groups are positioned in δ position with respect to the benzyl moieties, while in the previous cases the amines were all naphthilic and therefore positioned in β position to the aromatic ending moieties.

Compound **5** was subjected to deprotection in acidic conditions using HCl 1.25 M in MeOH (table 3). These conditions were chosen in order to have a milder cleavage agent with respect to TFA that showed a total unselectivity. In this case a selective cleavage of the Boc group was attained, tuning the acid concentration until a large excess was added.



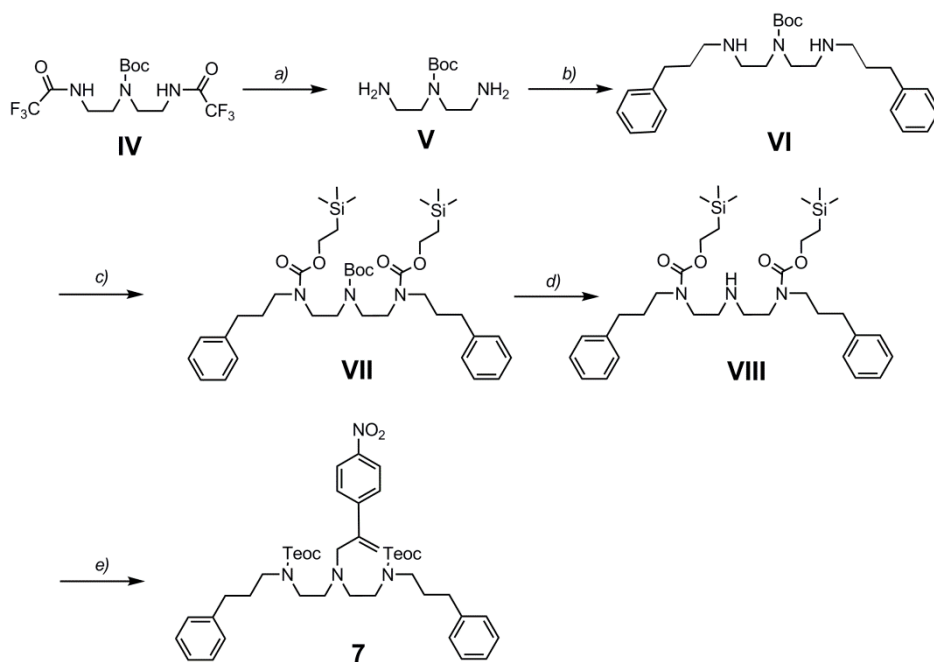
Scheme 11. Selective Boc deprotection reaction.

	Deprotection conditions	Result
a	HCl 1.25 M, large excess, 4 days	Selective deprotection of the Boc

Table 3. Deprotection condition tested and result obtained.

In the next step the efforts were focused on the synthesis of a simple three-amines model track with non benzylic ending amines necessary to hold the Teoc during the Boc deprotection conditions.

Model track synthesis. Model track 7 was synthesized according to the synthetic protocol shown in scheme 12. Compound IV was previously synthesized according to a literature procedure.⁷ The first step was the TFA deprotection using NaOH followed by reductive amination with 3-propionaldehyde, both reactions performed following a literature procedure. The protection of the amines with Teoc group was accomplished using a likewise procedure already used for tracks 1, 3 and 5 in scheme 8. The subsequent removal of the Boc was carried out in the presence of a large excess of HCl 1.25 M in MeOH and the final step was the attachment of α -methylene-4-nitrostyrene on the central amine in the presence of DIPEA.



Scheme 12. Synthesis of track VIII and attachment of the Michael walker. Conditions: a) NaOH, H₂O, MeOH, r.t., 4 h, yield 93%; b) 3-phenylpropionaldehyde, absolute EtOH, r.t., 24 h; NaBH₄, r.t., 4 h, yield 20%; c) 1-[2-(Trimethylsilyl)ethoxycarbonyloxy]pyrrolidin-2,5-dione, Cs₂CO₃, DCM, r.t., overnight, yield 35%; d) HCl 1.25 M in MeOH, r.t., overnight, yield 80%; e) α -methylene-4-nitrostyrene, DIPEA, MeOH, 60°C, 2 days, 57%.

Stability in walking conditions. Before performing the Teoc deprotection studies and monitoring the migration of the Michael walker, it was necessary to evaluate the stability of the molecule in the standard walking conditions that were developed in Leigh's laboratory. Dimethylformamide and dimethylsulfoxide proved to be the best solvents for walking conditions, so stability in both solvents was tested. The ^1H NMR in $\text{DMSO-}d_6$ over 2 hours (figure 5) showed that no significant changes in the diagnostic peaks of the Michael walker and of the track occurred (using DMF instead of DMSO led to the same result).

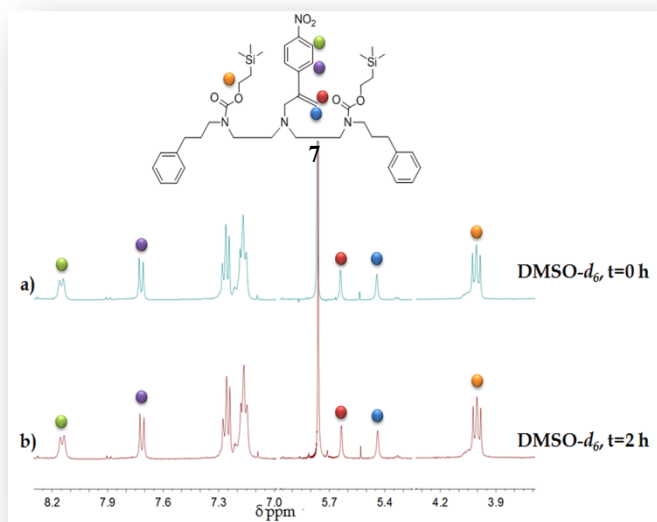


Figure 5. Relevant portions of ^1H NMR of compound 4 in $\text{DMSO-}d_6$. No changes occur over 2 hours.

The presence of a base in the solvent is necessary to assure that none of the amines present on the track could be protonated from the previous synthetic steps and therefore stop the walking process. The stability in both $\text{DMSO-}d_6$ and $\text{DMF-}d_7$ in the presence of 2 equivalents of DIPEA was tested. Below (figure 6) the behavior of compound 7 in $\text{DMSO-}d_6$ in the presence of 2 equivalents of DIPEA was monitored over 18 hours, showing neither shifts nor changes in the ^1H NMR.

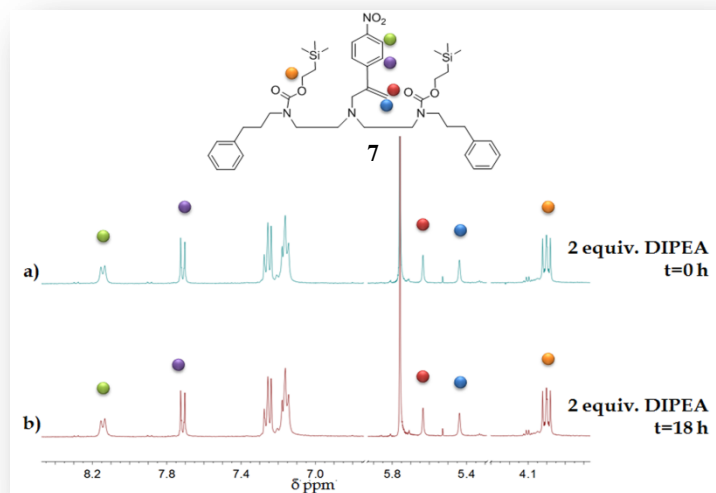


Figure 6. Relevant portions of ¹H NMR of compound 7 in DMSO-*d*₆ + 2 equivalents of DIPEA. No changes occur over 2 hours.

Teoc deprotection studies. After demonstrating the stability of the molecule in the standard walking conditions, the agent and conditions for Teoc deprotection were chosen.

KF cleavage agent. Since the cleavage of the Teoc group is usually achieved exploiting the nucleophilicity of the fluoride ion, KF was chosen.

Compound 7 was treated with a stoichiometric amount of KF (2 equivalents) and monitored over time. At time 0 (figure 7 entry a) no significant changes occurred to the sample. After 24 hours no deprotection of the Teoc group was present. The diagnostic signal of the protecting group showed no shift neither changes over the 24 hours. KF alone is a mild cleavage agent, and it is usually used in combination with other compounds, such as crown ethers that can trap the potassium, separating the ion couple and enhancing the nucleophilicity of the fluoride anion. In this case the use of the crown ether was avoided in order to have a clearer NMR spectra without additional interfering peaks.

Since TBAF acts like an efficient deprotection agent for TMS protecting groups, it was decided to add a stoichiometric amount of TBAF (3 equivalents) to harsher the deprotection conditions. At time 0 (entry c) a partial cleavage of

the Teoc was clearly visible and a splitting of the diagnostic signals of the Michael walker was occurring, meaning that it was starting to migrate to the adjacent amine. After 1 hour the new conditions led to the decomposition of the molecule and the complete detachment of the Michael walker (entry d).

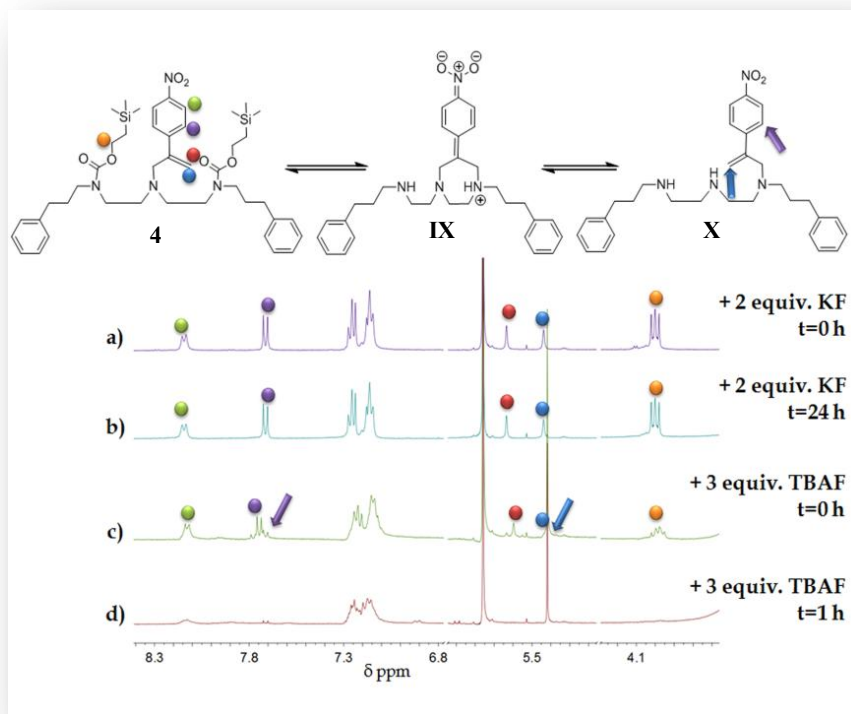


Figure 7. Relevant portions of deprotection study ^1H NMR spectra: a) compound 7 + 2 equivalents of KF at $t = 0$; b) compound 7 + 2 equivalents of KF $t = 24$ h; c) compound 7 + 2 equivalents of KF + 3 equivalents of TBAF at $t = 0$; d) compound 7 + 2 equivalents of KF + 3 equivalents of TBAF $t = 1$ h. Every spectra was recorded in $\text{DMSO-}d_6$ in the presence of 2 equivalents of DIPEA.

TBAF cleavage agent. Since TBAF attested to be an efficient deprotection agent for Teoc but at the same time a strong cleavage reagent also for the Michael walker, the next step was tuning his concentration in the buffer to enhance the Teoc removal and decrease to zero the Michael walker detachment. TBAF in catalytic amount was then tested (figure 8) in $\text{DMF-}d_7$. The solvent

switch was tried because previous study demonstrated that under certain conditions the walker detachment is favored in DMSO rather than in DMF.

After dissolving track **7** in DMF + 2 equivalents of DIPEA and monitoring its stability in these conditions, catalytic TBAF was added. Over 1 hour no changes in the proton NMR spectra were noticeable (entry **a** and **b**). Monitoring the reaction over 3 days showed that something was clearly changing in solution, but unfortunately no structure could be undeniably assigned to the new peaks formation controlling the reaction by ESI-MS.

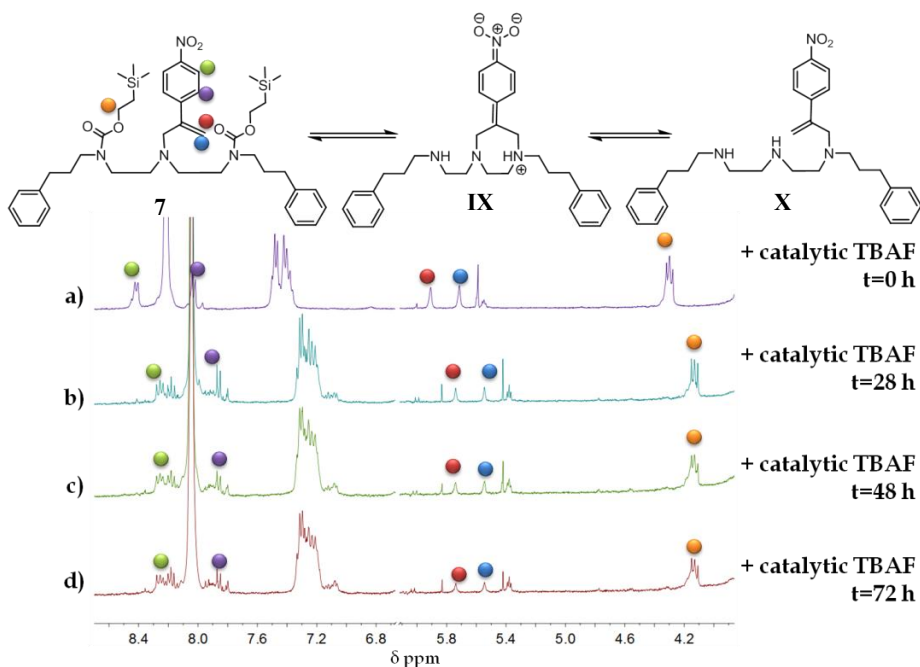


Figure 8. Relevant portions of ^1H NMR deprotection study with a catalytic amount of TBAF: the spectra monitor the response of compound **7** with TBAF over time a) $t = 0$; b) $t = 28$; c) $t = 48$ hours and d) $t = 72$ hours. Every spectra was recorded in DMF-d_7 in the presence of 2 equivalents of DIPEA.

TFA cleavage agent. In the first Boc deprotection studies (see table 1) it was showed that the use of trifluoroacetic acid was leading not only to Boc deprotection but also to the cleavage of the Teoc. This was exploited for the final deprotection study, using TFA as deprotecting agent for the Teoc group. In this case just a stoichiometric amount (3 equivalents) was used, since a larger

amount could give interference problems with the diagnostic peaks of the track. After the addition of the reagent, at time zero no deprotection of Teoc was observed (figure 9), instead there was a clear difference in the double bond protons of the Michael walker (entry **a** and **b**): from the spectra was not clear whether they were experiencing an upfield shift or a huge shape broadening. None of the two is anyhow related to the walking process. From the monitoring of the reaction over time (entry **c** and **d**), cleavage of the Teoc was not observed.

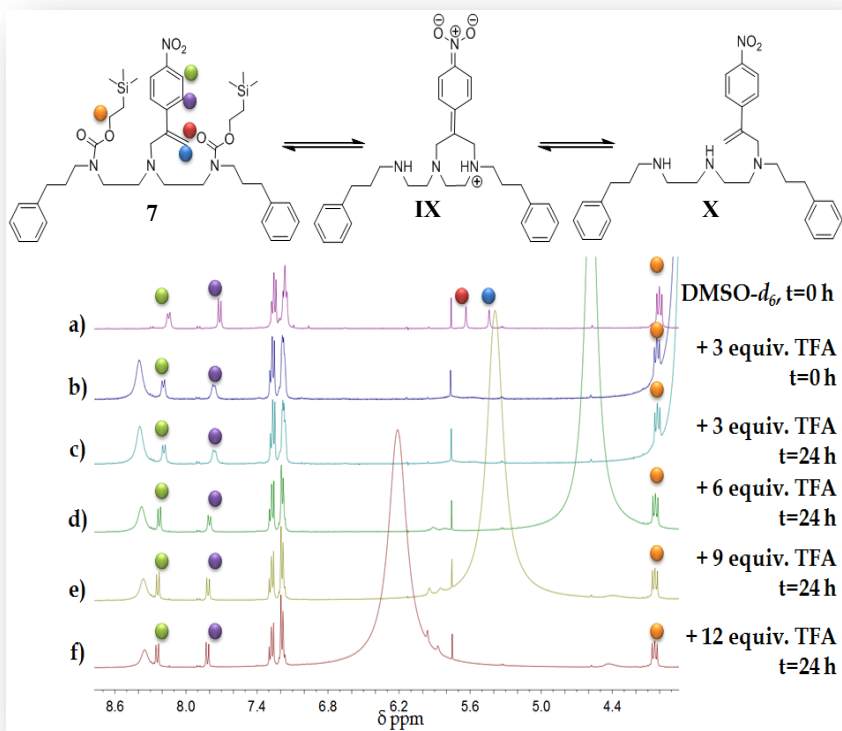


Figure 9. Relevant portions of ¹H NMR spectra of the deprotection study with TFA: the spectra shown monitors the response of compound **7** with TFA over time a) before the addition of trifluoroacetic acid; b) addition of 3 equivalents of TFA at t = 0; c) at t = 24 h; d) t = 24 h from the addition of further 3 equivalents; e) at t = 24 h from the addition of 9 equivalents in total; f) at t = 24 h from the addition of further 3 equivalents. Every spectra was recorded in DMSO-*d*₆ in the presence of 2 equivalents of DIPEA.

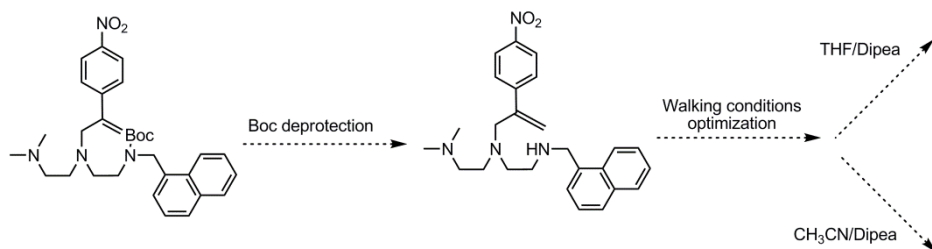
6.3 CONCLUSIONS

Teoc demonstrated to be one of the few amines protecting groups that can match all the requirements for a traffic lights on a branched track.

The selective deprotection of the Boc in the presence of Teoc was satisfied, and the synthesis of a mimic track of the final branched one was carried out with success, as the Michael walker attachment.

Unfortunately, the final Teoc deprotection studies did not pan out: when the deprotection occurs is always accompanied by cleavage of the Michael walker. A new tuning of the conditions is necessary and in particular two different approaches could be taken into account to finish the work.

1. A further optimization of Teoc deprotection in walking condition:
 - ∅ use again KF but in combination with a crown ether to enhance his reactivity;
 - ∅ try the catalytic TBAF deprotection but in DMSO- d_6 .
2. A tuning of the walking conditions to the TEOC deprotection conditions:
 - ∅ use TBAF in THF;
 - ∅ use TBAF in acetonitrile.



Scheme 13. Possible new approaches in the deprotection studies.

Acknowledgements

Special thanks to Professor D. A. Leigh and Urszula Lewandowska from the University of Edinburgh.

6.4 EXPERIMENTAL SECTION

General Methods. Unless otherwise stated, all reagents were purchased from commercial sources and used without further purification. Dry CH_2Cl_2 , CHCl_3 and THF were obtained by passing the solvent (HPLC grade) through an activated alumina column on a PureSolv™ solvent purification system (InnovativeTechnologies, Inc., MA). Dry DMF, MeOH and absolute EtOH were purchased from Sigma-Aldrich. Flash column chromatography was carried out using Kieselgel C60 (Merck, Germany) as the stationary phase. All commercial reagents were ACS reagent grade and used as received. Analytical TLC was performed on precoated silica gel plates (0.25 mm thick, 60F254, Merck, Germany) and observed under UV light. All ^1H and ^{13}C NMR spectra were recorded on Bruker AV 400, AV 500 (cryoprobe), at a constant temperature of 298 K. Chemical shifts are reported in parts per million and referenced to residual solvent. Coupling constants (J) are reported in Hertz (Hz). Mass spectrometric analysis was carried out by the mass spectrometry services at the University of Edinburgh. Synthesis of track **III** was already reported elsewhere together with compound **IV**,⁷ tracks **I** and **II** were synthesized according to the same literature procedure of **III** using 1-naphthaldehyde instead of 3-phenylpropionaldehyde for the reductive amination.⁷ Walker was synthesized following a published procedure.^{5a}

Synthesis.

Compound V

To a solution of compound **IV** (2g, 5.06 mmol) in 32 mL of methanol, a 40 mL water solution of NaOH (2.00 g, 50.6 mmol) was added. The reaction was stirred overnight at room temperature. The organics were evaporated under reduced pressure and the residue was washed with dichloromethane (x 3) leading to the desired product with a 87% yield.

^1H NMR (CDCl_3 , 400 MHz): δ (ppm) 3.29 (bt, 4H, CH_2NBoc), 2.29 (t, 4H, CH_2NH_2 , J = 6.6 Hz), 1.47 (s, 9H, $\text{OC}(\text{CH}_3)_3$), 1.39 (4H, bs, CH_2NH_2).

Compound VI

To a stirring solution of compound **V** (897 mg, 4.41 mmol) in 25 mL of absolute ethanol, the 3-phenylpropionaldehyde (1.07 g, 7.9 mmol) was added under nitrogen. After stirring the solution for 24 hours at room temperature, NaBH_4 (834 mg, 22.05 mmol) was added in portions and the resulting mixture

was stirred at room temperature for other 4 hours. Then 100 mL of water were added to the solution and the product extracted with dichloromethane and washed again with brine. The resulting organics were combined and dried over Na_2SO_4 . After filtration, the solvent was evaporated under reduce pressure and the product was subjected to flash column chromatography eluting with $\text{CH}_2\text{Cl}_2/\text{MeOH}/\text{NH}_3$ (96/4/1, v/v) affording pure product **VI** in 20% yield.

$^1\text{H NMR}$ (CDCl_3 , 400 MHz): δ (ppm) 7.31-7.28 (m, 4H, **aromatic**), 7.22-7.18 (m, 6H, **aromatic**), 3.34 (bt, 4H, CH_2NBoc), 2.80 (t, 4H, $\text{CH}_2\text{CH}_2\text{NBoc}$, $J = 6.5$ Hz), 2.69 (dt, 8H, CH_2Ar ; $\text{CH}_2\text{CH}_2\text{CH}_2\text{Ar}$), 1.84 (m, 4H, $\text{CH}_2\text{CH}_2\text{Ar}$), 1.49 (bs, 11H, $\text{OC}(\text{CH}_3)_3$; CH_2NH). **ESI-MS**: m/z : 440.09 [$\text{M}+\text{H}$] $^+$.

Compound 1, 3, 5 and VII

Similar procedures were followed for the Teoc attachment for products **1**, **3**, **5** and **VII**. herein we report the procedure and the quantities for the synthesis of product **VII**.

To a solution of compound **VI** (125 mg, 0.28 mmol) in 18 mL of dry dichloromethane, Cs_2CO_3 (365 mg, 1.12 mmol) and 1-[2-(Trimethylsilyl)ethoxycarbonyloxy]pyrrolidin-2,5-dione (Teoc, 174 mg, 0.67 mmol) were added. The resulting mixture was stirred under nitrogen at room temperature overnight. The solution was diluted with water and the product was extracted with dichloromethane (x 3), washed again with a saturated solution of NaHCO_3 and extract with dichloromethane (x 2). The organics were combined together and after evaporation of the solvent under vacuum, the product was purified on a column chromatography eluting with $\text{CH}_2\text{Cl}_2/\text{MeOH}/\text{NH}_3$ (98/2/0.5, v/v). The desired product **VII** was obtained with a 35% yield.

$^1\text{H NMR}$ (CDCl_3 , 400 MHz): δ (ppm) 7.31-7.27 (m, 4H, **aromatic**), 7.21-7.19 (m, 6H, **aromatic**), 4.16 (bt, 4H, $\text{OCH}_2\text{CH}_2\text{Si}$), 3.33 (bm, 12H, CH_2NBoc , $\text{CH}_2\text{CH}_2\text{NBoc}$, $\text{CH}_2\text{CH}_2\text{CH}_2\text{Ar}$), 2.61 (bt, 4H, CH_2Ar), 1.87 (bm, 4H, $\text{CH}_2\text{CH}_2\text{Ar}$), 1.49 (s+s, 9H, $\text{OC}(\text{CH}_3)_3$), 1.01 (bt, 4H, $\text{OCH}_2\text{CH}_2\text{Si}$), 0.09 (s, 18H, $\text{Si}(\text{CH}_3)_3$). **ESI-MS**: m/z : 1477.90 [M_2+Na] $^+$.

Compound VIII

To a stirring solution of compound **VII** (27 mg, 0.04 mmol), in 1 mL of MeOH, a 1.25 M solution of HCl in MeOH was added. The reaction was stirred overnight at room temperature. The solution was diluted in dichloromethane and suspended in a saturated solution of NaHCO_3 in water until the neutralization of the buffer. The product was extracted with dichloromethane (x

3), the organics were collected and concentrated under reduced pressure. The product was obtained with a 80% yield and used for the next stage without purification.

$^1\text{H NMR}$ (CDCl_3 , 400 MHz): δ (ppm) 7.31-7.28 (m, 4H, **aromatic**), 7.22-7.18 (m, 6H, **aromatic**), 4.19 (bt, 4H, $\text{OCH}_2\text{CH}_2\text{Si}$), 3.49-3.30 (overlapped, 8H, $\text{CH}_2\text{CH}_2\text{NH}$, $\text{CH}_2\text{CH}_2\text{CH}_2\text{Ar}$), 3.00 (bt, 4H, CH_2NH), 2.63 (t, 4H, CH_2Ar , $J = 7.3$ Hz), 1.89 (t, 4H, $\text{CH}_2\text{CH}_2\text{Ar}$, $J = 7.01$ Hz), 1.02 (t, 4H, $\text{OCH}_2\text{CH}_2\text{Si}$), 0.09 (s, 18H, $\text{Si}(\text{CH}_3)_3$). **ESI-MS**: m/z : 628.33 $[\text{M}+\text{H}]^+$.

Compound 7

To a degassed solution of compound **XI** (19 mg, 0.030 mmol) in 2 mL of dry MeOH α -methylene-4-nitrostyrene (10 mg, 0.030 mmol) was added in one portion. The reaction mixture was stirred at 60°C in the presence of DIPEA (12 mg, 0.090 mmol) for 2 days. The solvent was removed under vacuum and the product was purified on a preparative TLC on silica eluting with hexane/ethyl acetate (9/1, v/v) affording the desired product **7** with a 57% yield.

$^1\text{H NMR}$ (CDCl_3 , 400 MHz): δ (ppm) 8.16 (br, 2H, **walker aromatic**), 7.57 (br, 2H, **walker aromatic**), 7.30-7.28 (m, 4H, **aromatic**), 7.22-7.18 (m, 6H, **aromatic**), 5.33 (s, 1H, $\text{ArC}=\text{CHH}$), 5.41 (s, 1H, $\text{ArC}=\text{CHH}$), 4.17 (t, 4H, $\text{OCH}_2\text{CH}_2\text{Si}$, $J = 6.9$ Hz), 3.51 (br, 4H, $\text{CH}_2\text{CH}_2\text{CH}_2\text{Ar}$), 3.24-3.12 (overlapped, 8H, $\text{CH}_2\text{CH}_2\text{Nwalker}$, $\text{CH}_2\text{CH}_2\text{Nwalker}$), 2.62 (br, 4H, CH_2Ar), 1.82 (br, 4H, $\text{CH}_2\text{CH}_2\text{Ar}$), 0.99 (t, 4H, $\text{OCH}_2\text{CH}_2\text{Si}$, $J = 6.9$ Hz), 0.06 (s, 18H, $\text{Si}(\text{CH}_3)_3$). **ESI-MS**: m/z : 812.17 $[\text{M}+\text{Na}]^+$.

6.5 REFERENCES

- ¹ a) Von Delius, M.; Geertsema, E. M.; Leigh, D. A. *Nat. Chem.* **2010**, *2*, 96-101; b) Otto, S. *Nat. Chem.* **2010**, *2*, 75-76; c) von Delius, M.; Geertsema, E. M.; Leigh, D. A.; Tang, D.-T. D. *J. Am. Chem. Soc.* **2010**, *132*, 16134-16145; d) Barrell, M. J.; Campaña, A. G.; von Delius, M.; Geertsema, E. M.; Leigh, D. A. *Angew. Chem. Int. Ed.* **2011**, *50*, 285-290;
- ² a) Yin, P.; Yan, H.; Daniell, X. G.; Turberfield, A. J.; Reif, J. H. *Angew. Chem. Int. Ed.* **2004**, *43*, 4906-4911; b) Bath, J.; Green, S. J.; Turberfield, A. J. *Angew. Chem. Int. Ed.* **2005**, *44*, 4358-4361; c) Tian, Y.; He, Y.; Chen, Y.; Yin, P.; Mao, C. *Angew. Chem. Int. Ed.* **2005**, *44*, 4355-4358; d) Yin, P.; Choi, H. M. T.; Calvert, C. R.; Pierce, N. A. *Nature* **2008**, *451*, 318-322; e) Green, S. J.; Bath, J.; Turberfield, A. J. *Phys. Rev. Lett.* **2008**, *101*, 238101-238104; f) Omabegho, T.; Sha, R.; Seeman, N. C. *Science* **2009**, *324*, 67-71; g) Lund, K.; et al. *Nature* **2010**, *465*, 206-210; h) Gu, H.; Xiao, S. J.; Seeman, N. C. *Nature* **2010**, *465*, 202-205; i) He, Y.; Liu, D. R. *Nat. Nanotechnol.* **2010**, *5*, 778-782; j) Wickham, S. F. J.; Endo, M.; Katsuda, Y.; Hidaka, K.; Bath, J.; Sugiyama, H.; Turberfield, A. J. *Nat. Nanotechnol.* **2011**, *6*, 166-169; k) Muscat, R. A.; Bath, J.; Turberfield, A. J. *Nano Lett.* **2011**, *11*, 982-987; l) Sherman, W. B.; Seeman, N. C. *Nano Lett.* **2004**, *4*, 1203-1207; m) Shin, J.-S.; Pierce, N. A. *J. Am. Chem. Soc.*, **2004**, *126*, 10834-10835; n) Lund, K.; Manzo, A. J.; Dabby, N.; Michelotti, N.; Johnson-Buck, A.; Nangreave, J.; Taylor, S.; Pei, R.; Stojanovic, M. N.; Walter, N. G.; Winfree, E.; Yan, H. *Nature* **2010**, *465*, 206- 210.
- ³ a) Carter, N. J.; Cross, R. A. *Curr. Opin. Cell Biol.* **2006**, *18*, 61-67; b) Block, S. M. *Biophys. J.* **2007**, *92*, 2986-2995; c) Hirokawa, N.; Noda, Y.; Tanaka, Y.; Niwa, S. *Nat. Rev. Mol. Cell Biol.* **2009**, *10*, 682-696.
- ⁴ a) Koonce, M. P.; Samsó, M. *Trends Cell Biol.* **2004**, *14*, 612-619; b) Oiwa K.; Sakakibara, H. *Curr. Opin. Cell Biol.* **2005**, *17*, 98-103.
- ⁵ a) Sellers, J. R.; Veigel, C. *Curr. Opin. Cell Biol.* **2006**, *18*, 68-73; b) Sweeney, H. L.; Houdusse, A. *Annu. Rev. Biophys.* **2010**, *39*, 539-557.
- ⁶ Von Delius, M.; Leigh, D. A. *Chem. Soc. Rev.* **2011**, *40*, 3656-3676.

- ⁷ a) Astumian, R. D. *Phys. Chem. Chem. Phys.* **2007**, *9*, 5067-5083; b) Astumian, R. D. *Biophys. J.* **2010**, *98*, 2401-2409; c) Kay, E. R.; Leigh, D. A.; Zerbetto, F. *Angew. Chem., Int. Ed.* **2007**, *46*, 72-191.
- ⁸ a) *Molecular Motors* (Ed.: M. Schliwa), Wiley-VCH, Weinheim, **2003**; b) Vale, R. D. *Cell* **2003**, *112*, 467-480.
- ⁹ a) Mitra, S.; Lawton, R. G. *J. Am. Chem. Soc.* **1979**, *101*, 3097-3110; b) Liberatore, F. A.; Comeau, R. D.; McKearin, J. M.; Pearson, D. A.; Belonga, B. Q.; Brocchini, S. J.; Kath, J.; Phillips, T.; Oswell, K.; Lawton, R. G. *Bioconjugate Chem.* **1990**, *1*, 36-50; c) del Rosario, R. B.; Brocchini, S. J.; Lawton, R. G.; Wahl, R. L.; Smith, R. *Bioconjugate Chem.* **1990**, *1*, 51-59; d) del Rosario, R. B.; Baron, L. A.; Lawton R. G.; Wahl, R. L. *Nucl. Med. Biol.* **1992**, *19*, 417-421.
- ¹⁰ Campaña, A. G.; Carlone, A.; Chen, K.; Dryden, D. T. F.; Leigh, D. A.; Lewandowska, U.; Mullen, K. T. *Angew. Chem. Int. Ed.* **2012**, *51*, 5480-5483.
- ¹¹a) Greene, T. W.; Wuts, P. G. M. *Protective Groups in Organic Synthesis*, 2nd Edition, John Wiley and Sons: New York, **1991**. b) Carpino, L. A.; Tsao, J.-H.; Ringsdorf, H.; Fell, E.; Hettrich, G. *J. Chem. Soc., Chem. Commun.* **1978**, 358-359; c) Parlow, J. J.; Vazquez, M. L.; Flynn, D. L. *Bioorg. Med. Chem. Lett.* **1998**, *8*, 2391-2394.
- ¹²Hwu, J. R.; Jain, M. L.; Tsay, S.-C.; Hakimelahi, G. H. *Tetrahedron Lett.* **1996**, *37*, 2035-2038.

Acknowledgements

Ci siamo. Scrivere le pagine conclusive della tesi è come sigillare la fine di un periodo, racchiudendo dietro a tutte le righe scritte, i sorrisi, le risate e diciamo celo... talvolta anche le frustrazioni di questi ultimi tre anni.

Innanzitutto un grazie di cuore ad Enrico per la passione che non manca mai di trasmettere e per tutte le possibilità e gli insegnamenti che mi ha dato.

Il secondo grazie va alla mia splendida famiglia: alla mia bellissima mamma (ti voglio bene!), a mio padre (sei sempre una roccia), ai miei fratelli Paolo (le nostre cenazze continueranno per sempre), Claudio (devo strapparti la promessa di fare molte più cene insieme!), Marcello (sei il nostro Mel Gibson). Grazie per tutti i consigli, le chiacchiere, il sostegno morale (e non solo), siete stati la luce nei miei momenti bui, insomma siete i miei punti di riferimento e lo sarete sempre, vi devo tantissimo. Grazie anche alle mie cognate Mary e Cri e ai miei meravigliosi nipoti Sara, Ale, Dany, Franci, Marco e Silvia.

E adesso un grazie a chi ha reso speciale questo dottorato, a partire dall'ineguagliabile 213: a Roger (porto nel cuore le lezioni che mi hai dato e le risate che ci siamo fatti durante la tesi), Sarto (non dimenticherò mai le pazzie che facevamo ai concerti di Lady Gaga e Beyoncé, anche se ora sono diventate due sciacquette), alla Monica (grazie per la calma che riuscivi ad instillarmi), alle mie compagne di chiacchiere e gossip Vero e Robby (mi avete sempre allietato con i giusti consigli e i gossip più gustosi!), a Kuby e Kassy... datemi tutti i soldi! (È da quando siete arrivati in Italia che aspetto il super polish party, ma che fine ha fatto?? Va beh rimarrete sempre i miei polacchi preferiti!), alla Giuliy (il laboratorio ha smesso di essere fashion da quando te ne sei andata). Un grazie anche all'Ely ed ai suoi consigli che mi hanno accompagnata in questi 3 anni, a Tahnee, e ai super nuovi arrivi: a Fedè per le sane risate che mi ha fatto fare in un periodo così stressante come la tesi (non per niente hai la stellina), ad Ale per aver reso stressante un periodo così stressante come la tesi... dai che scherzo, appena smetto di scrivere la tesi torno simpatica e via che andiamo al blabli tutti insieme!

E ora passiamo ai ringraziamenti per il 187, che più che un laboratorio è uno stile di vita (cit. Merc): al Bedò (dai... che il count down è quasi finito, anche se non riesco proprio ad immaginare i prossimi mesi senza le tue perle), a Dany (ci manchi! Torna, il Bedò non è più lo stesso senza te), alla Maffi (per essermi venuta a trovare a Edimburgo, per le risate a Tarragona... insomma... senza di te non sarebbe mai stato lo stesso), al Merc (pensavi mi fossi dimenticata? Come potrei scordare l'allegria, i consigli, le lezioni che mi hai dato? Questa università ha perso un grande pezzo, ma che dico grande, ENORME!).

Thanks to Professor Leigh for the great opportunity to join his group, and special thanks to Ula, Bartek, Victor, Alan, Tug, John, Miriam, Daniel, Kenji and all the group for those great seven months.

Un grazie in generale a tutti i miei ex compagni di università, Mary, Mara, Vezza, Mone, Fantì, Sanna, Monichina, Nencio, Adò, Nico, Fra, Piero, Matty (anche se sei un intruso) ci vediamo poco ma ogni volta che ci riuniamo è come far finta per un momento di essere ancora gggiovani.

Ma chi è davvero gggiovane è la mia super amichetta lovvì del cuoricino Ire... sei stata una compagna di viaggio unica... ti voglio bene... ma smettila di cercare di diventare bionda come me... non ci riuscirai mai.

Un grazie ai miei amici di sempre, in particolare all'Ele, all'Ilo, alla Cerez e alla Marghe, siete i miei fiori, le mie gioie e so che potrò sempre contare su di voi.

E l'ultimo grazie va a chi mi è stato vicino dall'inizio di questa avventura, a chi mi ha sopportato nei periodi in cui ero nervosa, rallegrato quando ero triste... sei la mia forza Marco... grazie per aver reso speciale fin dall'inizio la nostra storia e per far durare questa magia tuttora.

Daniela

The author



born in Carpi (Modena, Italy) on the 22nd of October 1984

- July 2003* **High School Diploma**
Liceo Linguistico Matilde di Canossa
Reggio Emilia, Italy
- March 2007* **Bachelor in Industrial Chemistry**
University of Parma, Italy
Supervisor: Prof. M. Catellani
- April 2009* **Master in Industrial Chemistry**
University of Parma, Italy
Supervisor: Prof. E. Dalcanale
- April 2009-December 2009* **Post-graduate Research**
University of Parma, Italy
Supervisor: Prof. E. Dalcanale
- January 2010-December 2012* **Doctoral Research**
University of Parma, Italy
Supervisor: Prof. E. Dalcanale
- January 2012-July 2012* **Research exchange**
University of Edinburgh, Scotland
Supervisor: Prof. D. A. Leigh

Parma, January 2013